FUNCTIONAL STUDIES OF TYPE II HETERODIMERIC PHYTOCHROMES AND END-MODIFIED TYPE I PHYAS IN ARABIDOPSIS

by

Peng Liu

A dissertation submitted in partial fulfillment
of the requirements for the degree

of

Doctor of Philosophy

in

Plant Sciences

MONTANA STATE UNIVERSITY
Bozeman, Montana

July 2011

©COPYRIGHT

by

Peng Liu

2011

All Rights Reserved

APPROVAL

of a dissertation submitted by

Peng Liu

This dissertation has been read by each member of the dissertation committee and has been found to be satisfactory regarding content, English usage, format, citation, bibliographic style, and consistency and is ready for submission to The Graduate School.

Dr. Robert A. Sharrock

Approved for the Department of Plant Sciences & Plant Pathology

Dr. John E. Sherwood

Approved for The Graduate School

Dr. Carl A. Fox

STATEMENT OF PERMISSION TO USE

In presenting this dissertation in partial fulfillment of the requirements for a doctoral degree at Montana State University, I agree that the Library shall make it available to borrowers under rules of the Library. I further agree that copying of this dissertation is allowable only for scholarly purposes, consistent with "fair use" as prescribed in the U.S. Copyright Law. Requests for extensive copying or reproduction of this dissertation should be referred to ProQuest Information and Learning, 300 North Zeeb Road, Ann Arbor, Michigan 48106, to whom I have granted "the exclusive right to reproduce and distribute my dissertation in and from microform along with the non-exclusive right to reproduce and distribute my abstract in any format in whole or in part."

Peng Liu

July 2011

ACKNOWLEDGEMENTS

First and foremost I would like to thank my advisor, Dr. Robert A. Sharrock, who introduced me to this interesting research area of plant light signaling, for the ideas, support, and kindness. I sincerely thank for his understanding and patience.

Second, I would like to thank Ted Clack, whose technical expertise facilitated most aspects of my research. This work would not have been possible without his help and support.

I would also like to thank the other members of my graduate committee, Dr. Norman Weeden, Dr. Li Huang, and Dr. Chaofu Lu for the detailed and constructive comments, and for being a part of my education, research and career.

I wish to extend my warmest thanks to all those who have helped me. A special 'thank you' goes to: Irene Decker, Jinling Kang, Matt Moffet, Joanna Dumas, Jill Scarson, Ahmed Shokry. I am especially grateful to Ms. Jennifer Miller, who assisted in the formatting of this dissertation.

Finally, I dedicate this dissertation to my parents, Futian Liu and Xiuling Bai, and my fiancée Ming Yang, and, for their unconditional love, support and patience in every way possible throughout the process of this course, this dissertation and beyond.

TABLE OF CONTENTS

1. PHYTOCHROME-MEDIATED PHOTOMORPHOGENESIS
IN *Arabidopsis thaliana* 1

Overview 1
Phytochrome-mediated Plant Growth and Development 4
Phytochrome-mediated Responses 4
Low Fluence Response (LFR) 5
Very Low Fluence Responses (VLFR) 5
High Irradiance Response (HIR) 6
Seed Germination 6
Hypocotyl Growth and Development in Plants 7
Cotyledon Growth and Development in Arabidopsis 10
Shade Avoidance 11
Flowering 13
Phytochrome Genes in Higher Plants 14
Phytochrome Sequence Isolation and Identification 14
A Small Gene Family in Higher Plants 15
Type I and Type II Phytochromes in Higher Plants 16
Plant Phytochrome Evolution 17
Phytochrome: Inference of Protein Function from Protein Structure 19
The Chromophore 21
The N-terminus Three-dimensional Structures of Phytochrome 23
Pr/Pfr photoconversion based on Crystal Structures, 2VEA and 3C2W 24
Pr/Pfr photoconversion based on NMR Structures, 2KOI and 2KLI 25
The C-terminus 26
The Three-dimensional Structures of Phytochrome and Signaling 27
Conclusion 28
Phytochrome Nuclear Translocation and Degradation 29
Phytochrome Nucleo-cytoplasmic Transport 29
PhyA Localization 30
Type II Phytochrome Localization 32
The Types and Stages of NBs 33
Early and Late Phytochrome NBs 33
Four Stages of NB Formation 33
NBs- the Sites for Protein Degradation 34
Ubiquitin/Proteasome-mediated Proteolysis 35
PhyA Degradation 36
Ubiquitin/Proteasome-regulated PhyA Proteolysis 36
The Different Effects of PhyA Proteolysis 38

TABLE OF CONTENTS - CONTINUED

A Common Mechanism of PhyA Signaling is Expected in VLFRs and FR-HIRs 38
Phytochrome Interaction and Signaling 41
Phytochrome Function and Interaction in Plant Development 41
Additive and Synergistic Effects and Type II Heterodimerization 43
Phytochrome Signaling 45
The PIF Hub 46
The Feedback between Phytochrome and PIFs 47
PIFs Control Plant Hormone Expression 47
The Circadian Clock 48
High Temperature 48
The HY5 Hub 49
Conclusion 51

2. DIRECTED DIMERIZATION: AN *In Vivo* EXPRESSION SYSTEM FOR FUNCTIONAL STUDIES OF HETERODIMERIC PHYTOCHROMES IN *Arabidopsis* 52

Abstract 52
Introduction 53
Results 56
The PB1 Domains of the Yeast Bem1 and Cdc24 Protein Form Obligate Heterodimers 56
Bem/Cdc Domain-directed Dimerization *in vivo* of the NB PSR 58
Dimerization of the NB PSR with Itself or with Achromo-NB Induces Different R sensitivities in Seedlings 62
Yeast GAL4 Domain-directed Homodimerization of the NB or ND PSR, but not NC or NE, Induces Photosensing Activities 67
NB/ND Heterodimers are Functional and Mediate R Hypersensitivity 72
Directed Dimers Mediate Mature Plant R Light Responses 75
Discussion 78
Dimerization of PhyB PSRs in the Nucleus is Required for Signaling 78
The C-terminal Module of PhyB is Important for Regulating Signaling 80
PhyB/D Heterodimers may Have Higher Activity than PhyB Homodimers 82
Heterodimers Mediate Tissue-specific Growth and Development in De-etiolated Seedlings and Flowering 83
Phytochrome's Smart Evolutionary Way to Function in the Nucleus 84
Complexity in Light Signal Transduction 86

TABLE OF CONTENTS – CONTINUED

Materials and Methods....88
Plant Materials, Growth Conditions, and Measurement....88
Plasmid Construction and Plant Transformation....88
Proteasome and Protein Inhibitors....89
Yeast Two-hybrid Assay....90
Protein Extractions, SDS PAGE, and Western Blot....91
Immunoprecipitation....91
Size Exclusion Chromatography (SEC)....92

3. MODIFICATION OF THE ENDS OF PHYTOCHROME A INFLUENCES ITS ACTIVITY AND DEGRADATION PATTERN....93

Abstract....93
Introduction....94
Results....99
Myc_6 Epitopes Attenuate PhyA Biological Activity in FR-HIR Signaling....99
The PhyA N-terminus May be Important for VLFR than its C-terminus....103
Unmodified PhyA and Terminal-modified PhyA function similarly in Regulation of Flowering....103
PhyA Forms Only Homodimers *in vivo*....106
Myc_6 Epitope Tags Delay Degradation of PhyA in R Light....108
Interaction Regulates the Degradation Process of Native PhyA in the R Light....108
Discussion....110
Materials and Methods....114
Plant Materials, Growth Conditions, and Measurement....115
VLFR....115
Flowering Time....115

4. COMPLEMENTATION OF EARLY FLOWERING PHENOTYPE IN ARABIDOPSIS BY EXPRESSION OF PHYTOCHROME E....117

Introduction....117
Results....118
Discussion....119
Materials and Methods....123
Plant Materials, Growth Conditions, and Measurement....123

REFERENCES CITED....124

TABLE OF CONTENTS-CONTINUED

APPENDIX A: SEQENCES OF OBLIGATE DIMERS
OF THE N-TERMINAL PHY PSRS 152

LIST OF TABLES

Table Page

1.1 Phytochrome functions are summarized based on the research of *Arabidopsis* phytochrome-deficient mutants 42

2.1 Oligonucleotide primers used in PCR for the yeast two-hybrid analysis Table Two Name.....90

LIST OF FIGURES

Figure Page

1.1. Phytochrome general action machinery 4

1.2. Molecular phylogeny of the phy N-terminus 18

1.3. Schematic architecture of representatives of phy-type photoreceptors in plants, cynobacteria, bacteria and fungi 20

1.4. Biosynthesis of tetrapyrrole in higher plants 22

1.5. The proposed mechanism for phyA-mediated signaling in both VLFRs and FR-HIRs 40

1.6. Dimerization properties of Arabidopsis type II phytochromes 45

1.7. A simplified model of the phytochrome-mediated signaling network 50

2.1. The yeast Bem1 and Cdc24 proteins do not form homodimers 57

2.2. Co-expression of Bem and Cdc-mediated NB fusion transgenes stabilizes the NBs in the light 60

2.3. Quantitative analysis of phyB levels in the *phyB*(*PHYB*-myc$_6$) #210-3 line and the *phyB*(his$_6$-*PHYB*) #336-1 line 61

2.4. Monomeric phyB PSR is more stable in the dark than under R 61

2.5. Bem/Cdc domain and GAL domain-directed dimerization *in vivo* 64

2.6. PhyB/achromo-phyB dimers are non-functional in hypocotyls 65

2.7. Nuclear-localized chromophore-ligated NB dimers are required for hypocotyl inhibition 66

2.8. R light sensitivity is restored in the doubly transgenic *phyB*(NB-Cdc/NB-Bem) lines generated by crossing or double transformation 67

2.9. Expression of yeast GAL4 domain-mediated homodimeric phyB, phyC, phyD, and phyE 69

LIST OF FIGURES – CONTINUED

Figure Page

2.10. Activities of NB-containing and ND-containing dimeric phytochromes 70

2.11. Expression of the singly *phyB*(NX-Cdc) and doubly transgenic *phyB*(NX-Cdc/NB-Bem) (X=C, D and E) lines 71

2.12. Various R light responses of the singly *phyB*(NX-Cdc) and doubly transgenic *phyB*(NX-Cdc/NB-Bem) (X=C, D and E) lines 74

2.13. NB and ND transgene products are present at comparable steady-state levels in various transgenic lines 75

2.14. Directed NB/ND heterodimers suppress hypocotyl elongation very effectively 76

2.15. Diverse adult plant R-sensing activities observed in the NB and ND-containing transgenic lines 77

3.1. Generation of transgenic Arabidopsis lines expressing myc epitope-tagged phyA fusion transgenes 100

3.2. Expression levels of various phyA fusion proteins in 5-day-old FRc-grown seedlings 101

3.3. Myc6 epitopes attenuate phyA-mediated FR-HIR signaling 102

3.4. The N-terminus of phyA is critical for phyA-mediated VLFRs 104

3.5. Epitope-tagged phyAs are biological active and complement the late flowering phyA mutant phenotype 105

3.6. Assessment of coimmunoprecipitation of phyA-phyE with the phyA-m6 or phyA-m1 protein from seedling extracts 106

3.7. Kinetic analysis of phyA degradation following transfer to R 107

3.8. Interaction delays native phyA degradation in the WT(*PHYA*-m6) lines under R conditions 109

LIST OF FIGURES – CONTINUED

Figure Page

4.1. Biological activity of epitope-tagged phyE delays flowering.....120

4.2. Post-flowering phenotypes of representatives of Wild-Type, *phyB*, *phyBE*, *phyE*, WT(*PHYE*-m6), *phyE*(*PHYE*-m6) and *phyBE*(*PHYE*-m6).....121

4.3. The phyD/phyE heterodimers and the phyB/phyE heterodimers play major roles in controlling flowering time 121

ABSTRACT

Phytochromes (phys) are a family of dimeric chromoprotein photoreceptors that modulate plant physiological and developmental processes in response to red (R) and far-red (FR) light. In *Arabidopsis thaliana*, these fall into two functional groups, type I phyA and type II phyB-E. Previous findings have shown that heterodimerization occurs in type II phytochromes and suggest that diverse dimer forms may have specific functions. The first objective of this study was to characterize the activities of individual phytochrome dimer combinations by developing a novel *in vivo* protein engineering system. Either obligate homodimers or heterodimers of phytochrome N-terminal regions were produced in *phyB* mutant plants. With this system, a highly active phyB/D heterodimeric form was shown to rescue the *phyB* mutant phenotype. Dimers of phyB/achromo-phyB, phyB/C, and phyB/E mediated organ-specific growth in de-etiolation by functioning differentially in cotyledons but not in hypocotyls. Light labile phyA is critical in the plant transition from skotomorphogenic to photomorphogenic growth. To investigate possible *in vivo* phyA heterodimerization with type II phys and the relationship between phy quaternary structure and signaling mechanisms, transgenic plants were generated that express different myc-tagged N- or C-terminal end fusion phyA proteins in a Landsberg *erecta* (L*er*) *phyA* mutant or a wild-type background. Co-immunoprecipitation showed that phyA only forms homodimers with itself. Compared with fully active one myc epitope (myc1)-tagged phyAs, six myc epitopes attached to the ends of the N- or C- terminus of phyA impaired phyA-mediated far-red high irradiance (FR-HIR) signaling and also attenuated degradation in the light, indicating that alteration of phyA architecture may damage protein-protein interaction both in phyA downstream signaling and in its protein turnover. Overall, these findings have expanded the structurally complex R/FR sensing systems in plants and have implications for how plant growth and development may be fine-tuned through phy heterodimer-mediated tissue-specific growth or phy-modified activity.

CHAPTER 1

PHYTOCHROME-MEDIATED PHOTOMORPHOGENESIS IN *Arabidopsis thaliana*

Overview

After germination occurs, plants go through several successive growth stages, including seedling de-etiolation, plant maturity and flowering, followed eventually by seed production. A combination of internal genetic and external environmental factors determines the time frame of these processes. Light, as one of the most important environmental factors, not only provides solar energy for plant photosynthesis, but also informational signals, such as light quality, quantity, direction and duration, to synchronize plant adaptive development in response to the exigencies of the ambient conditions. Light-mediated plant growth and development is referred as photomorphogenesis.

A photoreceptor is a connector between light photons and cellular signaling intermediates, coupling two input/output processes: sensing light cues in the environment and directing various physiological and metabolic reactions in organisms. A diverse plant photoreceptor collection allows light to give plants a clear indication of time and space with the aim of acquisition of advantages for survival, and propagation in a constantly changing environment. Four major classes of photoreceptors have been described in flowering plants: the red/far-red (R/FR) light-absorbing phytochromes, the UV-A/blue light-absorbing cryptochromes and phototropins, and UV-B light-absorbing UVR8s

(Ballare, 2003; Briggs and Christie, 2002; Briggs and Huala, 1999; Quail, 1994; Rizzini et al., 2011).

The function of phytochrome is determined by its photosensory structure and photochemical properties. In early days, several phytochrome-induced responses known as LFRs, including germination, de-etiolation and photoperiodism in various plant species, were demonstrated to share basically the same action spectra with action maxima near 660 and 730nm. This indicated that a reversible photoreaction existed in plants which is regulated by two interconvertible forms of a photoreceptor (Nagy, 2006). The red/far-red light sensing photoreceptor -- phytochrome, was first observed and purified from maize tissue in 1959 by spectrophotometric approaches (Butler et al., 1959). Highly purified homogeneous phytochromes were finally obtained from oat and rye in the early 1980s, when new purification techniques were adopted to minimize the proteolytic loss of phytochrome (Cordonnier and Pratt, 1982; Vierstra and Quail, 1982). The purification of phytochrome became a precondition for the expression detection and subsequent phytochrome cloning, and also laid a solid foundation for studies of phytochrome structure, evolution and biological function.

Due to the innovation of highly sensitive spectroscopy and action spectroscopy, several phytochromes in different species were investigated and their common actions were observed. In summary, these findings showed that phytochrome is a dimeric chromoprotein, to which a linear tetrapyrrole bilin chromophore is covalently attached via a thioether linkage. Phytochrome acts like a light-regulated switch, reversibly altering various responses due to its two distinct conformational isoforms: inactive Pr and active

Pfr. Direct photoconversion between these forms occurs when Pr and Pfr absorb maximally in R (~660 nm) and FR (~730 nm), respectively. Therefore, when photoconversion between Pr and Pfr proceeds to a dynamic photoequilibrium state under natural light conditions, it reflects the ratio of R to FR light (the R:FR ratio), or more accurately, a specific fraction of total phytochrome in the Pfr form (Pfr/P_{total}), which was initially considered only as a function of light wavelength. However, from the 1950s to the 1980s, biologists also discovered other key properties of phytochrome, such as light lability, light-induced aggregation and dark reversion (Brockmann et al., 1987; Mackenzie et al., 1975; Pratt, Kidd, and Coleman, 1974). The combined effects of these properties give new consideration to the concept of the Pfr/P_{total} which is not only a function of light quality (wavelength) but also a function of light irradiance. From experimental data, theoretical calculation demonstrated that because of the overlap in R absorption, there is a balance of 86% Pfr and 14% Pr in R, whereas in FR, a balance of 97% Pr to 3% Pfr (Kelly and Lagarias, 1985; Lagarias et al., 1987).

As shown in Figure 1.1, the *de novo* synthesis of Pr occurs in the cytoplasm where phytochrome accumulates, reaching a relatively high level in the dark. Upon absorption of red light, Pr is converted to active Pfr which is imported from the cytoplasm into the nucleus, where phytochrome aggregates or is assembled into nuclear bodies (NBs) and induces various light transduction pathways resulting in their corresponding responses (Jiao, Lau, and Deng, 2007; Quail, 2002). Meanwhile, active Pfr is regulated by a destruction process carried out by the ubiquitin-proteasome machinery. Moreover, Pfr is

able to slowly reconvert to the Pr state in the absence of light, by a thermal process called dark reversion.

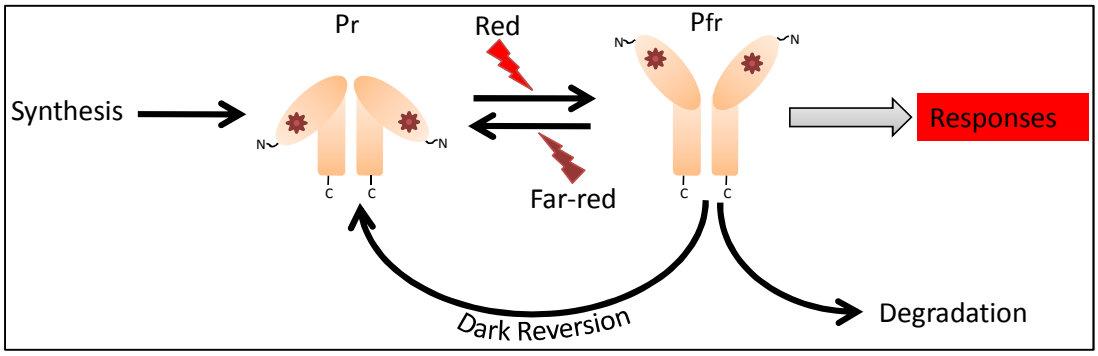


Figure 1.1. Phytochrome general action machinery. A model of the phytochrome photocycle within plant cells is depicted, where photoactivated phytochrome, the Pfr form, induces multiple responses to the environment. Pr, the inactive form, is converted to Pfr upon absorption of red light. For desensitizing responses, Pfr can undergo degradation in R. Alternatively, Pfr can be converted back into Pr either by exposure to FR, or by a thermal process in darkness known as dark reversion.

Phytochrome-mediated Plant Growth and Development

Phytochrome-mediated Responses

Phytochrome photoreceptors perform diverse functions throughout the life cycle of plants (Franklin and Quail, 2010). Generally, phytochromes promote seed germination, induce seedling de-etiolation and shade avoidance, repress flowering and entrain the circadian clock. But after the discovery of a small gene family in the model plant *Arabidopsis thaliana* and in other flowering species, we need to answer the question which phytochrome triggers what kind of responses more specifically (Clack, Mathews, and Sharrock, 1994). Associated with the most striking photochemical activities, phytochrome-mediated responses can be grouped into three categories as follows.

Low Fluence Response (LFR). The LFRs are all R/FR reversible responses, which are effectively induced by a single red light pulse and reversed by a subsequent far-red light pulse, obeying the rule of the "central dogma"—R/FR photoconversion. The first LFR was documented on the classic experiment of lettuce (*Lactuca sativa L.*) seed germination, in which germination of lettuce seeds was promoted by red light but inhibited by far-red light. The same induction/reversion action spectrum of a certain LFRs has also been recorded at the physiological, biochemical and biophysical levels. Meanwhile, LFRs obey the Bunsen-Roscoe reciprocity law, which states that the extent of response will be determined by the total exposure ($N \times t = \chi\, N \times t/\chi$, N: irradiance; t:duration of the light treatments; χ : an independent variable). The response may be saturated within a short period of irradiation (shorter than 20-30min) at low fluence rate (1 to 1000 μ mol m^{-2} s^{-1}), and establishes the ratio of Pfr/P_{total} between 0.01 to 0.87 (Smith and Whitelam, 1990).

Very Low Fluence Response (VLFR). In natural environments, a VLFR may promote seed germination when the seeds are exposed to a brief light during soil disturbances. The VLFRs can be fully induced by any light, including a green "safe" light used in many laboratory conditions and infrared light. Very low numbers of photons (10^{-4} to 10^{-1} μ mol m^{-2}) can saturate this response, which reflects very low values of Pfr/P_{total} between 10^{-6} to 10^{-3}. In fact, VLFRs can be induced with FR light and do not show R/FR reversibility. A biphasic fluence-response curve in the measurement of the rate of

germination, chlorophyll accumulation or cotyledon separation and expansion usually is interpreted as the occurrence of VLFRs (Yanovsky, Casal, and Luppi, 1997).

High Irradiance Response (HIR). The HIRs are prolonged irradiation responses with an action maximum in the far-red region. Continuous, long-term FR, R, blue (B), and UV can induce such HIRs individually. The extent of the HIR action is only determined by irradiance and duration of the light treatment, given the same wavelength of light. Reciprocity failure also shows in the HIRs, indicating that high irradiation may be inducing signaling feedback, or initiating unknown metabolic reactions required for these responses. Although R/FR reversibility and the reciprocity law do not apply to the HIRs, there are no clear boundaries between HIRs and LFRs in anthocyanin production, cotyledon expansion and hypocotyl inhibition (Beggs et al., 1980).

Seed Germination

The seed is the structure containing a fully developed plant embryo. It functions to promote survival of the embryo in the period between seed maturation and seedling establishment. Seed dormancy is an important checkpoint for seed development, allowing plants to choose the best place and time to germinate. After breaking dormancy, the seeds of an angiosperm or gymnosperm will undergo the germination process from which the sprouting of a seedling emerges. Therefore, seed dormancy and germination are two competitive processes, both of which are determined by the co-action of the growth potential of the embryo and the restraints imposed by environmental signals. The most important environmental cues are light, temperature, nutrients and water.

Light is a necessity for seed germination in many plant species. A light requirement for seed germination in the seeds of *Bulliarda aquatic* D.C. and other plant species was first documented by Caspary in 1860. Flint and McAlister showed in the 1930's that lettuce (*Lactuca sativa* L.) seed germination was promoted by red light but inhibited by far-red light. The involvement of phytochrome in mediating seed germination was discovered by Harry Borthwick and colleagues as a 'flip flop' phenomenon, showing that exposures to cycles of red and far-red light always alternated seed germination, dependent only on the last treatment given (Borthwick et al., 1952). Two years later, the action spectrum of lettuce-seed germination was shown to be similar to those for the phytochrome-mediated de-etiolation and flowering responses. Advanced studies in genetics and molecular physiology have taught us much about the control of germination using the model plant *Arabidopsis thaliana*. Besides phytochrome-mediated signaling, the interaction and balance between abscisic acid (ABA) and gibberellins (GA), the circadian clock, and some major growth-regulatory proteins play important roles in seed germination.

Hypocotyl Growth and Development in Plants

According to plant axial patterning, the hypocotyl in dicots is the embryonic and postembryonic seedling stem, which is located in the middle position between the two cotyledons and the seedling root. During the initial process of differentiation, hypocotyl cells emerge and are easily recognized in the middle region of the embryo at the heart stage in Arabidopsis. As the cells of the apical meristem undergo mitosis in embrogensis, the outermost cells, known as the protoderm generate the epidermis of the hypocotyl, the

ground meristem generates the cortex and the endodermis, and the procambium generates the vascular tissues. After seed germination, postembryonic cell elongation occurs in the epidermal and cortical cells which mainly grow through longitudinal cell expansion, rather than cell division. The hook, which is considered to protect the seedling apex from damage, emerges during growth through the soil with the apical end of the hypocotyl bending back on itself. Upon first sensing light, seedlings change their growth pattern from the dark-grown mode into the light-grown mode with the aim of survival, competition, and propagation.

Two distinct hypocotyl growth strategies, skotomorphogenesis (dark growth) and photomorphogenesis (light growth) have been studied extensively in the model plant Arabidopsis in the past decades. Gendreau et al. summarized three differences between light-grown and dark-grown hypocotyls (Gendreau et al., 1997). First, the epidermal cells under light-grown conditions show a characteristic differentiation, including a ridged surface and differentiated stomates, that are not observed in the dark-grown condition (Wei et al., 1994). Second, although cortical and epidermal cell divisions are rare during elongation growth, up to two endoreduplication rounds occur in photomorphogenesis, whereas a third round will happen only in skotomorphogenesis. Finally, all the epidermal and cortical cells under light conditions undergo a certain degree of elongation growth, with a zone of maximum growth rate moving up from the base to the middle of the hypocotyl. However, a gradient of elongation growth is observed from the base to the top in dark-grown hypocotyls.

Multiple endogenous and environmental cues such as hormones, light, temperature and gravity, strongly determine the growth rate of hypocotyl elongation. By now, nearly 50 genes or gene families have been isolated and characterized as principal regulators correlated with the process of cell elongation. In darkness, at least five classes of plant hormones mediate the process of hypocotyl growth. GA, brassinosteroids (BR) and auxin can promote hypocotyl elongation via downstream actuators, whereas, ethylene and cytokinin inhibit elongation of the hypocotyl (Nemhauser, 2008). Various light signals are received by diverse photoreceptors, transduced and amplified to trigger seedling photomorphogenic growth. The photoreceptors, such as cry, phy or phot mediate reduced hypocotyl elongation by inhibiting biosynthesis or action of the hormones GA, BR and auxin. Evidence also shows that in light conditions ethylene and cytokinin act to enhance hypocotyl elongation, rather than inhibiting it as they do in darkness. Other relatively isolated systems, such as the circadian clock and the ubiquitin system are also involved in the regulation of hypocotyl growth by their interaction with photoreceptors and plant hormone-related transduction pathways. Basic downstream actuators at the bottom of the plant hormone regulation system directly cause cell elongation. Xyloglucan endotransglycosylase, pectinase, expansin, cellulose-, and other cell-wall-related enzyme are involved in cell wall loosening. Aquaporins which regulate turgor pressure in cells, microtubule-severing katanin in microtubule orientation, and peroxidase mediation of hydroxyl radicals are also needed to help the process of cell wall relaxation. Furthermore, other environmental factors besides light also regulate the levels of ethylene and auxin in Arabidopsis. Low nutrition and high temperature result in longer hypocotyls because of

the elevation of ethylene and auxin concentrations, respectively. Although internal and external cues determine the final destination of hypocotyl growth, the elongation response is basically regulated by gibberellins, with the modulation of auxin and ethylene at the low hierarchy of signaling transduction.

Cotyledon Growth and Development in Arabidopsis

Cotyledons exist throughout the plant kingdom in gymnosperms, monocots, and eudicots (most dicot species). A distinct morphology of dicots, such as *Arabidopsis thaliana*, is that all the plants in this group contain two cotyledons. Cotyledons are radically different from true leaves in function. Cotyledons are formed during embryogenesis, at the same time as the root and shoot meristems, whereas true leaves are formed post-embryonically from the shoot apical meristem (SAM) (Tsukaya, Tsuge, and Uchimiya, 1994). After breaking of dormancy, seeds begin to develop in darkness characterized by heterotrophic growth. Cotyledons are the principal storage organs providing not only nutrients such as proteins, oil and starch but also hydrolytic enzymes including proteases, lipases and amylases during germination. Sensing the sun light, seedlings begin to photosynthesize within several hours, when the chloroplasts have differentiated in the cotyledons. In addition, morphological differences between cotyledons and leaves are easily observed, for example, the presence of trichome and stipule structures only on leaves.

The development of cotyledons in Arabidopsis is a complicated process, controlled by interactions between endogenous and environmental cues. In cells, gene hierarchies, programmed cell divisions, gene expression and signaling are united into a

gene-regulated network responsible for cotyledon development. The initiation of Arabidopsis cotyledons starts at the late embryonic globular stage or at the early heart stage. Outgrowths of cotyledons on either side of the future shoot apex give a bilateral symmetry to the embryo. Later, a clear boundary between the developing SAM and cotyledon primordia, visible in the apical region, is caused by the differential expression of several important genes such as Shoot Meristem Less (STM) and Cup-Shaped Cotyledon (CUC), KNAT6, miR164, TCP, DRN/DRNL (Aida, Ishida, and Tasaka, 1999; Belles-Boix et al., 2006; Chandler, Cole, and Werr, 2008; Koyama et al., 2007; Laufs et al., 2004). Cotyledon polarity during cell differentiation is established when the adaxial side derived from the embryo apical central domain and the abaxial side arise from the peripheral embryo domain. Three gene families, which are the class iii HD-ZIP, KANADI and YABBY, have been found to promote this polarization (Emery et al., 2003; Eshed et al., 2001). Auxin signaling is critical for cotyledon development, with the new primordia being initiated at sites where the auxin concentration is the highest. Furthermore, cotyledon growth is also influenced by some environmental cues. Cold weather, low nutrients and low light inhibit photosynthesis in cotyledons and limit cotyledon expansion.

Shade Avoidance

The spectral distribution of daylight measured by the use of a spectroradiometer is very complex. For many theoretical considerations, choosing a daylight quality parameter, the calculated ratios between specific pairs of wavelengths, is required to simplify spectral data. Because of the unique photoreversibility and specific absorption

spectrum of phytochrome, a dynamic equilibrium of the Pr and Pfr form is established in natural light environments, depending on the relative amounts of R and FR. Therefore, the ratio of the photon irradiance in the R region, to that in the FR region (termed R:FR ratio) can be considered as an important parameter to determine light quality of natural environments. In practice, R:FR is often defined using the following standardized formula:

$$\text{R:FR} = \frac{\text{Photon irradiance between 655 and 665nm}}{\text{Photon irradiance between 725 and 735nm}}$$

As a simplified parameter, the R:FR ratio can be seen as a bridge between the spectral distribution of natural light and calculated Pfr/P_{total}, which relates directly to phytochrome activity. Experimental data has shown that the R:FR ratio is remarkably constant in a certain environment (Smith, 1983). Usually, the values of R:FR in daylight, at twilight, under a canopy and under water are 1.05~1.25, 0.65~1.15, 0.05~1.15 and 1.15~max, respectively. When daylight is either transmitted through or reflected from plant leaves, photosynthetic pigments in mesophyll cells selectively absorb R light but not much FR light, causing a significant reduction in R:FR under the canopy.

As non-mobile organisms, plants must compete for limited local resources, especially sunlight for photosynthesis, with their neighboring vegetation for survival. The shade avoidance syndrome (SAS) is a series of responses that plants undergo when growing under a vegetational canopy. Thses responses include elongation of stems and petioles, earlier flowering and increased apical dominance. Undoubtedly, SAS is a phytochrome-mediated response. Under a high R:FR ratio, SAS is suppressed by

additional active Pfr forms, whereas a low R:FR ratio promotes SAS resulting from the loss of active Pfr forms. When a reduction in R:FR under the canopy is perceived by phytochromes, several downstream bHLH transcriptional regulators, which are involved in the initiation of SAS, are rapidly accumulated in the nucleus, and eventually initiate SAS-associated morphological and metabolic changes. This process will be considered further in the last section of this chapter.

Flowering

Flowering is also one of the most important checkpoints during plant development. During the floral induction process, the shoot apical meristem is transformed into the floral meristem, which generates the sepals, petals, stamens, and carpels of the flower. Early studies of flower timing mainly focused on daylength-induced flowering, and plants were divided into three categories: short day plants, long day plants and daylength neutral plants. After that, plant biologists found a graft-transmissible substance, which was named florigen, produced in the leaves, which acted as a stimulus to promote flowering. By using the model plant *Arabidopsis thaliana* and screening for late or early-flowering mutants, dozens of 'flowering time' loci were identified (Koornneef, 1991). The transcriptional regulator CONSTANS (CO) is one of the core factors in the photoperiod pathway and the circadian clock. CO protein promotes flowering by initiating transcription of the *FLOWERING LOCUS T (FT)* and *TWIN SISTER OF FT* (*TSF*). *CO* mRNA expression is controlled by the circadian clock, and CO protein stability is regulated by interaction with photoreceptors in plants including phytochromes. During the night, the CO mRNA level remains high, but without interaction with

photoactivated photoreceptors, most CO protein undergoes proteolysis. During the day, CO protein reaches a relatively higher level at twilight to promote flowering. Among the photoreceptors, phytochromes can activate or inactivate this CO-mediated pathway in response to changes in day length.

To date, ~180 genes related to flowering have been isolated in Arabidopsis on the basis of loss-of-function mutations and transgenic lines. The timing of floral induction is controlled by complicated regulatory networks, consisting of six major pathways: the vernalization and autonomous pathways, the photoperiod pathway and circadian clock, the gibberellin pathway, the ambient temperature pathway, the age pathway, and the meristem responses (Fornara, de Montaigu, and Coupland, 2010). Finally, the six pathways converge to regulate a small number of "floral integrator genes", including *FT* and *SUPPRESSOR OF OVEREXPRESSION OF CONSTANS 1 (SOC1),* which are both in charge of rapid promotion of floral development.

Phytochrome Genes in Higher Plants

Phytochrome Sequence Isolation and Identification

The detection and analysis of phytochrome gene expression was first accomplished when purified homogenous oat phytochrome was obtained from dark-grown tissue, followed by the generation of anti- oat phytochrome antibodies. Then, two mRNA expression pools of oat phytochrome between dark-grown tissue and light-grown tissue were observed, showing that translatable phytochrome mRNA was predominant (~5×10^{-3} % of total poly(A)-RNA) in etiolated oat seedlings but reduced rapidly (>95%)

within 2 hr R treatment (Colbert, Hershey, and Quail, 1983). By differential screening of a cDNA library, the oat phytochrome cDNA was successfully isolated and characterized and found to encode an 1128 amino acid sequence protein (Hershey et al., 1985; Hershey et al., 1984). Later, the first genomic sequence of the oat *phyA3* gene was published in 1987 (Hershey et al., 1987).

After its discovery, phytochrome sequences gradually accumulated with the extensive survey of other species, including zucchini (Sharrock, Lissemore, and Quail, 1986), pea (Sato, 1988), rice (Kay et al., 1989), corn (Sullivan, Christensen, and Quail, 1989) and Arabidopsis (Clack, Mathews, and Sharrock, 1994; Sharrock and Quail, 1989). It turned out designing hybridization probes according to the highly conserved amino acids around the chromophore attachment site was an efficient approach for phytochrome cloning in higher plants. Identification and characterization of multiple *PHYs* inaugurated a new era in phytochrome research at the molecular level and led to the establishment of a one to one relationship between phytochrome structure, activity and response.

A Small Gene Family in Higher Plants. Hershey et al. (1985) demonstrated that at least four oat phytochrome genes are present in the oat genome by use of polymorphic site analysis of restriction endonuclease digestion (Hershey et al., 1985). Five gene members (*PHYA*-*PHYE*) in Arabidipsis were then successfully identified from the *Arabidopsis* genome (Sharrock and Quail, 1989). Small *PHY* gene families are also widely distributed in other flowering plant species including the dicots tomato, potato, tobacco, pea, soybean, poplar, and cotton, and the monocots sorghum and rice

(Abdurakhmonov et al., 2010; Mathews, 2006a). Recent whole genome sequencing has confirmed the wide phylogenetic distribution of these *PHY* gene families.

Type I and Type II Phytochromes in Higher Plants. Previous evidence showed that two distinct phytochrome pools existed in a partially purified phytochrome mixture from light-grown pea seedlings, one of which was rapidly degraded and the other was more light stable (Abe et al., 1985; Furuya, 1989). Purified oat phytochrome (oat phyA) from etiolated seedlings was observed to degrade rapidly in the light, as a result of product destruction occurring at both the transcriptional and translational level (Colbert, Hershey, and Quail, 1983). Similar to oat phyA, any light-labile phytochrome can be called type I phytochrome. With high sequence similarity, the first deduced phytochrome in Arabidiopsis, which also belongs to type I phytochrome, is named phyA. However, the other four candidate phytochrome genes from Arabidopsis (designated *PHYB-E)*, which appear to be stable at the transcriptional and translational level in the light, are called type II phytochromes.

Type I/type II groups of phytochromes show differences in biochemical and spectral aspects, but more importantly, they function in both antagonistic and complementary ways. PhyA and phyB are the two major phy species that exhibit distinct roles in response to far-red and red light, respectively. PhyA, which is predominant in dark-grown tissue, induces non-FR reversible very low fluence responses (VLFRs) for seed germination and *CAB* gene induction (Hamazato et al., 1997; Shinomura et al., 1996a) and FR-HIRs of hypocotyl elongation and anthocyanin accumulation (Nagatani, Reed, and Chory, 1993; Parks and Quail, 1993). Conversely, phyB-phyE, which are

predominant in light-grown tissue, principally mediate responses to continuous R irradiation, the environmental R/FR ratio, and end-of day FR treatments (Aukerman et al., 1997; Devlin, Patel, and Whitelam, 1998b; Devlin et al., 1999; Reed et al., 1993b).

Plant Phytochrome Evolution

All plants are believed to derive from an eukaryotic cell that acquired a photosynthetic cyanobacterium as an endosymbiont. Plants consist of three groups of species: the glaucophytes (freshwater algae), rhodophytes (red algae), and the green plants (which include green algae and land plants) (Bowman, Floyd, and Sakakibara, 2007). Land plants comprise two major groups: bryophytes (liverworts, mosses and hornworts) and vascular plants (lycophytes, ferns, gymnosperms, basal angiosperms monocots and eudicots). When *PHY* gene sequences became available and the data accumulated, research began using comparative tools to address some of the major questions about phytochromes in plants, including the occurrence of phytochrome divergence, conservation of phy function, and potential structural/functional specificity among different phytochromes.

The genetic phylogeny suggests that diversified family members of phytochromes result from a single *PHY* gene lineage (Mathews, 2010). Amino acid sequence alignment showed ~50% identity shared among the five Arabidopsis phytochromes, with higher identity (~80%) shared between phyB and phyD representing their recent gene duplication (Clack, Mathews, and Sharrock, 1994). The five Arabidopsis genes are assigned to four subfamilies: *PHYA*, *PHYB/D*, *PHYC* and *PHYE*. The monocot plants sorghum and rice both contain a total of three *PHY* genes, which fall into the *PHYA*, *B/D*,

and C categories (Basu et al., 2000). Full or partial nucleotide sequences in all major subclasses of flowering plants, which include gymnosperm *PHY* (*PHYN*, *PHYO*, and *PHYP*), and sequences from ferns, lycophytes, and mosses, were analyzed, demonstrating that, almost all the tested genes fit into one of *PHYA*, *PHYB/D*, *PHYC*, *PHYE* gene lineages, except the *PHYE* lineage is missing in monocots (Mathews and Sharrock, 1997).

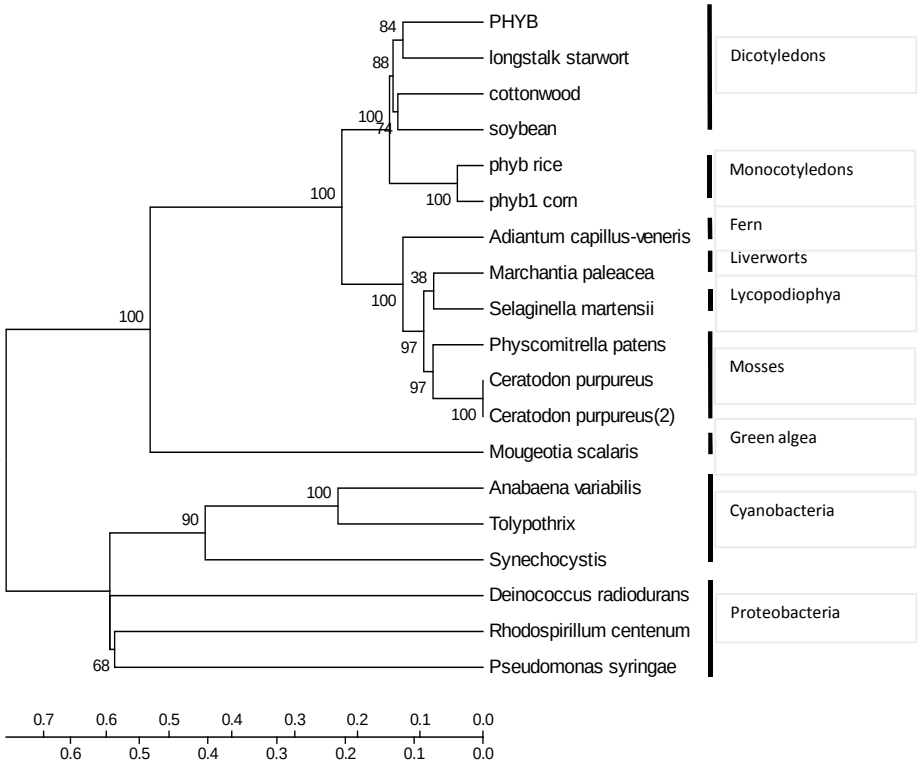


Figure 1.2. Molecular phylogeny of the phy N-terminus. 809 protein sequences which are correlated to the conservative phyB N-terminus were selected from NCBI database, and grouped them into 7 different categories. 19 sequences were chosen for the next step of alignment. The phylogenetic tree was generated using the neighbor-joining algorithm method in MEGA software. Bootstrapping with 500 replicates was used as a test for inferred phylogeny and distance values were counted as 0.913.

Early phylogenetic surveys successfully moved the occurrence of *PHYA/PHYB* spilt ahead to the divergence of seed plants and sporophytes (Mathews and Sharrock, 1997; Sharrock and Quail, 1989). Strong evidence with an increasing number of new data showed that *PHYN*, *PHYO*, and *PHYP* are the gymnosperm orthologs of angiosperm *PHYA*, *PHYC*, and *PHYB* in a recently deduced phytochrome peptide tree (Mathews, 2010). The tree suggested that the split between *PHYA* and *PHYB* occurred ~330 to 365 million years ago, when the seed plant ancestor began to diverge into angiosperms and gymnosperms (Figure 1.2). After that, the orthologous *PHYN/A*, *PHYO/C*, *PHYP/B* have been undergoing evolution independently. In gymnosperms, duplication of *PHYN*, *PHYO*, and *PHYP* are often seen (Mathews, Clements, and Beilstein, 2010). In angiosperms, *PHYA* and *PHYB* are duplicated more unlikely than phytochromes in gymnosperms, and their duplication sometimes generates a novel functional copy. For example, an early duplication of phyB led to the independently evolving *PHYE* lineage (Mathews, 2006b).

Phytochrome: Inference of Protein Function from Protein Structure

The unique spectral photosensitivity of phytochrome was observed upon its discovery (Butler et al., 1959). Light responses such as germination, de-etiolation and photoperiodism in several different plant species, were shown to share the same action spectra with response maxima near 660 and 730nm. These results indicated that a reversible photoreaction might be present in plants, regulated by two photoconvertible isoforms of a photoreceptor.

Early structural knowledge of phytochrome is derived from the studies on highly purified phytochrome proteins from dark-grown oat tissues. Native oat phytochrome is a soluble homodimer which is made up of two 124-kD identical subunits. Each subunit consists of two components: a tetrapyrrole chromophore and a polypeptide chain (Jones et al., 1986). Oxidative degradation analysis showed that the ring A of the chromophore is covalently attached to a cysteine residue of the polypeptide through a thioether linkage. Meanwhile, Lagarias and Mercurio showed that oat phytochrome, which is not an ideal globular protein, contains two dividable domains linked by a protease-sensitive hinge region (Lagarias and Mercurio, 1985). Using electron microscopy, researchers visualized the "Y' shaped Pr form of phytochrome, demonstrating the 70-Kd N-terminal domain bears the chromophore, whereas the smaller 55-Kd C-terminal domain binds with itself to form the dimer (Jones and Erickson, 1989; Romanowski and Song, 1992).

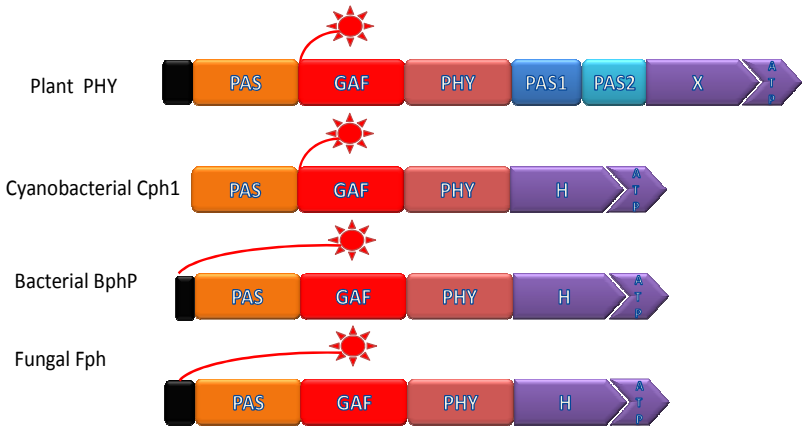


Figure 1.3. Schematic architecture of representatives of phy-type photoreceptors in plants, cynobacteria, bacteria and fungi. Black box, N-terminal extension. H-ATP, histidine kinase domain with ATP binding site. It is worth noting that the chromophore is attached to a cysteine residue either in the GAF domain in both PHY and Cph1, or in the N-terminal extension in BphP and Fph. X in plant PHY is non-functional histidine kinase-related domain.

The chromophore binding region of the first cloned phytochromes was highly conserved, and its coding sequence was used as a probe to explore novel phytochrome genes from a small range of higher plant species such as lettuce, squash, cauliflower, oat and mustard. Over 30 years, the search has been greatly expanded from flowering plants into green algae, photosynthetic bacteria (cyanobacteria and purple bacteria), nonphotosynthetic eubacteria and even fungi. Multiple sequence alignment analysis showed that phytochromes constitute a superfamily of photoreceptors with a photosensory bilin-binding pocket (BBP), which comprises a PER/ARNT/SIM domain (PAS), a cGMP phosphodiesterase/adenylate cyclase/FhlA domain (GAF), and a phytochrome-specific GAF-related domain (PHY), as a common feature shared by almost all phytochrome forms (Sharrock, 2008). Based on phylogenetic comparisons of the GAF domain alone, five distinct branches of the phytochrome superfamily have emerged which encompass the plant Phys (Phys), the cyanobacterial Phys (Cphs), the bacteriophytochrome photoreceptors (BphPs), the fungal Phys (Fphs) (Figure 1.3), and a large group of unclassified phy-like proteins.

The Chromophore

Biologically active tetrapyrrole cofactors in organisms have essential catalytic functions to support life systems. In higher plants, mainly four classes of tetrapyrroles are present: heme (oxidative metabolism and oxygen transport), biliverdin (photo signaling), chlorophyll (photosynthesis) and siroheme (sulfite and nitrite assimilation). In plants, plastids are the major sites of tetrapyrrole biosynthesis. As shown in Figure 1.4, all of the tetrapyrroles are derived from a common biosynthetic pathway, sharing four initial

synthetic steps: decarboxylation, methylation, metal ion chelation and porphyrin ring oxidation (Tanaka and Tanaka, 2007). Biosynthesis of bilins begins with the oxidative cleavage of heme to Biliverdin IXα (BV) by a heme oxygenase, and BV is further reduced and isomerized to yield phytochromobilin (PΦB) in plants or phycocyanobilin (PCB) in cyanobacteria.

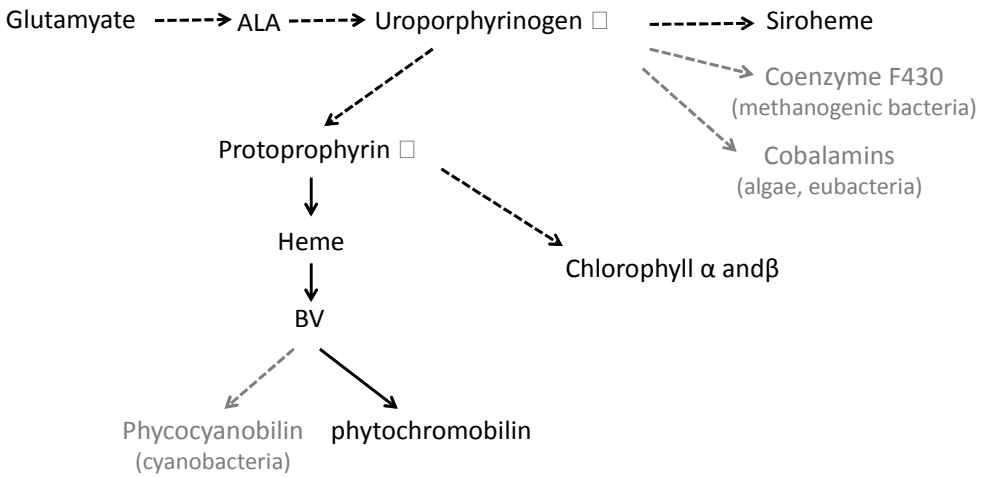


Figure 1.4. Biosynthesis of tetrapyrroles in higher plants. ALA, 5-aminolevolinic acid. BV, Biliverdin IXα. The gray fonts represent pathways that do not exist in higher plants, but are more important in other species.

The phytochrome chromophore is an open-chain linear tetrapyrrole, which absorbs a specific range of light wavelengths and induces subsequent phytochrome photoconversion. In higher plants, the chromophore is PΦB, which is covalently attached to the protein through a thioether link at a cysteine positioned at amino-acid residue 374 (numbering for oat phyA). Almost all phy-related molecules photoconvert between R- and FR-absorbing conformations. However, one of the cyanobacterial phytochromes, the well characterized *Synechocystis* Cph1 Ccas, which attaches PCB as the chromophore in

its unique GAF domain (Figure 1.3), causes reversible photoconversion between green- and red-absorbing forms (Hirose et al., 2008). BphPs, the largest number of phys in bacteria, bind BV as their chromophore and absorb red/far-red light for photoconversion similar to plant phytochromes. However, the BV attachment site of BphP phys is located at the end of the BphP N-terimnus, rather than in the GAF domain (Lamparter et al., 2002). According to sequence similarity, the architecture of Fphs is closely related to that of BphPs, showing the same chromophore located at the same position. Assembly of phytochrome apoprotein and chromophore occurs spontaneously *in vivo*, indicating that the phytochrome apoproteins contain inherent chromophore lyase activity. According to this property, recombinant phytochromes generated in planta or *in vitro* with the addition of chromophore are spectrally photoreversible and biologically active with either phytochromobilin or phycocyanobilin attached.

The N-terminus Three-dimensional Structures of Phytochrome

The first phytochrome-related crystal structure (1ZTU) was deduced in 2005 (Wagner et al., 2005), from a PAS/GAF bidomain (DrBph1-PAS/GAF or DrBph1-CBD) of a bacteriophytochrome DrBph1 from *Deinococcus radiodurans* in the Pr ground state. This Pr structure shows that the BV chromophore is partially cradled in deep pocket of the GAF domain, and the thioether linkage is generated between a conserved cysteine upstream of the PAS domain and the A-ring C3 vinyl side chain of BV. The most striking feature of this 3D structure is a deep trefoil knot which is formed at the interface between PAS and GAF, suggesting it may strengthen and stabilize the bidomain in signaling.

Unexpected dimeric interactions existing in the BBP were also seen in a subsequent DrBph1-PAS/GAF high resolution structure and a PAS/GAF/PHY structure from *Synechocystis* Cph1 (Esteban et al., 2005; Strauss, Schmieder, and Hughes, 2005; Wagner et al., 2007). Because the PHY domain as part of the BBP pocket is indispensable in photoperception, the crystal structures of the Pr state Cph1 of *Synechocystis* 6803 (2VEA) and the Pfr state PaPph from *Pseudomonas aeruginosa* (3C2W), have also included the PHY domain (Essen, Mailliet, and Hughes, 2008; Yang, Kuk, and Moffat, 2008). An interesting feature of these two structures is an elongated, tongue-like projection protruding from the PHY domain into the PAS/GAF lobe, in which the BV chromophore can be completely sealed in the BBP pocket both in the Pr state and in the Pfr state. This indicates that the tongue may play an important role in the Pr/Pfr transformation, the Pfr formation acceleration, and stability improvement in the Pfr state.

Pr/Pfr Photoconversion Based on Crystal Structures, 2VEA and 3C2W. The mechanism of Pr/Pfr photoconversion has been partially unveiled by comparisons of the conformational structures 2VEA and 3C2W. The previously solved BV chromophore structure within 1ZTU is a 5Zs/10Zs/15Za (ZZZssa) configuration, rather different from the predicted configuration from Raman spectroscopy. This ZZZssa configuration was re-confirmed in the crystal structures of the Bph RpBphP3-PAS/GAF (Yang et al., 2007) and in the Cph1-PAS/GAF/PHY, both of which are in the Pr state. The PaPph-PAS/GAF /PHY Pfr structure (3C2W) indicates that the active Pfr configuration is ZZEssa according to

hydrogen bonding interactions between the D ring of the chromophore and the surrounding residues. Therefore, it can be explained logically that Z to E isomerization of the double bond between C15 and C16 occurs in the Pr to Pfr photoconversion.

Several phy amino acid residues are critical for phytochrome photoconversion. The study of the crystal structure 3C2W indicates that direct interactions among Asp-194, Tyr-250, and Ser-459, with the chromophore at the interface of the GAF and PHY domains, benefit light-induced Pr to Pfr photoconversion. Meanwhile, several aromatic residues such as Tyr-163 and Tyr-190, interact with the D ring of the chromophore in the aim of stabilizing the two distinct Pr and Pfr configurations. The gain-of-function phyB Y276H mutant and the Cph1 Y176H mutant, which behave as a constitutive Pfr, confirm this conclusion (Su and Lagarias, 2007).

Pr/Pfr Photoconversion Based on NMR Structures, 2KOI and 2KLI. To understand in more detail the phytochrome photoconversion, two high-resolution NMR-based structures (a Pr form 2KOI and a Pfr form 2KLI) were obtained from a 20kDa GAF-domain of the "*SyB-Cph1*" phytochrome from the thermotolerant cyanobacterium *Synechococcus* OSB'(Ulijasz et al., 2010). Without interaction with the PAS domain, evidence showed that this GAF domain is able to bind PCB and undergo photoconversion smoothly from the Pr state into the activated Pfr state. As expected, the common features in these new NMR-based structures are deduced to be similar to these of the former X-Ray data, except for some differences in chromophore rotation. NMR spectroscopy showed that the Pr chromophore has more freedom in the binding pocket, and during photoconversion, the A pyrrole ring but not the

D ring rotate nearly 90° around the C4=C5 bridge (Cornilescu et al., 2008). Previous photochemical studies and NMR spectra of Cph1-PAS/GAF/PHY were also consistent with the result of the A ring rotation (Inomata et al., 2009; Seibeck et al., 2007; Strauss, Hughes, and Schmieder, 2005; van Thor et al., 2006). Several key residues have also been determined on the basis of the models. Phe 82, Tyr54, Asp86 and Tyr142 interact with the A and D rings of the chromophore to direct the subsequent protein rearrangement.

The C-terminus

As mentioned above, almost all phytochromes contain two relatively independent domains: a N-terminal photosensory domain and a C-terminal regulatory domain. The architecture of the N-terminal domain (or more specifically the BBP region) determines the spectral properties of the molecule and the phytochrome classification. The C-terminus contains a histidine kinase region (HKD) in prokaryotic and fungal phys and an "HKD-related" region in plants and is also critical for phytochrome structural and mechanical functions. One hypothesis has been partially accepted that microbial phytochromes function as light-regulated protein kinases in their entireties (Yeh et al., 1997). Most microbial phytochromes are typical two-component histidine kinases (TC-HKs), which are identified as dimeric protein kinases in bacteria for environmental adaptation. Sensing light signals by the microbial BBP domain, those phytochromes autophosphorylate themselves on a histindine side chain via the HKD, and transfer phosphate to an aspartate side chain on their downstream factors directly or through a response regulator (RR) protein to induce responses. The RcaE protein was the first

identified microbial phytochrome in the cyanobacterium *Fremyella diplosiphon,* showing a classic TC-HK phosphorelay in its signal transduction (Yeh et al., 1997). Bioinformatic analysis showed that the C-termini of plant phytochromes also possess a histidine kinase-related domain (HKRD),which cannot perform as a TC-HK because several key residues are missing in the TC-HK typical sequence (Krall and Reed, 2000a). Although still controversial, plant phytochrome has been shown to contain serine/threonine kinase activity and phosphorylation may play an important role in plant phytochrome signaling (Han et al., 2010c; Yeh and Lagarias, 1998).

The Three-dimensional Structures of Phytochrome and Signaling

Although no 3D structural information on the C-terminal region of phytochromes has been obtained yet, a full-length PaBphB structure was simulated by Yang et al (2007). through two crystal structures: the PaBphP-PAS/GAF/PHY dimer structure and a homologous sensor HK structure (2C2A), deduced from the thermophile *Thermotoga maritime* (Marina, Waldburger, and Hendrickson, 2005). Based on secondary structure predictions, a long continuous helix links the regions between the PHY and HK domains, indicating the dimer interface likely extends from the chromophore holding region into the HK domain. Consistent with the geometry of *in trans* phosphorylation of phytochromes, the phosphoacceptor histidine residue in one monomer is orientated toward the ATP binding site of the kinase domain from the other monomer (Yang et al., 2007).

When sensing light, the phy chromophore is activated and begins to rotate within the bilin-binding pocket. Although it is still controversial which one, the A ring or the D ring, is involved in the rotation, it may not be a real problem because binding of PΦB or PCB might cause different photochemical properties (Rockwell et al., 2009). Ring rotation induces the automatic adjustment of several contact sites between the chromophore and key chromophore-surrounding amino acid residues. Subsequently, a series of conformational changes result in the reorientation of the domains of phytochrome to facilitate the Pfr formation. The reorientation may also influence intermolecular GAF/GAF dimerization and intramolecular GAF/PHY interaction. When a cascade of structural rearrangements has spread along the dimeric backbone throughout the entire phytochrome, the photoconversion event is predicted be complete. Ultimately, the relatively stable Pfr form is generated with an altered biochemical output and a dramatic FR shift in absorption. Moreover, some phenomena such as chromophore protonation and deprotonation also occur in the process of photoconversion (Hughes, 2010), but the mechanisms are still unclear. In microbial phys, with activation of the histidine kinase region in the C-terminal output module, the phytochrome dimer undergoes (auto)phosphorylation, and triggers a series of reactions by transferring its phosphate to its downstream factors. In contrast to the microbial phy HKRDs, how plant phy Pfr signal is not resolved and is the subject of the following two sections.

Conclusion

The structure–function relationship in plant phytochromes can be explored intensively at three levels. In the early days, scientists began exploring the function of

phytochrome using purified oat and rye phytochromes as materials. Subsequently, structure/function studies have prevailed through genetics and genomic approaches when the *PHY* genes were deduced in Arabidopsis. In 2005, the first resolved crystal structure of bacterial phytochrome has lighted the way of actual 3D structural/functional research. Here, I have summarized our current understanding of phytochrome 3D structure. In the future, more 3D structures of phytochromes, especially plant phytochromes, need to be generated, and coupling of computer simulation, visualization of phytochrome function and signaling spacially and temporally would be expected.

Phytochrome Nuclear Translocation and Degradation

In plants, type I phyA controls VLFRs and FR-HIRs, whereas type II phytochromes mediate LFRs and R-HIRs. To fine-tune these light-induced responses, phytochrome acts like a light switch that turns on/off light signaling at the right time and place. Recent evidence shows that phy dynamic actions, such as distinct nucleo-cytoplasmic partitioning and rapid protein degradation, correlate tightly with these diversified phytochrome-mediated responses. In this section, mechanisms of phytochrome intracellular distribution and degradation will be mainly focused on and discussed in detail, largely based on the studies of *Arabidopsis* seedling de-etiolation.

Phytochrome Nucleo-cytoplasmic Transport

Until the 1990s', phytochrome was thought to exist only as a cytosolic protein, largely based upon early immunolocalization of native phytochrome in dark-grown seedlings. Phy light-dependent nuclear localization was first documented in 1996,

showing that endogenous phyB was detectable in isolated nuclei from *Arabidopsis* leaves (Sakamoto and Nagatani, 1996). The result was confirmed by direct observation of light-dependent phytochrome translocation, demonstrating that full-length phytochrome:GFP fusion protein molecules were imported into nuclei and then aggregated into speckles (nuclear bodies) in light quality- and quantity- dependent manners (Kircher et al., 2002; Kircher et al., 1999; Yamaguchi et al., 1999).

PhyA Localization. In darkness, native phyA is present exclusively in the cytosol (Kircher et al., 2002). A single, brief FR-, R- or B- pulse can successfully induce rapid nuclear translocation of phyA within several minutes. Subsequently, phyA gathers together and forms early nuclear bodies (NBs). In addition, a red pulse also promotes phyA spots in the cytosol, which are referred to as sequestered areas of phytochromes (SAPs), a designated place for phytochrome ubiquitination and degradation. High light intensity results in formation of large-size NBs (Kircher et al., 2002). Accumulation of phyA NBs in the nucleus reaches a peak after exposure to 10 min W light, and then drops markedly if the treatment is continued. However, continuous FR light needs a much longer time (approximate 2 h) to promote the highest level of phyA in the nucleus and maintains the level with prolonged treatment. Thus, it is possible that different sizes of NBs may directly correlate with diverse modes of phyA action.

Recent studies have revealed the general cellular transportation machinery for phyA movement to the nucleus in response to continuous FR. As shown in Figure 1.5, nuclear accumulation of phyA requires two small phyA-specific factors, FAR-RED ELONGATED HYPOCOTYL 1 (FHY1) and FHY1-LIKE (FHL) (Genoud et al., 2008;

Hiltbrunner et al., 2006; Hiltbrunner et al., 2005; Rosler, Klein, and Zeidler, 2007). Two transposase-related transcription factors, FHY3 and FAR1, indirectly affect phyA nuclear accumulation by controlling *FHY1* and *FHL* transcription (Yang et al., 2009). FHY1 and FHL are expressed and evenly distributed in cells in the dark. Upon exposure to continuous FR light, activated phyA Pfr directly binds to the C-terminal phyA binding domain (ABD) of the FHY1/FHL complex. The unmasked nucleus localization sequence (NLS) of FHY1/FHL leads the complex to translocate from the cytosol into the nucleus, and there, activated phyA aggregates into NBs and induces phyA-mediated FR-HIRs. A phyA:NLS fusion protein, although localized in the nucleus constitutively, fails to induce any of the responses in the dark, indicating the necessity of phyA photoactivation (Genoud et al., 2008).

In the past, phyA Pfr had been believed to be the only biologically active form in the FR-HIRs (Schfer, Schmidt, and Mohr, 1973; Wall and Johnson, 1983). Based on the theory of phytochrome photoconversion, high level FR light is proposed to suppress the transition from Pr to Pfr and therefore to produce fewer active Pfr phytochromes than low level FR. This observation conflicts with the evidence that the FR-HIRs are FRc fluence rate-dependent. A second short-lived "active component" was hypothesized to direct FR-HIRS during the process of photocycling from Pfr back to Pr (Shinomura, Uchida, and Furuya, 2000). Whether the photoconverted Pr (Pr*= cytosolic Pr → Pfr → nuclear Pr) of phyA or some transient intermediate phyA form(s) is responsible for the induction of the response is still unclear. One thing for sure is that Pr* is very stable in the FR light, because of the induction of large NBs in the nucleus. Shinomura et al. (2000)

hypothesized that phyA has two distinct mechanisms of photoperception, the photoirreversible VLFR mechanism and the FR-HIR mechanism. However, it is likely that these two phyA-mediated responses share one common mechanism, and this will be discussed at the end of this chapter.

Type II Phytochrome Localization. Observations of a phyB:GFP fusion protein expressed from the 35S promoter in the *phyB* mutant, were collected for the study of phyB nuclear translocation (Gil et al., 2000; Kircher et al., 2002). In the dark, phyB:GFP was mainly localized in the cytosol, but some fluorescence was always also detectable in the nucleus indicating that a small amount of phyB is constitutively nuclear. Under R light conditions, the movement of phyB:GFP into the nucleus was at least one order of magnitude slower than that of phyA:GFP. Further investigation showed that the NLS of phyB is located in the PAS region (594-917) of its own C-terminal domain (Chen et al., 2005). Therefore, phyB translocation appears to be a quite simple process in that light-induced conformational change of phyB causes the exposure of a phyB NLS protein sequence and allows phyB to transfer into nucleus. The amino acid sequences that comprise this phyB NLS have not been identified. Accumulation of nuclear phyB also results in the formation of NBs, of which the size and number depend on light quality, intensity and duration (Chen, Schwab, and Chory, 2003; Kircher et al., 2002; Yamaguchi et al., 1999). Upon transfer back into darkness, light-induced phyB-containing NBs start to dissolve, and disappear in about 12 h (Kircher et al., 2002). Hence, FRc light appears to effiectively reverse the process of phyB translocation and NB formation. A single pulse of R, FR or B light cannot induce detectable NBs of phyB:GFP.

GFP fusions to phyC-phyE are mainly localized in the cytosol, but still some of these proteins diffuse into nuclei in darkness. Upon white light (W) irradiation, phyC-GFP and phyE-GFP translocation kinetics are similar to the pattern of phyB-GFP movement into the nucleus. Interestingly, although phyD-GFP can be imported into the nucleus, the number of phyD NBs is maintained in a low steady state level even in a prolonged W light treatment (Kircher et al., 2002). Hence, the various type II phys in Arabidopsis all show some presence in the nucleus as Pr and some extent of light-induced movement into the nucleus, but may vary in the specifics of these pathways.

The Types and Stages of NBs

Early and Late Phytochrome NBs. Previous studies have shown that phyA NBs are formed within minutes, but the formation of phyB NBs is much more slower, in about 1.5-2 h after irradiation (Genoud et al., 1998; Kircher et al., 1999; Sakamoto and Nagatani, 1996). With improved techniques, Kircher et al. (2002) observed that type II phytochromes (phyB-D) in fact gathered into small "early" NBs very quickly within 2-3min in dark-grown seedlings when exposed to red light. These early type II phytochrome NBs were numerous in the nucleus and, after 10-15 min, gradually dissolved and finally totally disappeared. Under long-term continuous R light, the late-formed fewer and larger NBs of type II phytochromes appeared in 2-3 h. Components of the early NBs are likely to be different from the late ones, because phyA and some transcription factors which localized to early NB's such as PIFs are rapidly degraded in the light (Clack et al., 2009).

Four Stages of NB Formation. The dynamics of NB formation can be roughly divided into four stages by the observation of phyB:GFP translocation (Chen et al., 2003). At low fluence rates, nuclear phyB molecules which are translocated as a Pfr/Pr heterodimer, hardly form NBs. Higher R light fluences trigger NB formation progressively, leading to an increase in the number and size of NBs as well as NB activity by conversion into Pfr/Pfr dimers.

Stage 1: When Pfr/P_{total} is no more than 10%, phytochrome usually distributes in both the cytoplasm and nucleus, and apparent NBs can hardly be seen in the nucleus.

Stage 2: When Pfr/P_{total} is approximate 15%, there are small NBs, similar to the early NBs, in the nucleus under R.

Stage 3: When Pfr/P_{total} is about 24%, larger but fewer NBs show up in the nucleus.

Stage 4: When Pfr/P_{total} is 50% or above, only a few large NBs are seen in the nucleus, which are the late NBs as previously described.

NBs---the Sites for Protein Degradation

Several point mutations in *PHYA* and *PHYB* which do not affect nuclear translocation, result in phytochrome hyposensitivity and failure of NB formation (Chen, Schwab, and Chory, 2003; Chen et al., 2005; Kircher et al., 2002). This observation suggests that NB formation is correlated with phytochrome-induced signaling. Phytochrome NBs have been proposed to be the locations for protein degradation, because signaling factors such as phyA and PIF3 can directly interact with COP1 (an E3-ubiquitin ligase) in the early NBs (Al-Sady et al., 2006; Bauer et al., 2004; Seo et al., 2004). A new class of photomorphogenetic gene, *HEMERA* (*HMR*), was screened and

identified as being deficient in NB formation by mutagenesis of phyB-GFP seed lots (Chen et al., 2010c). The *hmr* mutant displays an etiolated phenotype under continuous R light with the phenomenon of NB destruction. Further investigation suggests HMR is required for the degradation of phyA, PIF1, and PIF3 in the NBs, which gives direct evidence that NBs play an important role in both light signaling and protein turnover.

Ubiquitin/Proteasome-mediated Proteolysis

The ubiquitin-proteasome system (UPS) is essential for eukaryotic organisms in regulating cellular signaling pathways by selective proteolysis of key regulatory proteins (Vierstra, 1996). The conserved ubiquitin/proteasome pathway begins with the ATP-dependent recognition and linkage between a ubiquitin polypeptide and a ubiquitin-activating enzyme E1. Ubiquitin is then transferred by E1 to a ubiquitin conjugating enzyme E2 and from there to a ubiquitin ligase E3. An E3 liagase can specifically recognize its substrate protein and conjugate a ubiquitin or a synthesized chain of ubiquitin to it. Subsequently, the ubiquinated substrate is shuttled into the 26S proteasome for degradation.

A series of pleiotropic Constitutive Photomorphogenic/De-etiolated/Fusca (COP/DET/FUS) proteins in the *Arabidopsis* UPS have been gradually characterized in seedling photomorphogenesis (Castle and Meinke, 1994; Chory et al., 1989; Deng, Caspar, and Quail, 1991; Sullivan, Shirasu, and Deng, 2003). Evidence shows that CONSTITUTIVELY PHOTOMORPHOGENIC1 (COP1), COP1-SUPPRESSOR OF PHYA (SPA), CULLIN4 (CUL4), CUL4-Damaged DNA Binding Protein1 (DDB1), DDB1 binding WD40 (DWD), RING-BOX1 (RBX1), Regulator of Cullins 1 (ROC1),

De-etiolated 1 (DET1) and other COP proteins are all involved in the COP/DET/FUS system (Chen et al., 2010a). These proteins are known to function in the process of proteasomal degradation in photomorphogenesis, and can be separated into three major entities: the COP1-SPA complexes, the COP9 signalosome (CSN), and the CDD complex (COP10, DDB1, and DET1). A working model of the proteolysis mechanism in photomorphogenesis has been proposed recently (Chen et al., 2010a). To direct the light-triggered degradation of downstream factors, two functional E3 ligase complexes, RBX1-CUL4-CDD and RBX1-CUL4-DDB1-COP1-SPA in Arabidopsis, are regulated by CSN complex-mediated rubylation and derubylation. A connection between these two E3 ligases is expected.

PhyA Degradation

Phytochrome destruction was first discovered in 1959, and well described in the 1970s. This work showed that after 3 h R irradiation, the concentration of *Avena* phytochrome drops to about 20% of its dark level, and eventually arrives at a new steady state at 1-3% of the initial level (Sage, 1992; Schafer, Lassig, and Schopfer, 1975). In Arabidopsis, phyA drops from original 85% of total phytochrome in etiolated seedlings to only 5% in de-etiolated seedlings (Sharrock and Clack, 2002). Although there is a 2-fold decrease of *PHYA* transcripts in the light, phyA destruction largely results from regulated protein degradation.

Ubiquitin/Proteasome-regulated PhyA Proteolysis. The molecular mechanism of the R-induced phyA rapid degradation has been partially elucidated to date. The basic E3

ligase COP1 specifically recognizes and ubiquitizes phyA (Seo et al., 2004). A nuclear SPA protein can directly bind to COP1 to form a COP1/SPA E3 complex which improves phyA recognition and later degradation (Hoecker, 2005; Laubinger, Fittinghoff, and Hoecker, 2004; Saijo et al., 2008a). Other photoreceptors, such as phyB, cry1 and cry2 (Wang et al., 2001; Yang, Tang, and Cashmore, 2001), and key transcription factors, such as LAF1, PIF3 and HY5(Khanna et al., 2004; Saijo et al., 2003; Seo et al., 2003), are also recognized and degraded by the COP1/SPA complexes. This indicates that efficient desensitization of phyA signaling may require the UPS blocking of several adjacent signal transduction pathways.

Upon exposure to R light, photo-activated phyA is targeted to be rapidly degraded, although phyA Pfr moves into the nucleus, while COP1 moves into the cytoplasm from the nucleus (Wu and Spalding, 2007). The rapid degradation process is also affected by light-induced phyA phosphorylation (Figure 1.5). Phytochrome contains apparent serine/threonine kinase activity, which can autophosphorylate itself or phosphorylate other substrates such as PKS1, Aux/IAAs, and crytochromes (Ahmad et al., 1998; Colon-Carmona et al., 2000; Fankhauser et al., 1999a; Yamaguchi et al., 1999). On the other hand, phytochrome may also be phosphorylated and dephosphorylated by downstream regulators, including Flower-specific Phytochrome-associated Protein Phosphatase (FyPP), Phytochrome-associated Protein Phosphatase 5 (PAPP5), and Phytochrome-associated Protein Phosphatase Type 2C (PAPP2C) (Kim et al., 2002; Phee et al., 2008; Ryu et al., 2005). (Auto)phosphorylated phyA preferentially interacts with the COP1/SPA complex and then is degraded quickly compared to unphosphorylated

phyA (Saijo et al., 2008b; Trupkin et al., 2007). Several autophosphorylation sites of phyA have been identified in the N-terminal extension (NTE) and the hinge regions of oat and *Arabidopsis* phyAs (Cherry et al., 1992; Han et al., 2010c; Lapko et al., 1999; Stockhaus et al., 1992).

The Different Effects of PhyA Proteolysis. Desensitization of activated receptors and regulatory factors is an important general mechanism for terminating signal transduction in many biological systems. Both autophosphorylation and COP1-mediated proteolysis play important roles in desensitizing phytochrome signaling in cells. Activated phyA undergoes desensitization in a two-step process involving, first, phosphorylation and subsequently, degradation by binding of COP1. However, the process of phyA degradation is just delayed, not completely shut down in the *COP1* mutant (Seo et al., 2004). This is consistent with the observation that phyA degradation occurs not only in the nucleus, but also in the cytosol (Rosler, Klein, and Zeidler, 2007). Thus, there might be another separate phyA degradation pathway in plant cells. HEMERA is a multiubiquitin-binding RAD23-like protein (Chen et al., 2010c). The study of the *hmr* mutants shows that in the absence of HMR native phyA accumulates in R light, while phyA response is absent. Chen et al. (2010) mentioned in the paper that " this suggests that phyA degradation is required for phyA function, rather than acting as desensitization mechanism for light signaling".

A Common Mechanism of PhyA Signaling is Expected in VLFRs and FR-HIRs. Unresolved questions about the mechanism of phyA degradation initiate from different perspectives in phyA signaling. With a broader

view, a common phyA signal transduction pathway may be fit to both the phyA-mediated VLFRs and FR-HIRs. As shown in Figure 1.5, light induces photoconversion from inactive phyA Pr to active Pfr in the cytosol. With the aid of FHY1/FHL, phyA Pfr translocates to the nucleus. R light also promotes the phyA Pfr phosphorylation process in the nucleus. When phosphorylated, phyA Pfr more easily interacts with its downstream factors, such as PIF3 and NAPK2, to induce multiple physiological responses. Likely, the majority of phyA molecules have already converted into a mixed active Pfr and phosphorylated Pfr at the beginning of exposure to R. After light pulse followed by darkness, the amount of Pfr/phosphorylated Pfr molecules gradually decreases via 26s proteosome. Thus, the whole VLFR process would match a desensitization mechanism for phyA-mediated signaling.

In contrast to the VLFR, FR-HIR depends on continuous irradiation with FR light and, therefore, is proposed to involve some type of short-lived phyA forms occurring in the photoconversion process of phyA back from Pfr to Pr. In my opinion, this short-lived functional phyA is neither Pr* nor some assumed intermediate phyA form, but is probably either phyA Pfr which is perhaps more active than phosphorylated Pfr, or in fact phosphorylated Pfr, which may be more efficient at signaling because of its affinity with its downstream factors. In the FRc light (FR-HIR), a small amount of Pfr molecules or phosphorylated Pfr (~3% total) constantly interact with their downstream regulators resulting in an open signaling state, whereas a light pulse in VLFR only generates Pfr once. The molecular mechanism in FR-HIR would occur like this: one portion of photocycled phyA Pfr molecules undergo a distinct interaction and co-degradation

process with PIFs, whereas rest of phyA Pfr are converted back, reentering into the big pool of Pr* in the nucleus (Figure 1.5). Active Pfr or phosphorylated Pfr generated from a round of phyA cycling may last up to 10-15 min (Shinomura, Uchida, and Furuya, 2000). High FR may enhance the speed of phyA cycling, and phyA function may be tightly related with its subsequent degradation. Therefore, the conclusion that "phyA degradation is required for phyA function" would be still right.

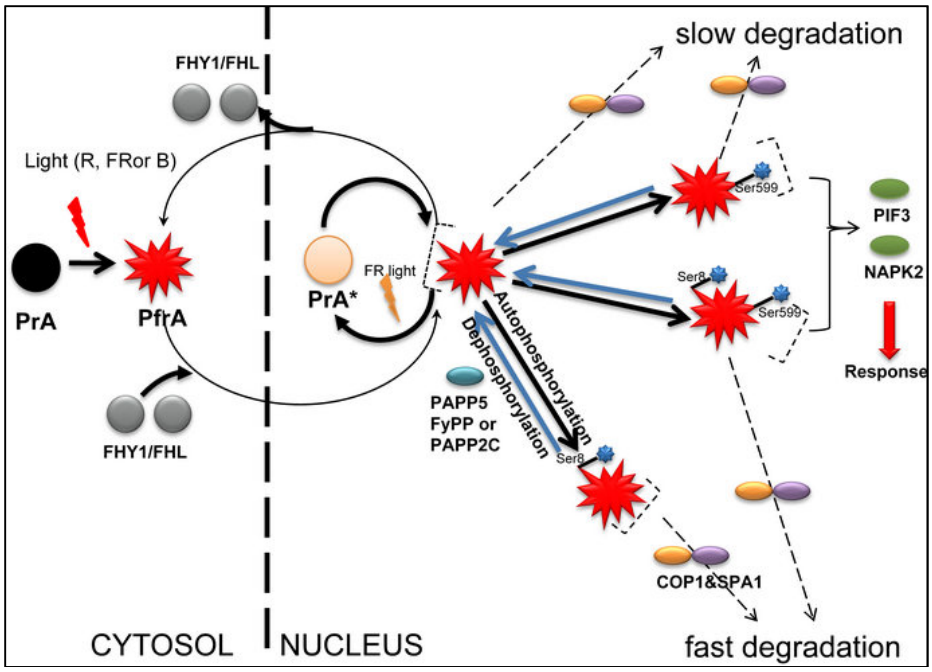


Figure 1.5. The proposed mechanism for phyA-mediated signaling in both VLFRs and FR-HIRs. The photon energy triggers photoconversion of inactive PrA to PfrA, which translocates into the nucleus with the help of FHY1/FHL. R light promotes PfrA phosphorylation, but phosphorylated PfrA can be reversibly dephosphorylated by some phosphatases. PfrA or phosphorylated PfrA is proposed to be the real active form in both VLFR and FR-HIR, because only this form possesses a lower/higher affinity toward signal transducers such as PIF3 and NAPK2. Meanwhile, Pfr/phosphorylated Pfr is unstable and can be differentially degraded. The difference between VLFR and FR-HIR is the period of induction time when Pfr can exist and function in the nucleus.

A brief R, FR or B pulse can give a jumpstart to saturate VLFRs by triggering the expression of early light responsive genes (Jiao, Lau, and Deng, 2007). By contrast, constant Pfr cycling in FRc can successfully induce the irreversible process of seedling establishment by signal amplification and transcriptome modification in FR-HIR. NB formation matches this hypothesis, showing that Rc exposure leads to photoconversion of a majority of phyA, rapid NB aggregation, phosphorylation, and degradation within several hours. After that, type II phys would take over the job from phyA to be co-degraded with PIFs in the large NBs and keep the signal transduction pathway open in plants. However, FRc light needs a much longer time (~2h) to reach the highest level of phyA in the nucleus, since only small amount of Pfr can be translocated into the nucleus at once in FR light.

Phytochrome Interaction and Signaling

Phytochrome Function and Interaction in Plant Development

Functions of different phytochrome family members in the model plant *Arabidopsis thanliana* have gradually been characterized by the analysis of individual and multiple null mutants, natural variants, and over-expression lines. According to the review by Frankin and Quail (2010), individual functions of phytochromes have been summarized at Table 1.1, showing that each phytochrome possesses unique as well as redundant activities in plant growth and development. PhyB is the predominant R-sensing phytochrome in Arabidopsis, but phyC-phyE have been proposed to play minor additional roles in R-sensing (Aukerman et al., 1997). PhyA is regarded as the major

FR-sensing receptor, but phyA activity is also significantly enhanced under high R irradiance (Franklin, Allen, and Whitelam, 2007).

Synergistic, additive or antagonistic effects have been observed in double or multiple phytochrome-deficient mutants, suggesting that phytochrome signaling pathways cross-talk with each other in regulation of plant growth and development. For

	phyA	phyB	phyC	phyD	phyE
Germination	Promotes germination in R and FR via the VLFR mode and in continuous FR in the HIR mode (Botto et al., 1996; Johnson et al., 1994b)	Regulates germination in R via the LFR mode (Shinomura et al., 1996b).		Only a small role was observed (Hennig et al., 2002).	Promotes germination in continuous FR (Hennig et al., 2002).
De-etiolation	Promotes de-etiolation in the FR-HIR mode (Parks and Quail, 1993).	Regulates de-etiolation in W and R (Reed et al., 1993a).	functions in de-etiolation through modulation of phyB activity (Franklin et al., 2003a).	Has minor role in de-etiolation and has synergistic effect with phyB (Aukerman et al., 1997).	Has small redundant role in seedling de-etiolation (Franklin et al., 2003b).
Gravitropic orientation	Regulates hypocotyl gravitropic orientation (Poppe et al., 1996)	Regulates hypocotyl and root gravitropic orientation (Correll and Kiss, 2005; Robson and Smith, 1996)			
Shade avoidance	Contains antagonistic activity in shade avoidance (Mathews, 2010).	Plays major roles in suppressing shade avoidance (Whitelam and Smith, 1991)		Has redundant function in suppressing shade avoidance (Aukerman et al., 1997).	Has relatively minor role in shade avoidance (Devlin, Patel, and Whitelam, 1998a).
Entrainment of the circadian clock	Acts as the low-intensity R for suppressing circadian period (Somers, Devlin, and Kay, 1998).	Acts as the primary high-intensity R photoreceptor for suppressing circadian period (Somers, Devlin, and Kay, 1998).		Plays a minor role in controlling circadian period (Devlin and Kay, 2000).	Plays a minor role in controlling circadian period (Devlin and Kay, 2000).
Flowering	Accelerates flowering (Johnson et al., 1994b)	Represses flowering (Goto, Kumagai, and Korrnneef, 1991)	Has redundant function in repressing flowering (Monte et al., 2003b).	Has redundant function in repressing flowering (Whitelam and Smith, 1991).	Has redundant function in repressing flowering (Goto, Kumagai, and Korrnneef, 1991).

Table 1.1 Phytochrome functions are summarized based on the research of *Arabidopsis* phytochrome-deficient mutants (Franklin and Quail, 2010).

example, in shade avoidance responses, phyA activity strongly antagonizes phyB signaling when sensing a low R:FR ratio (Devlin, Yanovsky, and Kay, 2003; Reed et al., 1994; Salter, Franklin, and Whitelam, 2003; Sharrock and Clack, 2002). PhyA and phyB also play opposite roles in the floral-transition, such that, under long day conditions, the *phyA* mutant shows delayed flowering, the *phyB* mutant shows accelerated flowering, and the *phyAphyB* double mutant is intermediate between these two single mutants (Goto, Kumagai, and Koornneef, 1991; Johnson et al., 1994a; Neff and Chory, 1998b; Takano et al., 2005). It should be noted that both the *phyB* and *phyD* mutants promote hypocotyl elongation, but the *phyB/phyD* double mutant surpasses the total amount of increased hypocotyl length of the *phyB* mutant plus that of the *phyD* mutant in either Ws or Ler genetic background (Aukerman et al., 1997).

Additive and Synergistic Effects and Type II Heterodimerization

An additive effect is the most common phenomenon seen in cross-talk among Type II phytochromes. However, a few examples of synergistic interactions have been also noted. As we mentioned above, a synergistic relationship between phyB and phyD was detected when a greater hypocotyl elongation was detected in the double *phyB/phyD* mutant, compared to the combined increases in the monogenic mutants. A phyD and phyE synergistic effect occurs in the time of flowering, with the double *phyD/phyE* mutant flowering much earlier than the additive acceleration in the two monogenic mutants (Clack et al., 2009). Synergistic effects may arise from direct interaction between the relevant type II phytochrome forms (Clack et al., 2009).

For many years, phytochromes had been assumed to form homodimers on the basis of the early biochemical analysis of oat phyA. In the 1980s, purified oat phyA from dark-grown tissues was identified as a homodimer by size-exclusion chromatography (Jones and Quail, 1986; Lagarias and Mercurio, 1985). Using co-immunoprecipitation (Co-IP), phytochrome heterodimerization of type II phytochromes was first discovered in 2004, suggesting phy heterodimerization is a common biological event in angiosperms (Sharrock and Clack, 2004). When the myc_6-phyB fusion protein was pulled down from seedling extracts, phyC-phyE were coprecipitated. Meanwhile, myc_6-phyD coprecipitated phyB and phyE. All these phy heterodimers exist not only in dark-grown seedlings but also in light-grown seedlings as well. PhyA forms only homodimers based on the observations that phyA failed to be coprecipitated with the type II phyB-phyE in these experiments, and in chapter 3 of this thesis, phyB-E also failed to be pulled down with myc-tagged phyA. Further investigation showed that phyC and phyE undergo obligate heterodimerization with phyB and phyD in seedlings (Clack et al., 2009).

As shown in Figure 1.6, type II phytochrome dimers can be divided into two categories: a phyB-related group and a phyD-related group, with the linkage of phyB/phyD dimerization (Clack et al., 2009; Sharrock and Clack, 2004). Because of the high amino acid sequence similarity of phyB and phyD, phyC and phyE may bind to them randomly. Therefore, a higher level of accumulation of phyC/phyD and phyE/D heterodimers is likely in *phyB* mutant plants. In the absence of phyB and phyD, phyC is degraded and phyE forms monomers (Clack et al., 2009).

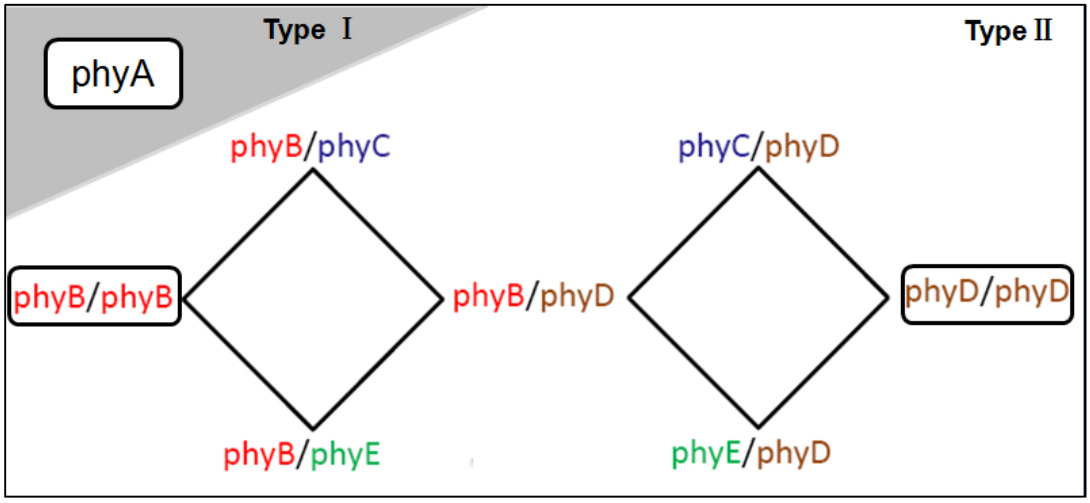


Figure 1.6. Dimerization properties of Arabidopsis type II phytochromes. Arabidopsis contains three homodimers phyA, phyB and phyD and five combined phytochrome heterodimers: phyB/E, phyB/C, phyB/D, phyD/E, and phyD/C.

Phytochrome Signaling

Photoactivated phytochromes translocate into the nucleus, modulate ~20% of the transcriptome (Kevei, Schafer, and Nagy, 2007) and ultimately induce diverse plant growth and developmental responses to optimize a plant's survival in a given environment. There are mainly two distinct transduction pathways, phyA and phyB-mediated pathways, both of which share some common transcriptional regulators in the complex light signaling network. The study of seedling photomorphogenesis shows that two integrated hubs are emerging in the network, a hub associated with the positive-acting HY5 transcription factor and a hub associated with the negative regulators PIFs (Lau and Deng, 2010). Here, a basic and simplified model of phytochrome signaling will first be discussed, followed by special emphasis on HY5 and PIF-mediated signaling in the de-etiolation process.

In the dark, the COP/DET/FUS group of regulators prevent photomorphogenesis by targeting a number of photomorphogenesis-promoting transcription factors (HY5, HYH, HFR1, LAF1 and others) for degradation. Meanwhile, nuclear-accumulated PIF proteins act as negative regulators promoting skotomorphogenesis by suppressing gene expression. Light irradiation rapidly changes skotomorphogenesis into the opposite direction, photomorphogenesis. Activated phytochromes promote HY5 accumulation in the nucleus, possibly by decreasing the expression of COP1 or dephosphorylating HY5, causing significant reduction of its physical interaction with COP1 (Hardtke et al., 2000; Osterlund and Deng, 1998; Osterlund, Wei, and Deng, 2000). Secondly, in the light, PIFs are phosphorylated and rapidly degraded following direct interaction with phytochromes. Therefore, a 'double check' mechanism ensures the right program for direction of plant growth and also coordinates phytohormone signaling pathways with light signaling in plant development.

The PIF Hub. The complete PIF-subfamily in Arabidopsis consists of fifteen phy-interacting basic helix-loop-helix (bHLH) transcription factors(Leivar and Quail, 2011). The most highly examined PIFs, PIF3 and PIF1, contain an Active Phytochrome B-binding (APB) region and an Active Phytochrome A-binding (APA) region, both of which are necessary for binding to the Pfr forms of phyA and phyB. Others such as PIF4, PIF5 and PIF7 only interact with phyB via their APB domain (Monte et al., 2007). PIFs are known to specifically target gene promoters with a conserved G-box core (CACGTG), indicating direct regulation of gene expression by these proteins through interaction with phytochromes (Shin, Park, and Choi, 2007). Some of these DNA

promoter motif-targeted PIFs may function as positive regulators. For example, dual transcriptional activation activities of PIFs have been discovered recently (Kidokoro et al., 2009). The activities of PIFs compose a cellular signaling hub, at which multiple signaling pathways converge together, including the phytochrome pathway, plant hormone pathways, the circadian clock and high temperature-mediated pathways (Koini et al., 2009). Thus, these functionally redundant but also somewhat differential PIFs can alter the plant transcriptional profile and significantly influence plant development.

The Feedback between Phytochrome and PIFs. Photoactivated Pfr phytochromes can directly bind to PIFs, and thereby trigger de-etiolation by repressing the expression of PIFs at the post-translational level via ubiquitin/proteosome-mediated proteolysis. Recent evidence shows that although monogenic *pif* mutants still exhibit an etiolation phenotype in the dark (Huq et al., 2004; Lorrain et al., 2009; Stephenson, Fankhauser, and Terry, 2009), the *pif1pif3pif4pif5* quadruple mutant shows constitutive photomorphogenesis (Leivar et al., 2008b). In the continuous R light, increasing the number of *pif* mutations significantly enhances phyB expression (Khanna et al., 2007; Leivar et al., 2008a). This indicates that interaction between phytochromes and PIFs via a negative feedback loop modulates phytochrome signaling.

PIFs Control Plant Hormone Expression. Plant hormone signaling is also interconnected with PIFs. In contrast to light signals, GAs promote skotomorphogenesis and repress photomorphogenic growth. In the dark, PIF1, as a negative regulator of seed germination, reduces GA responses by repressing the expression of GA-biosynthetic

genes and enhancing the expression of GA catabolic genes (Leivar et al., 2009). Meanwhile, PIF1 improves ABA biosynthesis and reduces ABA catabolism, resulting in an increase of ABA levels. PIF1 also desensitizes seeds to GA response by up-regulating GA-repressor (DELLA) expression. Conversely, in response to light, rapid PIF1 degradation increases the GA level and sensitivity, and decreases the ABA level, ultimately resulting in seed germination. Following germination, GA accumulation promotes the expression of PIF3 and PIF4, through the suppression of the expression of DELLAs. When growing seedlings are exposed to light, DELLAs are released from degradation, interact with PIF3 and PIF4 factors and sequester them from their targeted genes (de Lucas et al., 2008; Feng et al., 2008). In addition to this overexpression of PIF5 may promote the triple response in the dark by altering ethylene biosynthesis (Khanna et al., 2007).

The Circadian Clock. PIFs are a major convergence point of both phytochrome--regulated signaling and the circadian clock. Phytochromes are involved in both input to the clock and controlling output from the clock. By interacting with activated phytochromes, the circadian clock can regulate the transcriptional expression of PIFs, such as PIF4, PIF5 and PIF7, (Kidokoro et al., 2009; Yamashino et al., 2003). For example, at dusk, hypocotyl elongation rate reaches its maximum as a result of the high level of PIF proteins accumulated in the nucleus at that time (Kidokoro et al., 2009).

High Temperature. High temperature-induced responses in plant development include rapid extension of plant axes, leaf hyponasty, and early flowering. The *pif4*

mutant does not exhibit dramatic changes in plant architecture, but causes an early flowering response under high temperature conditions, suggesting that isolated temperature-initiated signaling may be linked together through PIF factors (Koini et al., 2009).

The HY5 Hub. The HY5 transcription factor protein is another major downstream regulator of the light signaling pathway and plays a critical role in promoting plant photomorphogenesis. In darkness, the COP1-SPA1 complex interacts directly with HY5 in the nucleus to down-regulate its activity (Saijo et al., 2003). In the light, phytochrome indirectly enhances the expression of HY5 mainly at the transcriptional level (Oyama, Shimura, and Okada, 1997). The subsequent accumulation of HY5 improves its binding affinity for specific G-box promoter sequences upstream of photomorphogenesis genes and induces photomorphogenesis responses (Chattopadhyay et al., 1998). Recent studies have shown that, HY5, as a convergence point of multiple signaling pathways, regulates the transcriptional network to coordinate plant development. Potential HY5 binding sites have been identified by chromatin immunoprecipitation and >3000 chromosomal sites have been revealed as putative HY5 binding targets (Lee et al., 2007). More than one thousand genes, including regulators and signaling components of plant hormone pathways, have been affected at their transcription level by genome-wide mapping of the HY5-mediated gene networks in Arabidopsis (Zhang et al., 2011).

In promoting photomorphogenesis, HY5 interacts with several plant hormone pathways, including GA signaling, auxin signaling and ABA signaling. Reduction of auxin results in a light-grown phenotype in the dark. HY5 may directly activate auxin

negative regulators, such as *AXR2* and *SLR*, in order to suppress auxin signaling (Woodward and Bartel, 2005). LONG1, an ortholog of Arabidopsis HY5 in pea, decreases the GA level during photomorphogenesis through activation of a GA catabolic enzyme gene *GA2ox2* (Weller et al., 2009). GA represses photomorphogenesis by two distinct mechanisms. GA can either repress the accumulation of the DELLA proteins, which promotes the abundance of PIFs, or, GA can down-regulate the expression of HY5 at the translational level by modulating COP1 activity (Alabadi et al., 2008). HY5 enhances ABA signaling by directly binding to the promoter of a bZIP transcription factor ABI5 (Finkelstein and Lynch, 2000). Crytochrome and cytokinin signaling pathways, which increase HY5 protein levels, are also integrated in the HY5 hub (Vandenbussche et al., 2007).

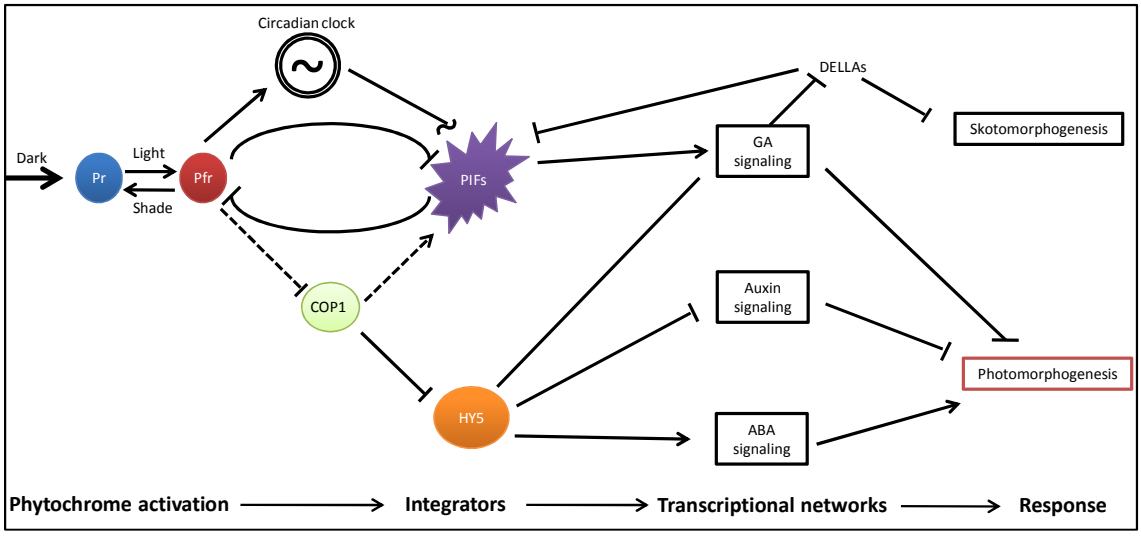


Figure 1.7. A simplified model of the phytochrome-mediated signaling network. There are at least three hierarchies in this signaling network: the activation of phytochrome, the integration of signaling, and the modification of the plant transcriptome through plant hormone signaling pathways. When sensing light, plants turn on one pattern of growth, skotomorphogenesis, and switch off the other one, photomorphogenesis. Dotted lines represent putative or indirect interactions.

Conclusion

Current evidence favors the existence of two convergence hubs, through which phytochromes and phytohormones build an extensive communication. PIFs play a major role in integrating light and GA signals in photomorphogenesis. HY5 tightly co-operates GA, auxin and ABA signaling. These two hubs are relatively independent because interactions between PIFs and HY5 have not been observed yet. As shown in Figure 1.7, there are at least three hierarchies in this signaling network: the activation of phytochrome, the integration of signaling, and the modification of the plant transcriptome. Phytochrome photoactivation and nuclear translocation are the primary events in the first level. Signal transduction in the second level mainly relies on protein-protein interactions, phosphorylation, and degradation. Most regulators like PIFs and HY5 are transcription factors, functioning within the nucleus. Signal amplification occurs in the third level, resulting in a relatively fast shift of a major part of the plant transcriptome. Moreover, much more fundamental hormone-regulated metabolic and physiological pathways can be expected at the basic level (the fourth level). Meanwhile, endogenous hormones and the feedback of hormones direct signaling factors interacting back into the top hierarchy. Clearly, this simple model can hardly explain the whole process of phytochrome- -mediated signaling. Lau and Deng (2010) also pointed out that more integrators or other hormone interactions will need to be identified in the future. Combination of the use of traditional genetic approaches, crystallography, imaging and bioinformatics may some day allow us to truly understand the mechanisms of photosensory signaling in plant growth and development.

CHAPTER 2

DIRECTED DIMERIZATION: AN *In Vivo* EXPRESSION SYSTEM FOR FUNCTIONAL STUDIES OF HETERODIMERIC PHYTOCHROMES IN *Arabidopsis*

Abstract

Phytochromes (phys) are a family of dimeric chromoprotein photoreceptors that modulate plant physiological and developmental processes in response to red (R) and far-red (FR) light. Identification of heterodimers of type II phys in *Arabidopsis* has revealed that plant R/FR sensing systems are structurally complex and suggests that diverse forms may have specific functions. Here, we report a novel *in vivo* protein engineering system for use in characterizing the activities of individual phytochrome dimer combinations. A series of singly and doubly transgenic *Arabidopsis* plants expressing functional truncated phy transgenes were developed. One set of transgenes consisted of the wild-type phyB N-terminal (amino acids 1-651) domain (NB) with the C-terminal domain replaced by the SV40 nuclear localization sequence (SV40 NLS) and a short yeast protein domain that mediates either homodimerization or obligate heterodimerization. Particularly, monitoring seedling growth responses to R in a *phyB*-deficient background is a convenient and sensitive assay system for plant photoreceptor function. Using this system, biological activity of chimeric NB/NB homodimers but not monomeric NB subunits was demonstrated in control of hypocotyl elongation, cotyledon separation and expansion, rosette leaf morphology, and flowering time. Yeast domain-mediated homodimerization of the NC, ND, and NE domains from the

phyC-phyE receptors, and directed heterodimeriztion of these with the NB domain, were used to probe the individual activities of these phy forms. Notably, NB/ND heterodimers show stronger activity than NB/NB homodimers in this system. Heterodimers of the wild-type NB sequence with the chromophoreless NB^{C357S} mutant, which may mimic phyB Pr/Pfr heterodimers, differentially mediate sensitivity of plant tissues to R. These findings have implications for understanding the mechanism of plant R/FR photosensory signaling and this experimental approach of directed production of specific protein dimer combinations *in vivo* may be applicable to other systems.

Introduction

The emerging field of synthetic biology seeks to rationally engineer novel molecular structures and mechanisms in cells that facilitate predictable biological outputs (Haynes and Silver, 2009). Implementation of synthetic signaling circuits within living cells, as opposed to induction of engineered gene expression patterns, is a relatively new approach to this goal. To succeed, such circuits will need to operate reliably to transmit environmental stimuli into predictable responses within the context of very complex and dynamic ongoing cellular processes (Kiel, Yus, and Serrano, 2010; Lim, 2010). Development of this capability will likely require targeted manipulation of the assembly of multi-protein complexes. In eukaryotes, the structural domains and molecular mechanisms that connect naturally-occurring signaling proteins into circuits or networks are frequently modular (Bhattacharyya et al., 2006). Modular organization is essential to integration of multiple diverse signaling pathways in cells and also likely facilitates

evolution of new circuitry. In this study, I demonstrate use of heterologous modular protein binding domains to achieve biologically-relevant protein quaternary structure changes that alter light sensing and response in plants.

Phytochromes (phy) are dimeric plant photoreceptors for red (R) and far-red (FR) light, which undergo a reversible photo-induced conformational change between a R-absorbing Pr form and a FR-absorbing Pfr form (Quail, 2002). Phy-related R/FR light-sensing receptors have been identified in eubacteria, cyanobacteria, fungi, and plants (Karniol et al., 2005; Sharrock, 2008). Phy apoproteins are highly modular. They contain a covalently-attached linear tetrapyrrole chromophore embedded in a 500-700 amino acid N-terminal globular module (photosensing region, PSR) of the apoprotein (Quail et al., 1995; Rockwell, Su, and Lagarias, 2006). This conserved PSR is comprised of three recognized protein domains, PAS (Period/ARNT/SIM), GAF (cGMP phosphodiesterase/adenylcyclase/FhlA), and PHY (Phy-associated), and contains all of the amino acid sequences needed to mediate reversible Pr-Pfr conformational photo-transformation. In bacteria, fungi, and algae, the C-terminal modules of phy apoproteins are light-regulated two-component histidine kinases (Davis, Vener, and Vierstra, 1999; Froehlich et al., 2005; Yeh et al., 1997). In higher plants, phy C-termini have a more complex domain structure, containing two adjacent PAS domains and a histidine kinase-related sequence (HKRD) that lacks some amino acid residues essential to histidine kinase activity but has an ATP binding domain-like sequence (Rockwell and Lagarias, 2006). The PSR and the C-terminal module of plant phys are connected by a "hinge" sequence, which is readily accessible to protease cleavage (Grimm, 1988;

Lagarias and Mercurio, 1985). Moreover, the cellular functions of the two phy ends are, to a significant extent, independent. The N-terminal PSR mediates R light sensing/signaling and the C-terminal region mediates dimerization and nuclear translocation (Chen, Schwab, and Chory, 2003). It has been shown that the PSR of *Arabidopsis* phytochrome B (phyB) alone can confer hypersensitivity to R in the absence of the C-terminal module, but only if it is fused to a heterologous protein that causes the fusion protein to dimerize (β-glucuronidase) and to a nuclear-localization signal (NLS) that promotes import into the nucleus (Matsushita, Mochizuki, and Nagatani, 2003).

One complicating feature of plant phy structure/function is that multiple, divergent *PHY* genes are expressed in the same plant cells, such as the *PHYA-PHYE* genes in *Arabidopsis* (Goosey, Palecanda, and Sharrock, 1997). These paralogous phy apoproteins have distinct regulatory functions as judged by analysis of their respective null mutants (Devlin, Patel, and Whitelam, 1998b; Devlin et al., 1999; Monte et al., 2003a; Reed et al., 1994). The most prominent difference is in the function of phyA, which mediates very low fluence responses (VLFR) and high irradiation responses to continous FR (FR-HIR), versus the functions of phyB-phyE, which signal in R/FR reversible responses and shade sensing (Mathews, 2010). Because of the striking functional distinction between them, phyA is often referred to as type I phy and phyB-phyE as type II phys. An additional factor that complicates the plant phy photoreceptor array is that the type II phys assemble in many heterodimeric forms (Clack et al., 2009; Sharrock and Clack, 2004). It is an open question whether each of these phy forms has a distinct regulatory activity.

In this thesis, I have used a synthetic biology approach to characterize the functions of discrete homodimeric and heteromeric *Arabidopsis* phytochromes. Small protein-protein interaction domains from the yeast GAL4, Bem1, and Cdc24 proteins were substituted for the phy C-termini in order to produce either obligate homodimers or obligate heterodimers of the N-terminal phy PSRs (NX). I demonstrate that engineered NB/NB homodimers and ND/NB heterodimers are highly active as photoreceptors in seedling de-etiolation and flowering. Dimers of NB with chromophore-less NB^{C357S} subunits, and NC/NB or NE/NB heterodimers are active in cotyledons but not in hypocotyls. These findings confirm and extend the model for modular organization of the plant phy proteins. They are relevant to questions regarding the origins of *PHY* gene diversity and its physiological implications and they reveal novel aspects of tissue-specific phy regulation in plant development. Moreover, they illustrate the utility of a directed protein dimerization system, used in plants here but likely applicable in many *in vivo* systems, to study the roles of protein quaternary interactions.

Results

The PB1 Domains of the Yeast Bem1 and Cdc24 Proteins Form Obligate Heterodimers

Analysis of the establishment of cell polarity in budding yeast *Saccharomyces cerevisiae* has shown that the C-terminal PB1 domains of the Bem1 and Cdc24 proteins interact directly with each other to form a Bem1/Cdc24 heteromeric complex (Ito et al., 2001). To test whether the Bem1 and Cdc24 dimerization domains bind to themselves in addition to binding to each other, yeast two-hybrid assays were performed with

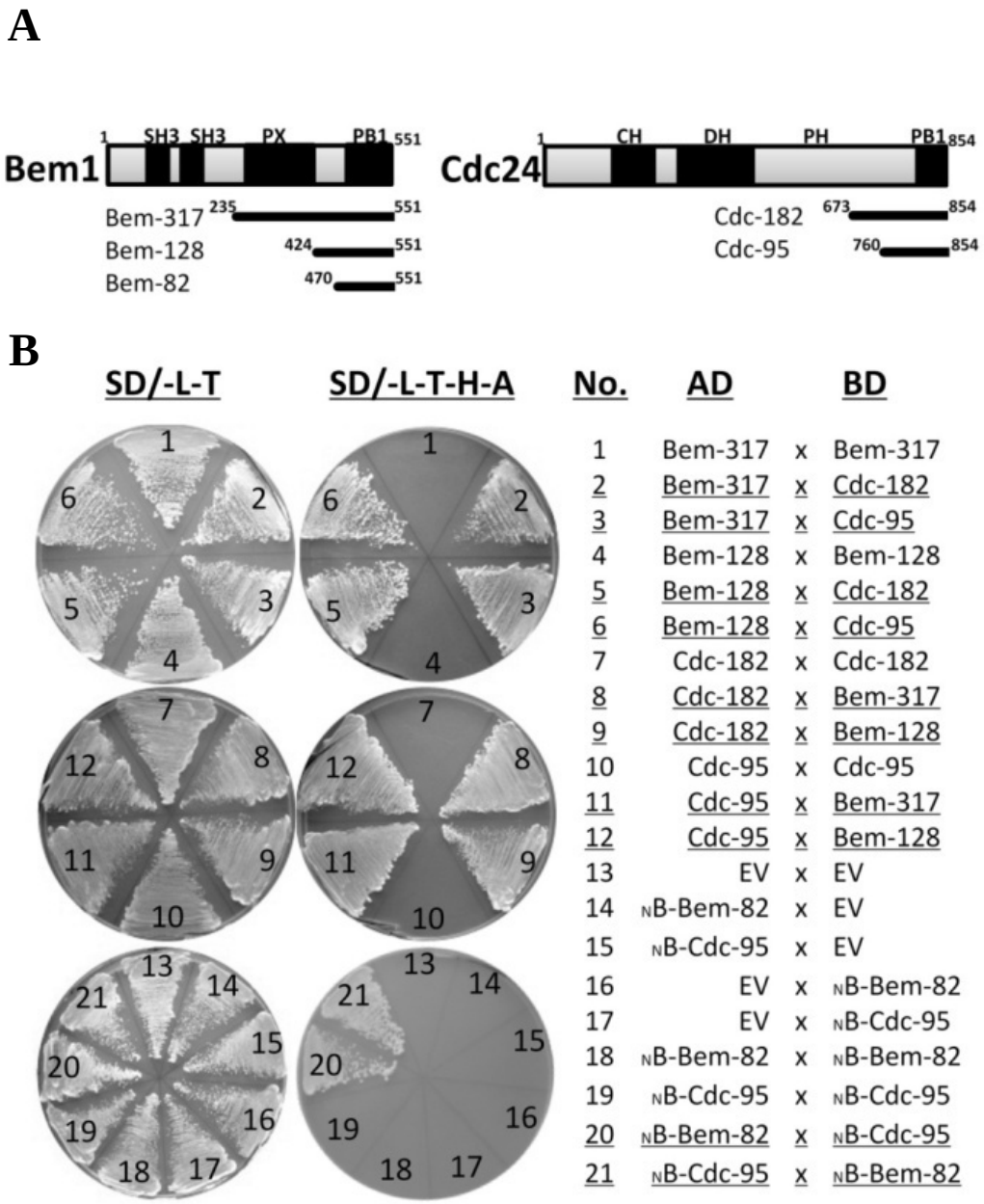


Figure 2.1. The yeast Bem1 and Cdc24 proteins do not form homodimers. Interactions between PB1-containing Bem1 and Cdc24 regions in yeast two-hybrid assay. (A) Different lengths of PCR products of Bem1 (Bem-317, Bem-128 and Bem-82) and Cdc24 (Cdc-182 and Cdc-95) were fused to the Gal4 activation domain (AD) and the Gal4 DNA-binding domain (BD). (B) Yeast strains expressing the indicated constructs were streaked on –Leu/–Trp medium to select for plasmids (on the left) and on –Leu/-Trp/-His/-Ade medium to test the interactions (on the right).

various-sized protein sequences containing the PB1 domains of Bem1 (Bem-317, Bem-128 and Bem-82) and Cdc24 (Cdc-182 and Cdc-95). As shown in Figure 2.1, no interaction of the Bem1 regions or the Cdc24 regions with themselves is detected, whereas all combinations of Bem1 PB1 domains with Cdc24 PB1 domains show interaction with each other. In addition, strong interaction is also observed in yeast two-hybrid assays when the Bem-82 and Cdc-95 sequences are fused to the N-terminal 651 aa phyB sequence (NB-Bem-82 and NB-Cdc-95). These results suggest that these small yeast protein domains may be used to assemble phytochrome N-terminal PSR modules into dimers in a directed manner *in vivo*.

Bem/Cdc Domain-directed Dimerization *in vivo* of the NB PSR

Transgenes called NB-Bem and NB-Cdc were constructed in which epitope-tagged nuclear-localized phyB fusion proteins are expressed from the cauliflower mosaic virus 35S (35S) promoter (Figure 2.2A). The NB-Bem transgene product consists of the phyB PSR (aa 1-651 = NB) fused to Bem-82, followed by a myc_6 epitope tag and the SV40 NLS. The NB-Cdc transgene product is NB fused to the Cdc-95 region, followed by the his_6 epitope tag and the SV40 NLS. These two chimeric coding sequences were constructed in vectors that confer either kanamycin or gentamicin resistance in plants. Singly and doubly transgenic *Arabidopsis* plants were generated, in which the NB-Bem and NB-Cdc transgenes are expressed individually or are co-expressed in a *phyB* null mutant background. Single-locus kanamycin-resistant *phyB*(NB-Bem) #100 T3 lines and gentamicin-resistant *phyB*(NB-Cdc) #97 T3 lines were identified and crossed to each

other to produce doubly-transgenic true-breeding *phyB*(NB-Cdc/NB-Bem) F_3 progeny lines (CBC). Extracts of seedlings of these lines were analyzed by immunoblotting with anti-myc_6 and anti-his_6 antibodies. Figure 2.2B shows that the chimeric NB-containing proteins are detected at their predicted sizes on blots. In order to compare the expression levels of these proteins to the normal wild-type phyB level, extracts of *phyB*(*PHYB*-myc_6)#210 and *phyB*(his_6-*PHYB*) #336 lines, in which epitope-tagged full-length (FL)-phyB coding sequences are expressed from the *PHYB* promoter, were include on the blots. Both of these FL-phyB transgenes complement the *phyB* mutant phenotype and their expression levels could be quantified relative to the native WT phyB level on immunoblots with anti-phyB antibody MAb B6B3 (Figure 2.3). The expression levels of the NB chimeric proteins, which lack the MAb B6B3 epitope, were then estimated by comparison to these proteins on immunoblots that detect the epitope tags (Figure 2.2B).

Despite being transcribed from the 35S promoter, the NB-Bem and NB-Cdc proteins are present in plants at steady-state levels similar (0.8-1.2X) to native phyB. Under white light or R, the *phyB*(NB-Cdc/NB-Bem) CBC lines contain two to three-fold higher levels of both the NB-Cdc and NB-Bem proteins than the progenitor #97 and #100 lines (Figure 2.2B), suggesting that dimerization stabilizes these chimeric proteins in the light. This is not seen in seedlings grown in the dark (Figure 2.4). Moreover, the NB-Bem protein is not stabilized by MG132 under R, indicating the light-dependent degradation of the NB fusion proteins is not mediated by the ubiquitin/26S proteasome pathway (Figure 2.4)

(Jang et al., 2010). An $_{N}B^{C357S}$-Cdc transgene, with the same sequence as $_{N}$B-Cdc but containing a mutation changing the chromophore attachment cysteine 357 residue to

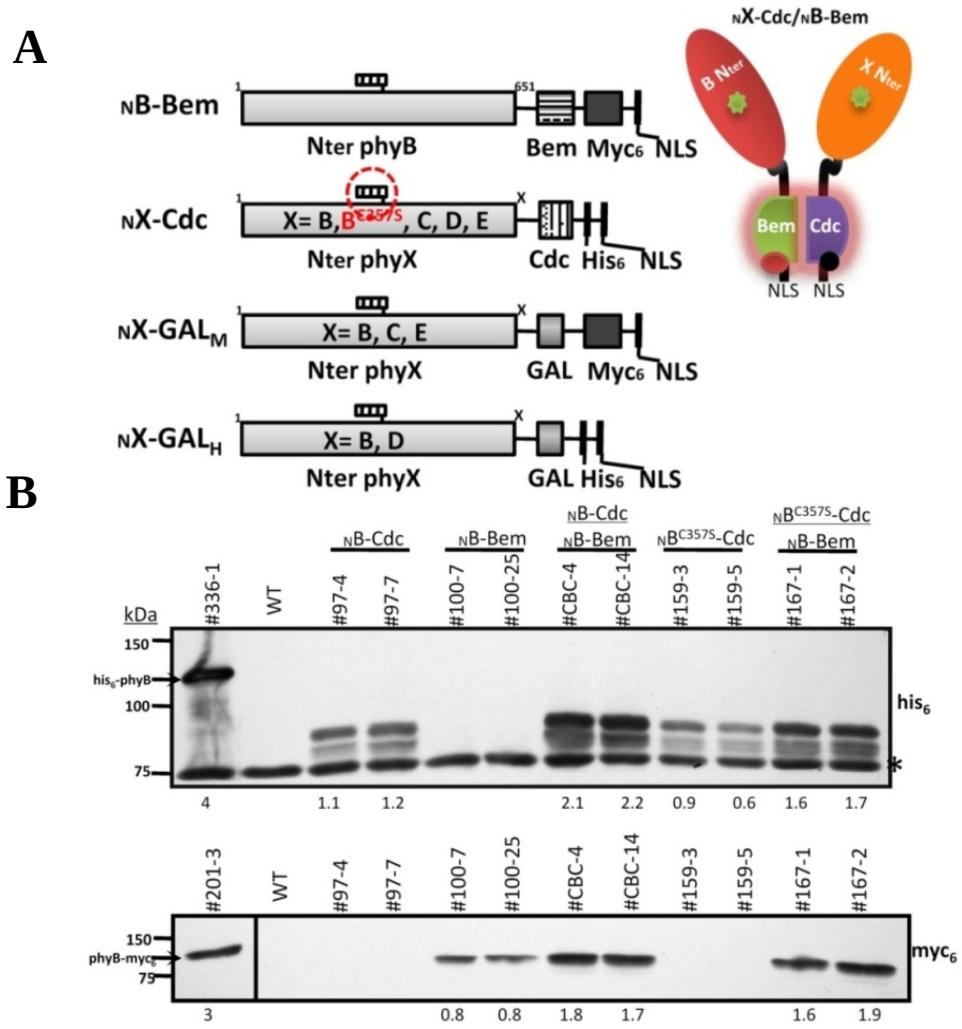


Figure 2.2. Co-expression of Bem and Cdc-mediated $_{N}$B fusion transgenes stabilizes the $_{N}$Bs in the light. (A) Structures of the four groups of synthesized phytochrome transgenes, $_{N}$B-Bem, $_{N}$X-Cdc, $_{N}$X-GAL$_{M}$, $_{N}$X-GAL$_{H}$ (various phytochrome coding sequences in each transgene group denoted by X), and the expected heterodimeric phytochrome model of each directed dimer phy chimera. The phy N-terminal domain or PSR is abbreviated Nter. Bem and Cdc are the Bem-82 and Cdc-95 regions in yeast, respectively. GAL is the homodimers-directing GAL4 domain from yeast. (B) Immunoblot analysis of the levels of the truncated phyB products in singly and doubly transgenic lines: the *phyB*($_{N}$B-Cdc), *phyB*($_{N}$B-Bem), *phyB*($_{N}$B-Cdc/$_{N}$B-Bem), *phyB*($_{N}B^{C357S}$-Cdc), *phyB*($_{N}B^{C357S}$-Cdc/$_{N}$B-Bem) lines and two full-length phyB control lines, the *phyB*(P_B-phyB-myc$_6$) and the *phyB*(P_B-his$_6$-phyB) lines. Total protein extracts from 5-d-old white light-grown seedlings of the indicated lines were fractionated on

SDS-PAGE gels. Blots were probed with anti-his_6 or anti-myc_6 antibody. Numbers at the bottom indicate the relative phyB expression levels in the transgenic lines. The asterisk indicates a non-specific band detected by the anti-his_6 Ab (same as below).
serine, was also transformed into the *phyB* host. The *phyB*($_N$B^{C357S}-Cdc) #159 lines and the *phyB*($_N$B^{C357S}-Cdc/$_N$B-Bem) #167 lines contain similar transgene product levels to their corresponding phyB WT sequence #97 and #100 lines and the two proteins are again stabilized when they are co-expressed (Figure 2.2B).

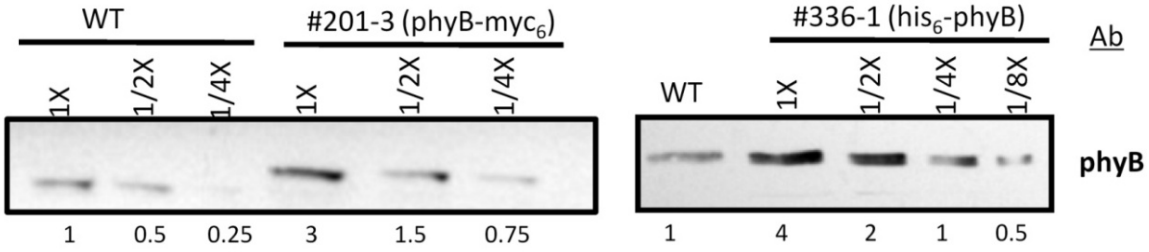


Figure 2.3. Quantitative analysis of phyB levels in the *phyB*(*PHYB*-myc_6) #210-3 line and the *phyB*(his_6-*PHYB*) #336-1 line. Extracts of 5-d-old white light-grown seedlings were fractionated by SDS-PAGE, blotted, and probed with anti-phyB antibody. Numbers at the bottom of lines indicate the phyB expression levels of each line relative to WT.

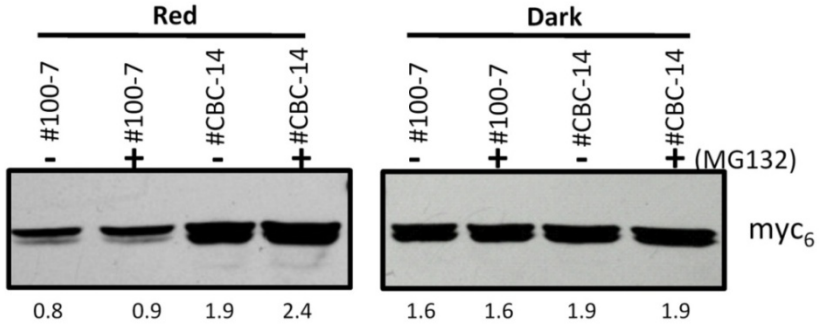


Figure 2.4. Monomeric phyB PSR is more stable in the dark than under R. Protein immunoblot analysis of $_N$B-Bem protein levels of in the transgenic *phyB*($_N$B-Bem) and *phyB*($_N$B-Cdc/$_N$B-Bem) lines under R or D for 24h in the presence or absence of MG132. Numbers at the bottom of lines indicate the phyB expression levels of each line relative to WT.

To directly demonstrate Bem/Cdc domain-mediated dimerization of the transgene products, extracts of *phyB*(NB-Bem) #100-7 and *phyB*(NB-Cdc/NB-Bem) CBC-4 were fractionated by size exclusion chromatography (SEC) by Brian Eilers in Martin Lawrence's lab. Fractions were analyzed on immunoblots probed with the anti-myc_6 or anti-his_6 Abs and the immunoblots were scanned. Figure 2.5A shows that the NB-Bem (93.2 kDa) and NB-Cdc (85.2 kDa) proteins are recovered in fractions consistent with their monomer MWs when expressed by themselves, and are ~50% shifted to a dimer MW (178.4 kDa) when co-expressed in the CBC line. This demonstrates that the proteins do not bind to themselves and that, although not completely efficient, interaction of the Bem and Cdc domains is sufficient to mediate formation of discrete dimers. To further confirm this, the NB-Bem protein was immunoprecipitated with anti-myc antibody from extracts of the *phyB*(NB-Cdc/NB-Bem) CBC and *phyB*(NB^{C357S}-Cdc/NB-Bem) #167 lines. Figure 2.5B shows that the his_6-tagged NB-Cdc and NB^{C357S}-Cdc proteins co-precipitate with NB-Bem.

Dimerization of the NB PSR with Itself or with Achromo-
-NB Induces Different R Sensitivities in Seedlings

Figure 2.6 illustrates that, while the singly-transformed *phyB*(NB-Cdc) #97 and *phyB*(NB-Bem) #100 control lines have highly elongated hypocotyls under R like the *phyB* mutant, co-expression of the fusion proteins in the *phyB*(NB-Cdc/NB-Bem) line significantly complements this phenotype. There is no difference seen between the doubly transgenic *phyB*(NB-Cdc/NB-Bem) lines generated by crossing or by double transformation (Figure 2.8). Therefore, an active R-sensing dimeric photoreceptor is

reconstituted in seedlings from two inactive monomers via interaction of the fused Bem and Cdc domains. In contrast, both the *phyB*(NB^{C357S}-Cdc) #159 and *phyB*(NB^{C357S}-Cdc/NB-Bem) #167 lines show almost no R-induced suppression of hypocotyl elongation (Figure 2.6). It is predicted that, in the #167 line, NB^{C357S}-Cdc/NB-Bem dimers assemble and these form Pr/Pfr-like photo-conformational dimers when exposed to R light. These appear to be inactive in mediating R sensitivity in hypocotyl cells. A control *phyB*(*PHYB*^{C357S}) #139 line, which expresses full-length phyB^{C357S} (Clack et al., 2009) is also not sensitive to R. However, different effects of the directed dimers are observed in other seedling tissues. R-induced increases in cotyledon expansion and cotyledon angle are both fully restored in *phyB* lines containing NB-Cdc/NB-Bem dimers, but these responses are also strongly complemented in the *phyB*(NB^{C357S}-Cdc/NB-Bem) #167 lines (Figure 2.6-2.7). Time courses of hypocotyl length and cotyledon area under continuous R demonstrate that cotyledon area is much more sensitive to the presence of NB^{C357S}-Cdc/NB-Bem dimers than is hypocotyl length throughout seedling development (Figure 2.7A). It is notable that, particularly in their first week of growth, the singly transgenic *phyB*(NB-Cdc) #97 and *phyB*(NB-Bem) #100 lines have a small degree of light-induced cotyledon expansion (Figure 2.7A lower panel), suggesting this response is very sensitive and that either the NB-Cdc and NB-Bem monomers can signal weakly in this pathway or a small fraction of these proteins homodimerizes *in vivo*. The activity of the NB^{C357S}-Cdc/NB-Bem construct in the cotyledon expansion and angle phenotypes directly demonstrates that a chromo/achromo

dimer can drive significant signaling, confirming an assumption that Pr/Pfr photo-heterodimers of phytochromes are biologically active.

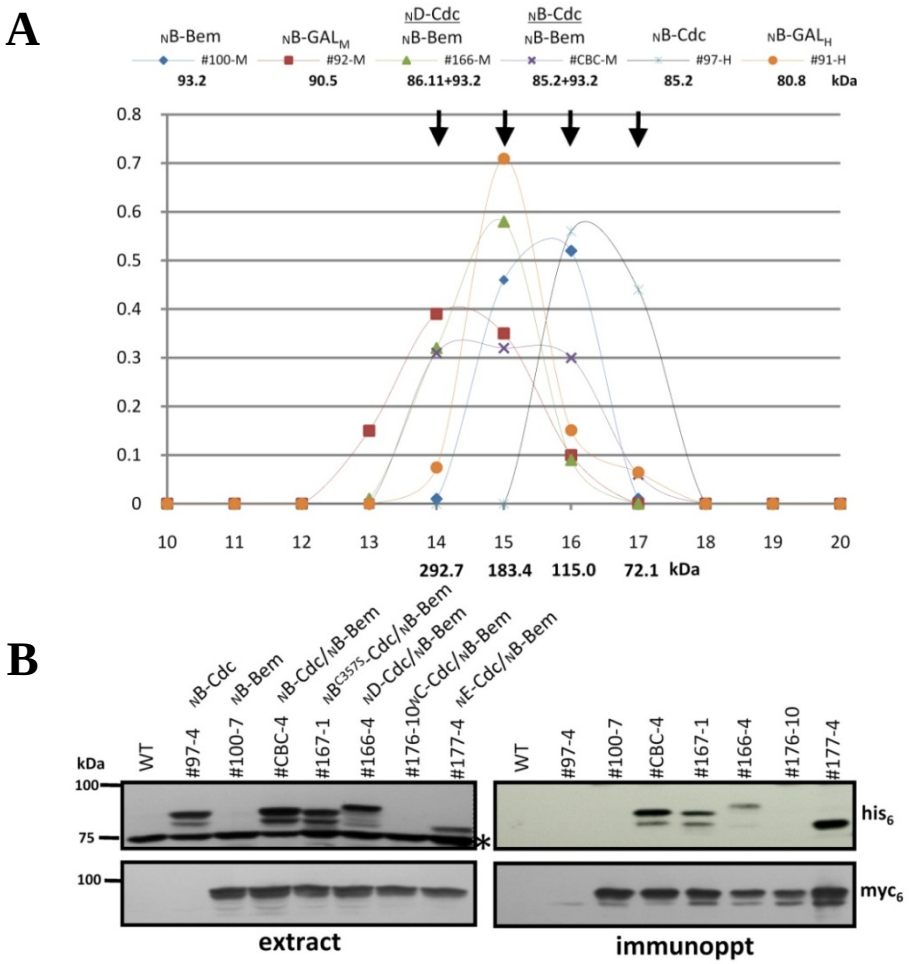


Figure 2.5. Bem/Cdc domain and GAL domain-directed dimerization *in vivo.* (A) Size exclusion chromatography (SEC) analysis. Extracts of WLc-grown seedlings were fractionated on a Superose 6 SEC column and 1.0ml fractions were collected. Aliquots of the fractions were separated on SDS-PAGE gels, blotted and probed with the anti-myc_6 or anti-his_6 Abs. Profiles of scanned immunoblots for the NB-Bem, $NB\text{-}GAL_M$, NB-Bem/ND-Cdc, NB-Bem/NB-Cdc, NB-Cdc, $NB\text{-}GAL_H$ transgene products from SEC of the indicated transgenic lines. (B) Immunoblots of extracts and myc antibody IPs from doubly transgenic lines expressing NB-Cdc, NB-Bem, NB-Cdc/NB-Bem, NB^{C357S}-Cdc/NB-Bem, ND-Cdc/NB-Bem, NC-Cdc/NB-Bem and NE-Cdc/NB-Bem transgenes. Seedlings of the indicated lines were grown for 5d under white light conditions, extracts were prepared and immunoprecipitated with anti-myc_6 antibody, and immunoblotting was performed with the anti-his_6 antibody. A small amount of degradation of each extract occurs under white light conditions.

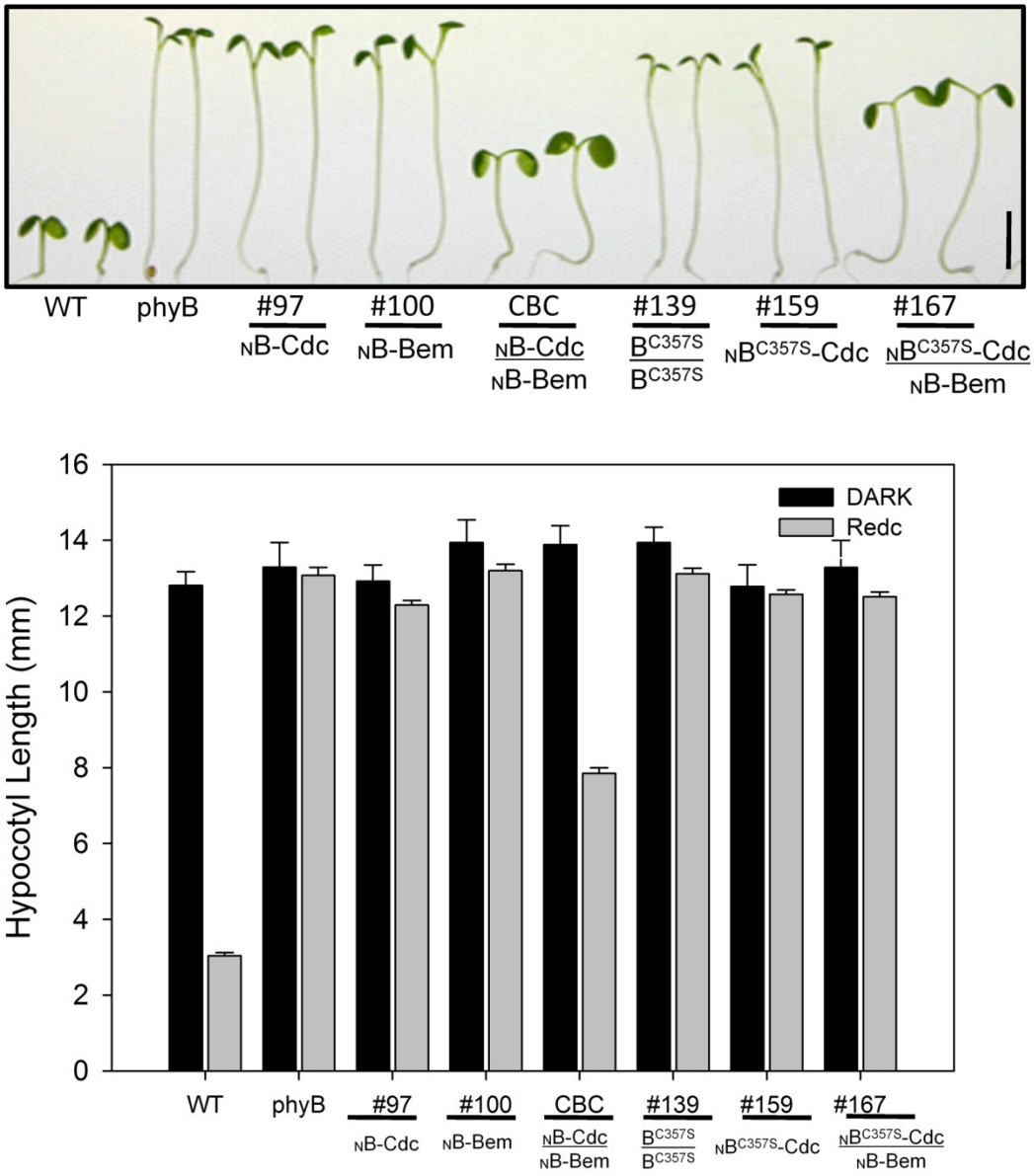


Figure 2.6. PhyB/achromo-phyB dimers are non-functional in hypocotyls. Morphology (top) and hypocotyl measurement (bottom) of the *phyB* mutant seedlings expressing NB-Cdc, NB-Bem, NB-Cdc/NB-Bem, full-length phyB^{C357S}, NB^{C357S}-Cdc and NB^{C357S}-Cdc/ NB-Bem. Seedlings of two independent lines of each indicated construct were exposed to 3h white light to induce germination and then grown for 5 days in the dark or under continuous R (25umolm^{-2}s^{-1}). Error bars represent the SE of 2×(20-30) seedlings (mean ± SE; n=40-60). Bar=3mm.

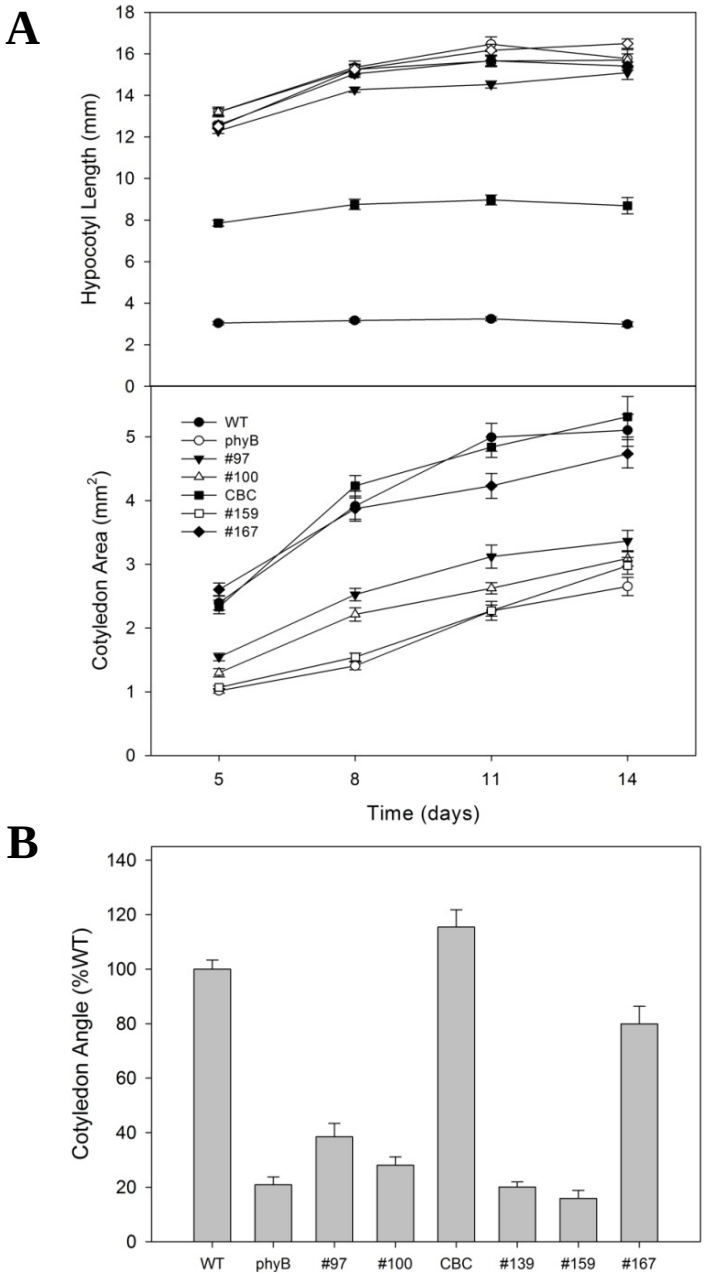


Figure 2.7. Nuclear-localized chromophore-ligated NB dimers are required for hypocotyl inhibition. (A) PrPfr-like $_{N}B^{C357S}$-Cdc/ NB-Bem does not affect hypocotyl growth but promotes cotyledon growth. Seedling hypocotyl elongation and cotyledon expansion measurements of the indicated lines were recorded following growth on MS agar under continuous R (25umolm^{-2}s^{-1}) for 5, 8, 11 or 14 days (mean ± SE; n=40-60). (B) Cotyledon angles in the indicated lines grown in the continuous R (25umolm^{-2}s^{-1}) for 5 days (mean ± SE; n=40-60).

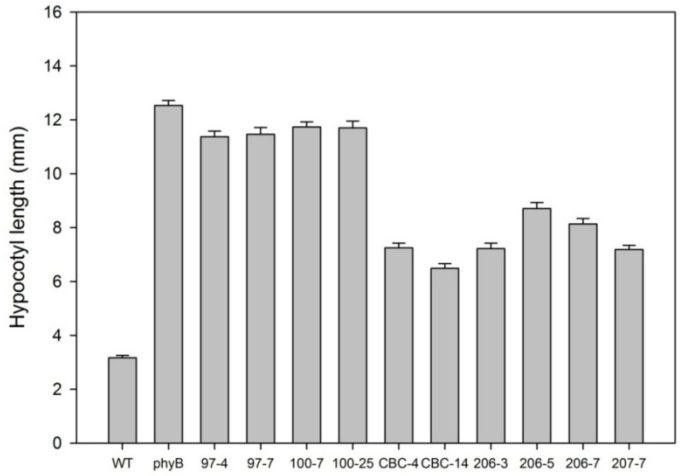


Figure 2.8. R light sensitivity is restored in the doubly transgenic *phyB*(NB-Cdc/NB-Bem) lines generated by crossing or double transformation. Hypocotyl measurement of the *phyB* mutant seedlings expressing NB-Cdc, NB-Bem and NB-Cdc/NB-Bem. The #206 and #207 lines were generated by sequential transformation either starting from NB-Cdc to NB-Bem, or the opposite direction, respectively. Seedlings of each independent line were treated with 3h white light to induce germination and then grown for 5 days under continuous R (25umol$m^{-2}s^{-1}$). Error bars represent the SE of 1×(20-30) seedlings (mean ± SE; n=20-30).

Yeast GAL4 Domain-Directed Homodimerization
of the NB or ND PSRs, but not NC or NE,
Induces Photosensing Activities

As a second approach to assembling phy PSR regions in a directed way *in vivo*, the homo-dimerization domain of the yeast GAL4 protein (Carey et al., 1989; Marmorstein et al., 1992) was fused to the C-terminus of the NB PSR region, followed by an epitope tag and the SV40 NLS (Figure 2.2A). Figure 2.9 shows that *phyB*(NB-GAL[his_6-NLS]) #91 and *phyB*(NB-GAL[myc_6-NLS]) #92 lines, which differ only in their epitope tags, express their transgene products at approximate 3-fold and 10-fold that of endogenous phyB respectively, suggesting that homodimerization via the GAL4 sequences, like dimerization mediated by the Bem/Cdc interaction, yields a stable NB PSR construct. The homologous N-terminal 600-650 residue long regions of phyC,

phyD, and phyE were also incorporated into GAL4-based chimeric transgenes and transformed into *phyB* host plants. These chimeric proteins are present in the *phyB*(ND-GAL[his_6-NLS]) #189, *phyB*(NC-GAL[myc_6-NLS]) #109, and *phyB*(NE-GAL[myc_6-NLS]) #125 lines at 5-fold, 1/4-fold, and 4-fold that of endogenous phyB in WT *Arabidopsis* respectively (Figure 2.9). To demonstrate the self-interaction of the yeast GAL domain used in these constructs, SEC of extracts of the lines expressing the NB-GAL-[myc_6–NLS] (Abbreviated NB-GAL_M) and NB-GAL-[his_6–NLS] (Abbreviated NB-GAL_H) proteins shows that they migrate as dimers (Figure 2.5A).

Seedlings of lines expressing the NX-GAL fusion proteins grown under continuous R light (25 $umolm^{-2}s^{-1}$ $\times$5 days) are shown in Figure 2.10A. The NB-GAL homodimers in lines #91 and #92 are both more active in complementing the *phyB* hypocotyl elongation and cotyledon expansion phenotypes than are NB-Bem/NB-Cdc dimers. The #336 and #210 lines, which over-express his_6 or myc_6 tagged full-length phyB by two to four-fold, show the expected mild R hypersensitivity compared to wild-type (Wester et al, 1997), but none of the chimeric receptors mediates hypersensitivity to R light at this fluence. Compared to the NB-GAL_H in line #91, the ND-GAL fusion protein in line #189 is more highly expressed (Figure 2.9) but is much less active in R sensing/signaling, particularly with regard to hypocotyl elongation (Figure 2.10A). This suggests that phyD/phyD homodimers, which do form in cells (Sharrock, Clack, and Goosey, 2003), may signal less effectively through hypocotyl cell light transduction pathways than phyB/phyB homodimers. The NC-GAL (line #109) and NE-GAL (line #125) transgene products are inactive. Native full-length phyC and phyE

do not form homodimers in *Arabidopsis* (Clack et al., 2009), so this latter finding is not unexpected.

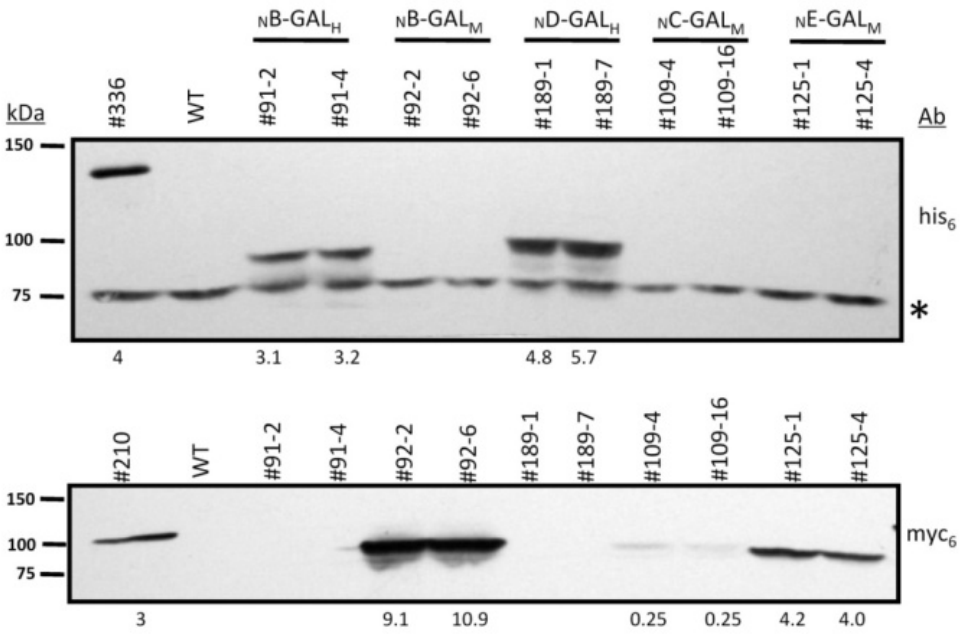


Figure 2.9. Expression of yeast GAL4 domain-mediated homodimeric phyB, phyC, phyD, and phyE. Immunoblot analysis of relevant transgene-encoded phy levels in *phyB*(NX-GAL) lines (X=B, C, D and E), and two control lines, the *phyB*(*PHYB*-myc$_6$) and the *phyB*(his$_6$-*PHYB*) lines. Total protein extracts from 5-d-old de-etiolated seedlings were probed with anti-his$_6$ or anti-myc$_6$ antibody.

Figure 2.10B shows R fluence response curves for hypocotyl elongation in representative *phyB*(NB-GAL), *phyB*(ND-GAL), and *phyB*(NB-Cdc/NB-Bem) CBC lines, and for the two full-length epitope-tagged *phyB*(*PHYB*) #210 and #336 lines. Seedlings expressing full length phyB, including the WT and the transgenic #210 and #336 lines, show the expected negative slope of hypocotyl length when exposed to increasing R fluence rates, with the 2 to 4-fold over-expressing #210 and #336 lines exhibiting hypersensitivity relative to WT at fluences over 0.1 umolm^{-2}s^{-1}, in the range of R-HIR

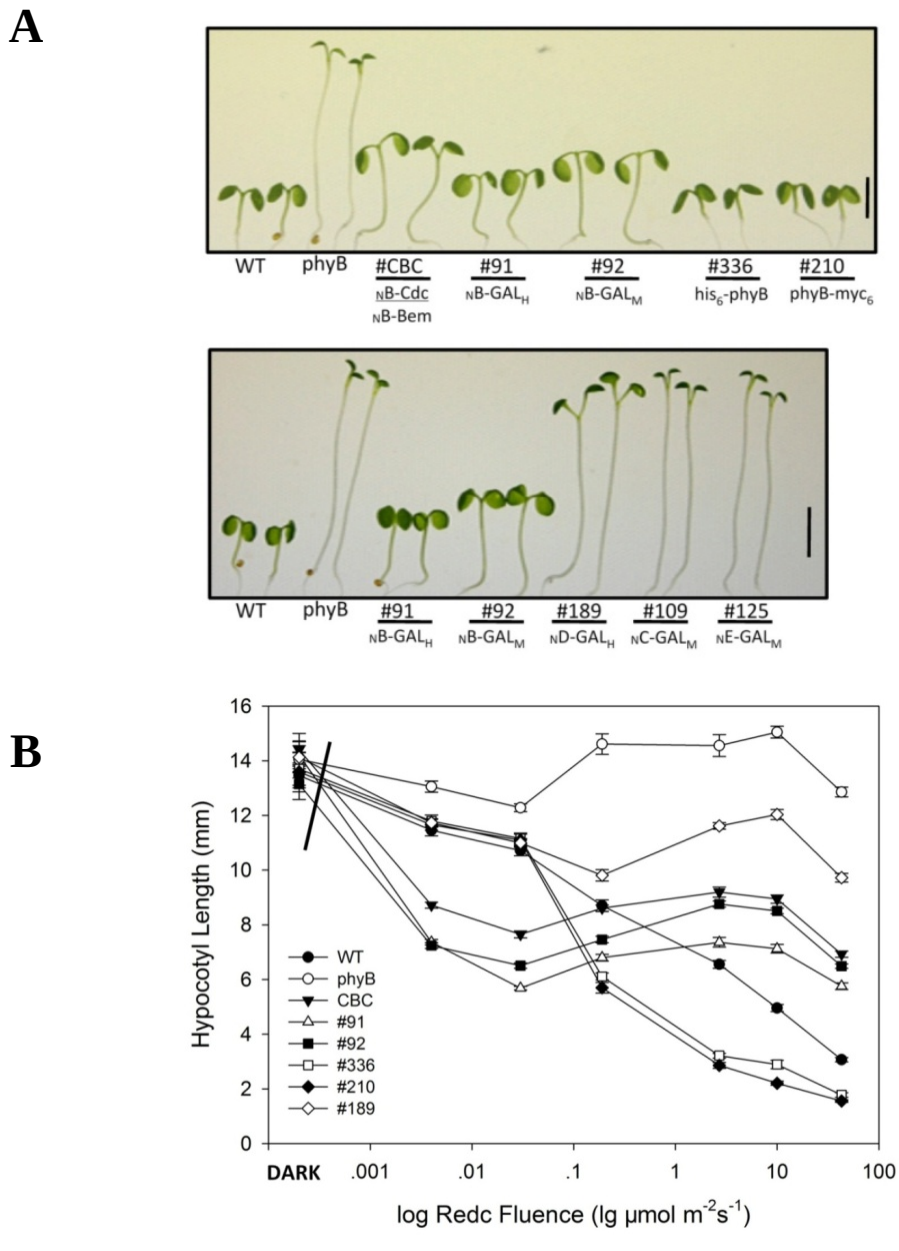


Figure 2.10. Activities of NB-containing and ND-containing dimeric phytochromes. (A) Morphology (top) of 5-day-old WT, *phyB*, *phyB*(NB-Cdc/NB-Bem), *phyB*($_N$B-GAL$_H$) and *phyB*($_N$B-GAL$_M$), *phyB*(P_B-phyB-myc$_6$) and *phyB*(P_B-his$_6$-phyB) seedlings grown in 25umolm^{-2}s^{-1} R light for 5 days. Morphology (bottom) of 5-day-old representative seedlings of the WT, *phyB*, *phyB*($_N$B-GAL$_H$) and *phyB*($_N$B-GAL$_M$), *phyB*($_N$D-GAL$_H$), *phyB*($_N$C-GAL$_M$), and *phyB*($_N$E-GAL$_M$) lines. Bar=3mm. (B) Fluence response of hypocotyl length to dark and continuous R. Seedlings of the WT, *phyB*, *phyB*(NB-Cdc/NB-Bem), *phyB*($_N$B-GAL$_H$), *phyB*($_N$B-GAL$_M$), *phyB*(*PHYB*-myc$_6$) and *phyB*(his$_6$-*PHYB*) and *phyB*($_N$D-GAL) lines were incubated for 3h white light to induce germination and then grown for 4 days in the dark or under a range of continuous R (mean ± SE; n=40-60).

responses. In contrast to this, all of the directed dimer NB-containing PSR constructs cause a striking hypersensitivity to low fluences of R (< 0.1 $\mu molm^{-2}s^{-1}$) but lack response to increasing amounts of R (Figure 2.10B). Therefore, NB-GAL and NB-Cdc/NB-Bem dimers mediate stronger inhibition of hypocotyl elongation than is seen in the WT under low fluence R, but they are not further activated over a 10^4-fold increase in R fluence. This suggests that the fusion proteins can signal very efficiently to regulatory circuitry at low Pfr/Ptot ratios, but they cannot convert an increase in Pfr into higher signaling output.

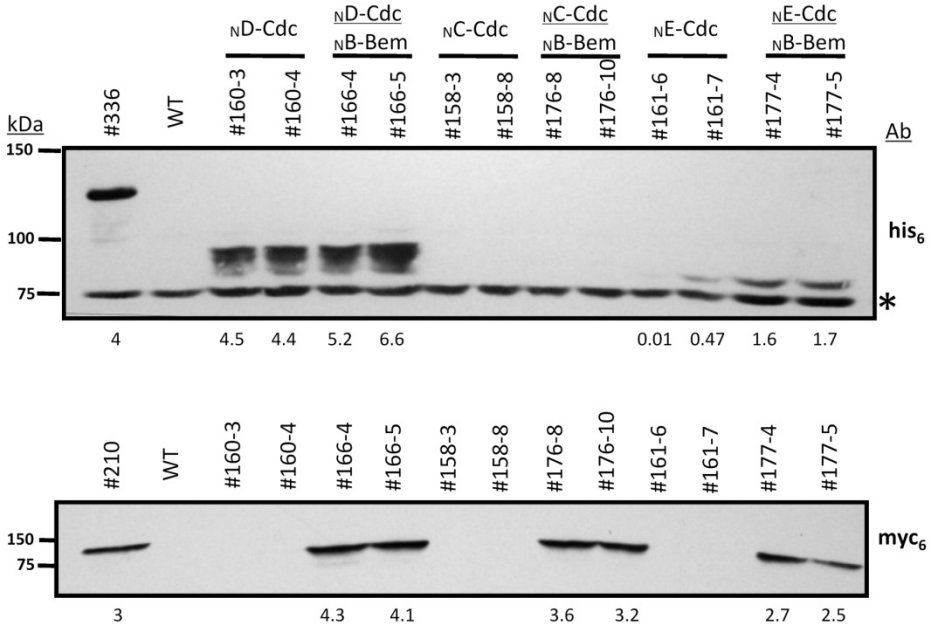


Figure 2.11. Expression of the singly *phyB*(NX-Cdc) and doubly transgenic *phyB*(NX-Cdc/NB-Bem) (X=C, D and E) lines. Immunoblot analysis and relative NX chimeric protein levels in transgenic *phyB*(ND-Cdc), *phyB*(ND-Cdc/NB-Bem), *phyB*(NC-Cdc), *phyB*(NC-Cdc/NB-Bem), *phyB*(NE-Cdc), *phyB*(NE-Cdc/NB-Bem), and two control lines, the *phyB*(*PHYB*-myc$_6$) and the *phyB*(his$_6$-*PHYB*) lines. Total protein extracts from 5-d-old WL-grown seedlings were probed with anti-his$_6$ or anti-myc$_6$ antibody.

NB/ND Heterodimers are Functional and Mediate R Hypersensitivity

The directed dimer system has been used to investigate the activities of discrete phy heterodimer forms. NX-Cdc transgenes (X= C, D, or E), containing the N-terminal halves of the different type II phytochromes, were constructed and introduced into the *phyB* mutant and into *phyB*(NB-Bem) line #100-7, generating doubly transgenic *phyB*(NX-Cdc/NB-Bem) lines and the corresponding *phyB*(NX-Cdc) control lines (Figure 2.2A). As shown in Figure 2.11, the ND-Cdc protein is expressed well and, unlike NB-Cdc, is not less stable in the absence of a binding partner NB-Bem protein than in its presence. The NE-Cdc is weakly expressed on its own and is stabilized when co-expressed with NB-Bem. The NC-Cdc protein is present in extracts in very low amounts when expressed either alone or with NB-Bem and was detected on blots only at very long exposures. Figure 2.11 also shows that all of the doubly transgenic lines express the NB-Bem dimerization partner protein at similar levels. An immunoblot comparing the levels of the his_6-tagged NB-GAL, NB-Cdc, NB^{C357S}-Cdc, ND-GAL, and ND-Cdc proteins in key lines used in these experiments confirms that they are present in transgenic lines at comparable steady-state levels (Figure 2.13). Size exclusion chromatography analysis shows that, when co-expressed, the NB-Bem and ND-Cdc proteins form a dimer (Figure 2.5A).

Representative seedling phenotypes of transgenic lines expressing NX-Cdc monomers, NX/NB heterodimers, or NX-GAL homodimers (X = C, D, or E) are quantified in Figure 2.12. The *phyB*(ND-Cdc/NB-Bem) #166 lines are strongly complemented for hypocotyl elongation, cotyledon expansion, and cotyledon opening, demonstrating that

this heterodimeric NB/ND form is strongly active in R sensing/signaling. *phyB*(NE-Cdc/NB-Bem) #177 lines are not complemented for hypocotyl elongation but show expanded cotyledons compared to the NE-Cdc alone control (Figure 2.12A). Surprisingly, *phyB*(NC-Cdc/NB-Bem) #176 lines, which contain nearly undetectable levels of the NC-Cdc subunit, show marked opening of their cotyledons relative to their monogenic control lines and relative to the *phyB*(NE-Cdc/NB-Bem) #177 lines, which are more active in cotyledon expansion (Figure 2.12B). Hence, various combinations of phy PSRs that have been assembled with each other, have differential regulatory activities. These results suggest that B/B, D/D, B/D, B/C, and B/E dimers, which all form from full-length phy monomers *in vivo* (Clack et al., 2009), have differential activities in seedling hook and cotyledon tissues.

R fluence response curves and representative 5-day old seedlings from these curves for *phyB*(ND-Cdc/NB-Bem) #166 and *phyB*(NB-Cdc/NB-Bem) CBC lines compared to WT are shown in Figure 2.14. Cotyledon expansion, cotyledon angle, and hypocotyl elongation are all hypersensitive to low R fluences (0.1 $umolm^{-2}s^{-1}$ or less) in the two PSR fusion lines (Figure 2.14A). This effect is stronger in ND-Cdc/NB-Bem than NB-Cdc/NB-Bem lines, likely because these protein partners dimerize more efficiently (Figure 2.5A). Whereas hypocotyl length in the directed dimer lines shows almost no change with increasing R fluence and cotyledons are maximally open even at the lowest fluence, cotyledon area in these lines progressively increases over the entire fluence range. Hence, directed NB/NB and ND/NB PSR dimers promote markedly different light sensitivities for different responses.

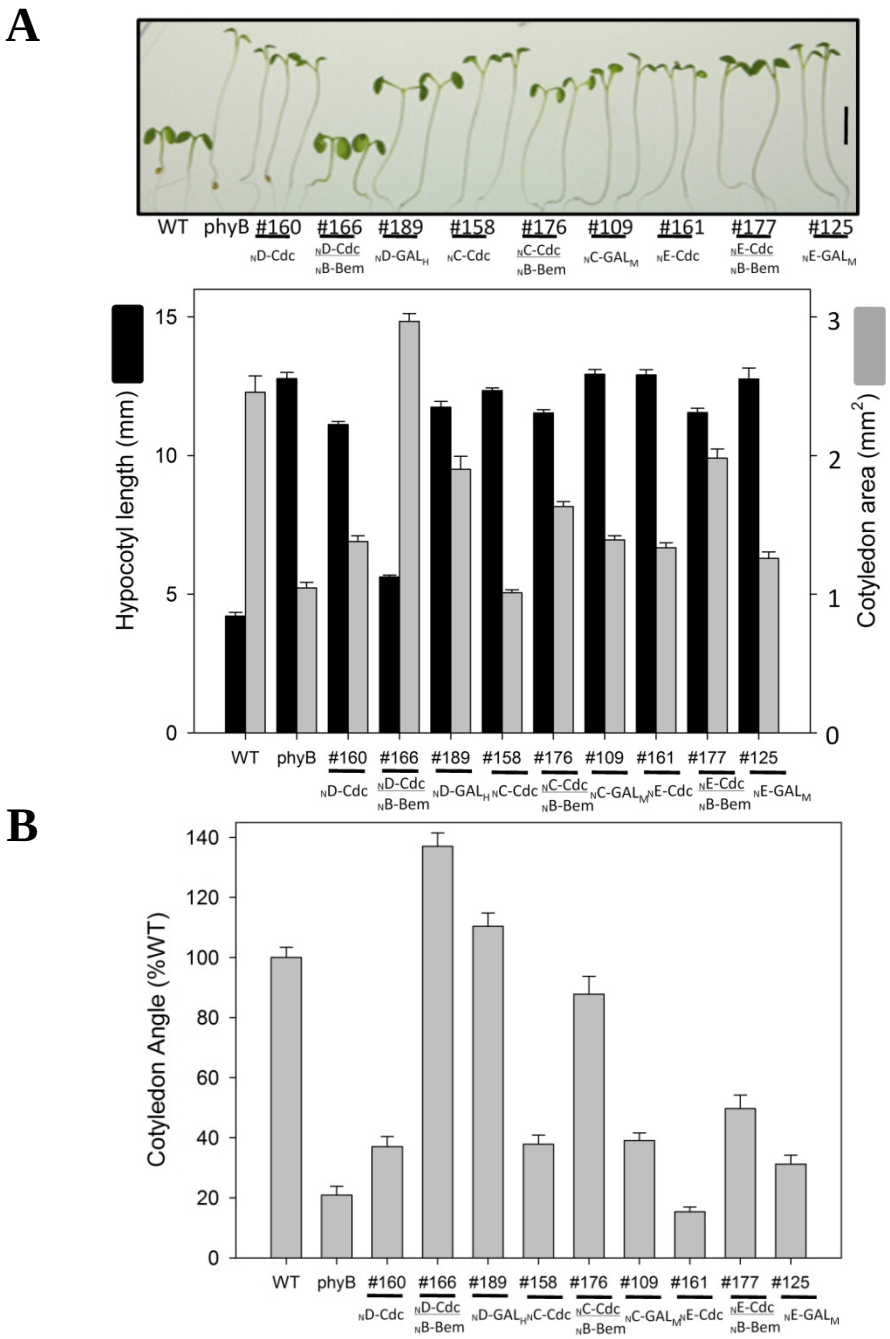


Figure 2.12. Various R light responses of the singly *phyB*(NX-Cdc) and doubly transgenic *phyB*(NX-Cdc/NB-Bem) (X=C, D and E) lines. (A) Representative seedling phenotypes of the indicated lines. Seedlings of two independent lines of each indicated construct were incubated for 3h white light to induce germination and then grown for 5 days in the dark or under continuous R (25umolm^{-2}s^{-1}). Bar = 3mm. Hypocotyl lengths and cotyledon areas of lines from part B grown under continuous R (25umolm^{-2}s^{-1}) for 5 days (mean ± SE; n=40-60). (B) Cotyledon angles of lines from part B grown under continuous R (25umolm^{-2}s^{-1}) for 5 days (mean ± SE; n=40-60).

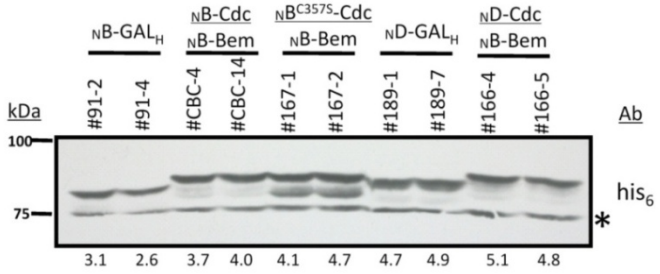


Figure 2.13. NB and ND transgene products are present at comparable steady-state levels in various transgenic lines. Immunoblot analysis and relative transgene-encoded protein levels in the *phyB*(NB-GAL), *phyB*(NB-Cdc/NB-Bem), *phyB*($^{NB^{C357S}}$-Cdc/NB-Bem), *phyB*(ND-GAL), and *phyB*(ND-Cdc/NB-Bem) lines. Total protein extracts from 5-d-old WLc seedlings were fractionated by SDS-PAGE, blotted, and probed with anti-his_6 antibody.

Directed Dimers Mediate Mature Plant R Light Responses

Directed phy PSR dimers remain active as plants mature and can influence light responses throughout the life cycle. Figure 2.15A shows the morphologies of control and dimer-producing lines following growth for 40 days under continuous R (15 $umolm^{-2}s^{-1}$). The first true leaves emerge from the apical meristem in all lines, including the *phyB* parent, however all of the dimer-producing lines exhibit more robust rosettes with more and larger leaves. The *phyB*($^{NB^{C357S}}$-Cdc/NB-Bem) #167 line is complemented for many aspects of adult morphology compared to the #100 and #159 control lines, demonstrating a surprisingly strong capacity for chromo-NB/achromo-NB structural heterodimers to mediate R responsiveness. In Figure 2.15A, the ABO 35S:phyB line (Wagner, Hoecker, and Quail, 1997) exhibits the well-known FL-phyB overexpression dwarf phenotype. It has been observed that the ABO line also flowers early compared to both the WT and *phyB* mutant, which is counterintuitive (Bagnall et al., 1995). Nevertheless, like the ABO line, the various lines expressing NB/NB, ND/ND,

or ND/NB dimers flower early while the control lines flower similar to the *phyB* parent (Figure 2.15B). Interestingly, pronounced early flowering is seen in the *phyB*(ND/ND) #189 line, which shows little effect of the transgene on seedling phenotypes (Figure qq).

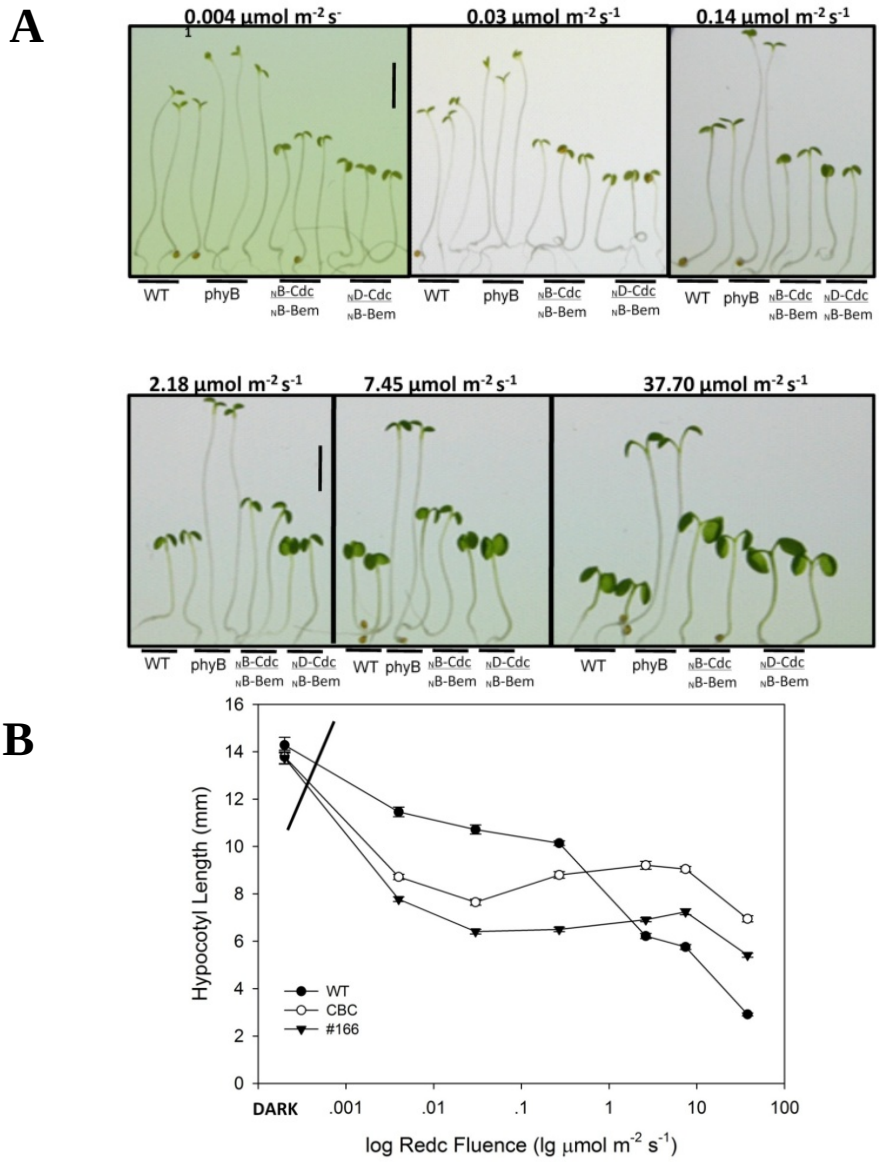


Figure 2.14. Directed NB/ND heterodimers suppress hypocotyl elongation very effectively. (A) Seedling morphologies of the WT, *phyB*, *phyB*(NB-Cdc/NB-Bem) CBC and *phyB*(ND-Cdc/NB-Bem) #166 lines under a range of continuous R. Plants were incubated for 3h white light to induce germination and then grown for 4 days in the dark or under the continuous R fluences. Bar=3mm. (B) Fluence response of hypocotyl length to continuous R. 5-day-old seedlings of the lines from part (A) were grown in the dark or under varying continuous R fluences (mean ± SE; n=40-60).

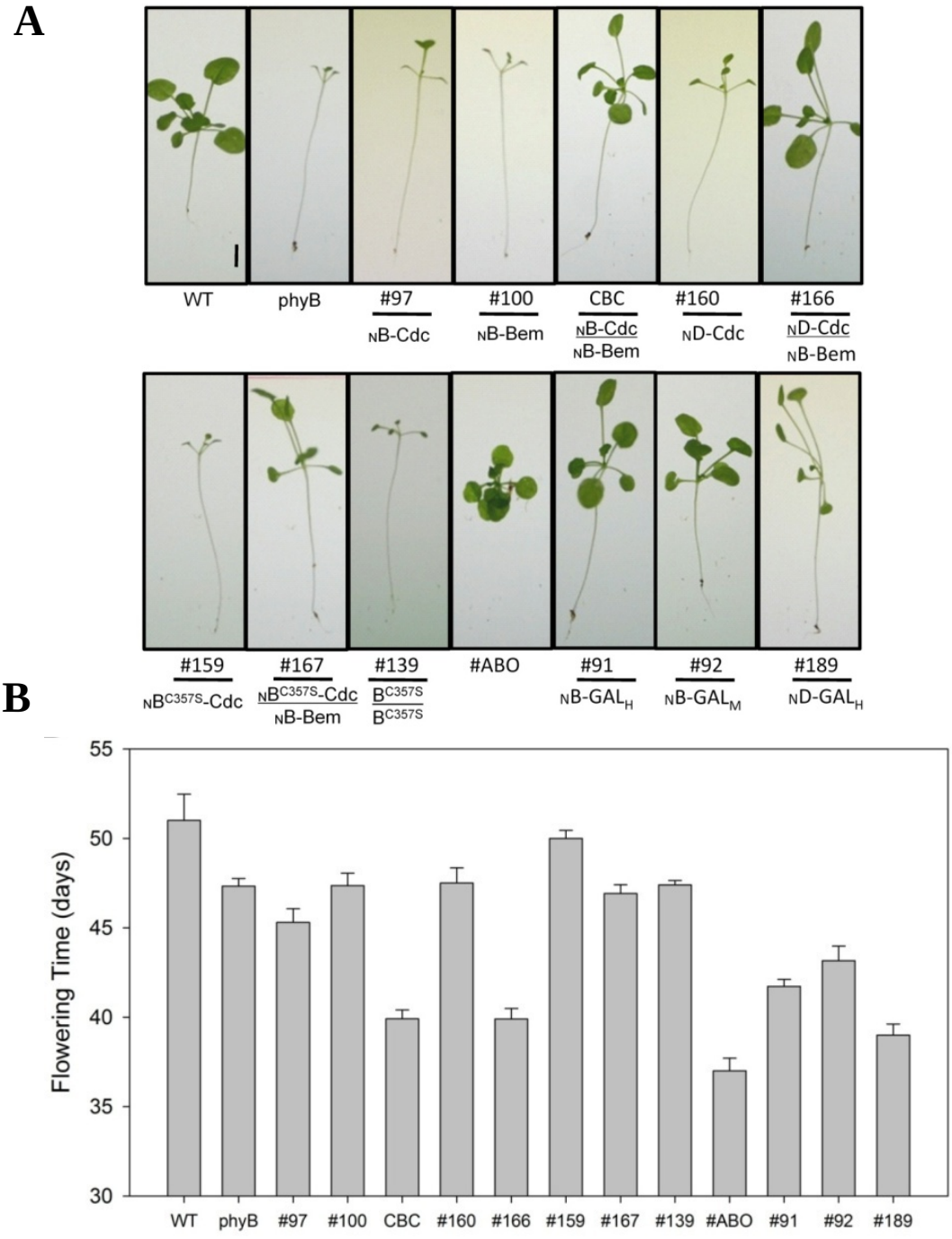


Figure 2.15. Diverse adult plant R-sensing activities observed in the NB and ND-containing transgenic lines. (A) Rosette leaf phenotypes of 40-day-old seedlings grown under a low continuous R (15 umolm^{-2}s^{-1}). Bar=3mm. (B) Flowering times under a high continuous R (90 umolm^{-2}s^{-1}) were observed for the indicated lines. Error bars represent the SE for 12 plants.

Discussion

Plants have evolved sophisticated photosensory systems to optimize their growth and development in response to a changing environment. Previous work has shown that Arabidopsis contains mixed phytochrome homodimers and heterodimers (Clack et al., 2009). Unlike the two major homodimeric phyA and phyB, the functions of other phy are difficult to elucidate by traditional genetic approaches. Here, we describe a novel *in vivo* expression system to extend functional studies to these type II heterodimers and to assess whether homodimers of phyC or phyE, which do not normally form in plant cells, have any biological activity.

Dimerization of PhyB PSRs in the Nucleus is Required for Signaling

R/FR sensing phytochrome functions as a collection of interchangeable modules. Three synthetic phytochrome-mediated signaling systems have previouly been successfully engineered into bacteria, yeast and mammalian cells (Levskaya et al., 2005; Levskaya et al., 2009; Shimizu-Sato et al., 2002). To investigate the N-terminal PSR of phyB in signal transduction, a plant *in vivo* expression system was first developed by expressing a NB-GFP fusion protein (NG) attached to GUS and NLS (NG-GUS-NLS) in the *phyB* mutant (Matsushita, Mochizuki, and Nagatani, 2003). The analysis of the NG-GUS-NLS transgene product showed that the N-terminal 651 aa phyB alone was sufficient for signaling when dimerized in the nucleus. Palágyi et al. (2010) reported both B651-NLS and B450-NLS were effective in hypocotyl suppression (Palagyi et al., 2010). Here, I present the following evidence to support that dimeric phyB PSRs in the nucleus

participate in signal transduction in plants. (1) Three nuclear chimeric NB dimers without the C-terminus of phyB, NB-Cdc/NB-Bem, NB-GAL_H and NB-GAL_M all show strong photoactivities in control of seedling establishment and flowering. (2) Monomeric NB-Cdc and NB-Bem are inactive in plants. (3) The chimeric C-terminus of NB^{C357S}-Cdc and the full-length B^{C357S} intact C-terminus do not mediate light signal transduction due to loss of chromophore in the phyB PSR.

Different activities for the NB module were generated from different C-terminal dimeric modules in the transgene products. Figure 2.10B shows that NB-Cdc/NB-Bem has weaker photoactivity than either of the NB-GAL constructs in hypocotyl inhibition under R. SEC analysis in Figure 2.5A demonstrates that NB-GAL_M forms almost entirely homodimers in the *phyB*(NB-GAL_M) line, but a significant portion of NB-Cdc and NB-Bem monomers still exists in the *phyB*(NB-Cdc/NB-Bem) line. This suggests that stronger phyB C-terminal dimeric interactions improve phyB activity. The NG-GUS-NLS chimeric protein (Matsushita, Mochizuki, and Nagatani, 2003) shows hypersensitivity to R, probably resulting from the C-terminal GFP-GUS-NLS module providing strong interaction with itself. Evidence has been presented that the two GUS modules used by Matsumura et al form not only dimers but a majority of tetramers, perhaps providing very strong interaction with themselves (Geddie and Matsumura, 2007), and GFP molecules also readily form dimers (Ward and Cormier, 1979). Because of these considerations, the new *in vivo* directed dimer expression system presented here may facilitate direct comparison of interactions of two sets of novel proteins.

PhyB instability in the light mainly results from a direct interaction between the phyB PSR and its E3 ligase COP1 in the nucleus (Jang et al., 2010). The observation that formation of NB-Cdc/NB-Bem or $_{N}B^{C357S}$-Cdc/NB-Bem dimers stabilizes their two monomer components in the light (Figure 2.2B), suggests that monomeric phyB PSR is differentially targeted for degradation in the light and dimerization of phyB PSRs may protect some key residues on the flank of the molecule from ubiquitination. This is the first time it has been demonstrated that phytochrome dimerization improves protein stability in the light. Although phy nuclear bodies are regarded as the likely cellular location for phy proteolysis, strong phy activity also correlates with the formation of large nuclear bodies (Chen, Schwab, and Chory, 2003). This implies that phy dimerization and assembly with other proteins in the nucleus results in signal magnification in cells. In contrast to this, the similar steady state levels of the NB-Bem proteins as monomers in the *phyB*(NB-Bem) lines and as dimers in the *phyB*(NB-Cdc/NB-Bem) lines in the dark (Figure 2.4) indicates that, even when localized to the nucleus, the phyB Pr form is not targeted by COP1 and degraded.

The C-terminal Module of PhyB is Important for Regulating Signaling

When exposed to R from low to high fluences, the full-length phyB-containing lines #336, #210 and WT all have the ability to sense light intensity, showing a continuous decline of hypocotyl elongation with increasing R fluence (Figure 2.10B and 2.14B), whereas the yeast domain-mediated transgenic lines, are equivalently responsive at all fluences (Figure 2.10B and 2.14B). This suggests that the lack of the native

C-terminal domain of phyB results in loss of R fluence rate sensitivity. Interestingly, the directed NB-Cdc/NB-Bem and NB-GAL dimers show hypersensitivity in very low to low fluence rates of continuous R, but exhibit hyposensitivity under high R irradiation (Figure 2.10 and 2.14B). There are several possibilities to explain this. One is that there may be different molecular mechanisms involved in the dim light and strong light conditions. With regard to this, evidence has been presented that the native C-terminal module attenuates the R-sensing N-terminal module on transfer from dark to light (Matsushita, Mochizuki, and Nagatani, 2003). A more likely explanation is that the chimeric NB localized in the nucleus in the dark due to presence of the SV40 NLS may have some advantages in sensing dim light. Under higher R fluences, the non-native R-sensing structures of NB-Cdc/NB-Bem and NB-GALs, compared with a more compact native phyB, may impede photo signaling and transduction. Recent experiments not included in this thesis demonstrate that phyB-NLS-EYFP fusion protein shows stronger hypersensitivity than NB-Cdc/NB-Bem and NB-GALs in the same low R fluence conditions, while a phyB-EYFP fusion protein even overexpressed in the *phyB* mutant, only shows a normal wild-type phenotype.

Previous evidence has also shown that the C-terminal domain of phyB is critical for phyB activity. The B651-NLS transgene product (Palagyi et al., 2010) and several phyB C-terminal mutations (Elich and Chory, 1997; Krall and Reed, 2000b), which do not affect dimerization or nuclear translocation, also have hyper- or hypo-activities. Some important signaling factors have been shown to physically interact with the phyB C-terminus. In a yeast two-hybrid system, E3 ligase COP1 shows a direct interaction with

the C-terminal region of phyB (Yang, Tang, and Cashmore, 2001). Phytochrome kinase substrate 1 (PKS1) which acts as a negative regulator of phytochrome signaling can directly bind the HKRD subdomain of the phyB Pr form in cytosol (Fankhauser et al., 1999b). Phy heterodimer formation also requires that the phyB C-terminus directly bind to the C-terminus of other type II phys, so the normal phyB-containing heterodimeric phys will not form in NB-expressing transgenic lines.

PhyB/D Heterodimers may Have Higher Activity than PhyB Homodimers

The phenotypes of phy individual and multiple null mutant lines indicate that phytochrome synergistic effects exist in hypocotyl inhibition and flowering. Under white light, continuous R light or end-of-day FR light conditions, the amount of increased hypocotyl length of the *phyBphyD* double mutant surpasses the total amount of increased hypocotyl length of the *phyB* mutant plus that of the *phyD* mutant in either the Ws or L*er* genetic background (Aukerman et al., 1997). And the difference in flowering time is also greater between the double *phyB/phyD* mutant and WT than the total difference between the *phyB* mutant and WT plus the difference between the *phyD* mutant and WT (Clack et al., 2009). Although NB-Cdc/NB-Bem and ND-Cdc/NB-Bem exhibit similar protein expression levels (Figure 2.13), ND-Cdc/NB-Bem has a relatively higher effect on seedling growth in response to R. Therefore, it is possible that the synergistic effect arises from the direct interaction between phyB and phyD.

It has become clear that correct phytochrome folding and chromophore position are important for function. For example, the $PHYB^{Y276H}$ and $PHYA^{Y242H}$ mutants exhibit

constitutive photomorphogenesis in the dark (Bae and Choi, 2008; Su and Lagarias, 2007). The proposed quaternary structure of the bacteriophytochrome (DrBphP) dimer derived from both cryoelectron microscopy (cryoEM) and crystal structures shows that the C-terminal region and the N-terminal bilin-binding region of DrBphP provide a dimerization interface (Li, Zhang, and Vierstra, 2010). Tight interaction occurs between ND-Cdc and NB-Bem (Figure 2.5A). Since the ND monomer is more stable in cells in the light than the NB monomer (Figure 2.11), the phyB/D heterodimer chimera may be more stable in the nucleus than the phyB/B chimera. Therefore, it is possible that the NB/ND quaternary structure might be more suitable for light perception and signal transduction.

Heterodimers Mediate Tissue-specific Growth and Development in De-etiolated Seedlings and Flowering

Recently, a crystal structure of a point mutant (Q188L) of the *Pseudomonas aeruginosa* bacteriophytochrome photosensory core module (PaBphP-PCM) was reported, which displays a mixed Pfr and Pr state, distinct from either the Pr state or the Pfr state (Yang, Kuk, and Moffat, 2009). This indicates that phytochromes may contain a unique function in this Pr/Pfr state. The $_{N}B^{C357S}$-Cdc/NB-Bem achromo/chromo transgene products are likely to resemble the phytochrome intermediate PrPfr in the light, in which the NB-Bem half is functional and the $_{N}B^{C357S}$-Cdc half is nonfunctional. Figure 2.7A shows that when exposed to R, $_{N}B^{C357S}$-Cdc/NB-Bem can fully complement the cotyledon phenotype of the phyB mutant, but has no effect on hypocotyls. Cotyledon expansion shows light duration- dependence. (Figure 2.7A). In addition, the observation of post seedling development and flowering shows that both NB-Cdc/NB-Bem and

$_{N}B^{C357S}$-Cdc/$_{N}$B-Bem significantly promote the emergence of true leaves, but only $_{N}$B-Cdc/$_{N}$B-Bem enhances early flowering (Figure 2.15A &B).

It is perhaps difficult to draw firm conclusions about the specific activities of the different naturally-occuring phy dimers from results with the directed dimer system because the protein structures produced in the directed dimers are highly engineered. Positioning of phy PSRs relative to each other may be altered or constrained in the chimeric dimers compared to native full-length molecules. Nevertheless, it is clear that synthetic association of phy PSRs both activates their signaling functions and results in differential activities depending upon which PSRs are dimerized. This may quite closely recapitulate the situation with wild-type phys, where differential activities can at least in part be associated with phy heterodimers by genetic comparisons (Clack et al., 2009).

Similar to the PrPfr-like $_{N}B^{C357S}$-Cdc/$_{N}$B-Bem, both $_{N}$C-Cdc/$_{N}$B-Bem and $_{N}$E-Cdc/$_{N}$B-Bem in this novel *in vivo* expressing system show strong effects on cotyledons, but not on hypocotyls (Figure 2.12). Despite the low expression level of $_{N}$C, synthesized $_{N}$B/$_{N}$C dimers are more active in cotyledon separation, while the $_{N}$B/$_{N}$E dimers function more in cotyledon expansion. I have also demonstrated that phyB/D heterodimers are very active in hypocotyl inhibition, seedling morphology and flowering (Figure 2.14A-B & 2.15). Despite comprising only approximately 10% of total phytochromes present in these transgenic plants, these engineered heterodimeric molecules have significant potential to fine-tune plant growth and development through heterodimer-mediated tissue-specific growth.

Phytochrome's Smart Evolutionary Way to Function in the Nucleus

Analysis of the distribution of phytochromes in prokaryotic and eukaryotic organisms has been beneficial for understanding their origins and evolution. Protein oligomerization is a ubiquitous phenomenon in living systems and is fundamental to many biological functions. Protein oligomers, frequently being homodimers and heterodimers, facilitate fast quaternary structural formation, enhance protein stability, and improve specific interactions with their downstream substrates.

The origin of plant phytochromes is believed to have arisen from a cyanobacterium phy (Cph) when a photosynthetic cyanobacterium was captured by an ancient eukaryotic plant cell. To optimize functioning in a new environment, ancient Cph evolved significantly, which adjusted the N-terminal light absorption region to better regulate plant photosynthesis, recruited the PAS-PAS domain to lead phytochrome into the nucleus, and converted the histidine-kinase activity into Ser/Thr activity for autophosphorylation. Phytochrome gene duplication presumably began and gave rise to three major lineages, *PHYA*, *PHYB* and *PHYC*, at the early emergence of the ancestor of seed plants. The duplicated *PHYB* genes, *PHYE* and *PHYD*, arose early in flowering plants and Brassicaceae, respectively. Based on our findings of various functional phytochrome heterodimers, increased complexity of R/FR light sensing and signaling systems, arising from combinations of type II phytochromes, may have played many important roles in the evolution of new biological abilities and phenotypes in higher plants.

PhyC and phyE homodimers do not exist in nature (Clack et al., 2009). To address the question of whether such homodimers could have signaling activity, I generated a series of *phyB*(NX-GAL) lines expressing phyX PSR-GAL (X= B, C, D, or E) in the *phyB* mutant. Analysis has shown that, unlike the functional chimeric phyB and phyD homodimers, these phyC and phyE chimeras are inactive in plants (Figure 2.12A). This indicates that during the long period of evolution, the phyC and phyE homodimer structures became non-functional, and ceased to exist, but they retained regulatory activity when bound as heterodimers to phyB and phyD monomers.

Complexity in Light Signal Transduction

Phytochrome-mediated signaling pathways or networks in flowering plants can be divided at least into three levels: phy activation, signal integration, and transcriptome modification involving integration with complicated phytohormone signaling pathways. Today, two downstream integrators in light signaling, PIFs and Long Hypocotyl 5 (HY5) have been discovered and well-characterized (Bae and Choi, 2008; Chen et al., 2010b; Leivar and Quail, 2010) (Lau and Deng, 2010). The basic helix-loop-helix (bHLH) PIFs bind preferentially to the Pfr form of phytochrome homodimers and heterodimers, and chiefly negatively regulate photomorphogenesis. Phytochrome indirectly interacts with HY5, a positive regulator of photomorphogenesis, by up-regulating its expression level (Osterlund et al., 2000). Compared with the nonfunctional full-length phyB^{C357S}/B^{C357S}, it is likely that, NB^{C357S}-Cdc/NB-Bem which can mediate tissue-specific growth, is not functional in one signaling pathway in hypocotyls but is functional in a somewhat different pathway in cotyledons. In fact, monomer NBs in the *phyB*(NB-Cdc) and

phyB(NB-Bem) lines also show very weakly detectable activities in cotyledons (Figure 2.7A). One hypothesis would be that in Arabidopsis, some downstream regulators require recognition of Pfr/Pfr phyB homodimers before triggering hypocotyl suppression, whereas other regulators can interact with a single phyB Pfr N-terminus in a PrPfr dimer to induce cotyledon expansion. Alternatively, PrPfr and PfrPfr dimers utilize the some regulators. It is also possible that the specialized NX-Cdc/NB-Bem (X= D, C and E) heterodimers, as biological fine-tune switches, may possess their own signaling pathways to generate differential hormone distribution in cells and direct specific-tissue growth in seedling de-etiolation.

Analysis of expression patterns of *PHYB*, *PHYD* and *PHYE* have previously shown that *PHYB* and *PHYC* are expressed broadly in tissues, while *PHYD* and *PHYE* are expressed differentially, especially in cotyledons, rather than in hypocotyls (Clack et al., 2009; Goosey, Palecanda, and Sharrock, 1997). HEMERA (HMR), a multiubiquitin-binding RAD23-like protein, regulates phy-mediated responses. Interestingly, *HMR* shares a similar expression pattern with *PHYD* and *PHYE* in seedling developmental stage (Chen et al., 2010c). Transcriptomics studies on light-regulated *Arabidopsis* genes has shown that the cotyledon expression profile has small overlaps with the hypocotyl gene expression profile in light-grown seedlings (Tepperman et al., 2004). Thus, our hypothesis may partially explain the dilemma that a R light signal can trigger distinct tissue-specific expression patterns in seedling organs through the same photoperception and signaling systems. The directed dimer *in vivo* expression system described in this thesis may also be useful for screening new downstream regulators,

which could be tissue-specific-inducing factors that bind homodimeric or heterodimeric phytochrome N-termini. We anticipate this work can greatly help us to understand the mechanisms of light signal transduction in *Arabidopsis*, and to improve crop quality and productivity in the future through fine-tuning their signaling.

Materials and Methods

Plant Materials, Growth Conditions, and Measurement

The *Arabidopsis thaliana phyB*-null allele *Bo64* line (*phyB-1*) and the established transgenic lines were in the Nossen (No-0) background. Seeds were surface sterilized and planted on Murashige and Skoog medium containing 0.8% agar with or without 3% sucrose. The plates were incubated at 4°C in the dark for 4 d, exposed to fluorescent light at room temperature for 3 h to induce uniform germination, and then transferred to the respective light conditions described in the figure legends. R (670 nm) and FR (735 nm) light were supplied by LEDs in an E-30LED growth chamber (Percival), or a growth chamber (Conviron) providing low Rc by red filter-wrapped fluorescent bulbs.

For hypocotyl length and cotyledon area measurements, after being given a 3h white light treatment, the seeds selected from at least two independent lines were grown on MS plates without sucrose for 5 d at 22°C, then laid out on 0.8% agar plates, photographed, and measured (40~60) of seedlings per treatment using ImageJ software (National Institutes of Health). For rosette leaf morphology and flowering time experiments, seeds were either sown directly on pots, treated at 4°C for 4 d, and grown at

22°C under low Rc (15 umolm^{-2}s^{-1}), or planted on MS plates with 3% sucrose for 1 week at 22°C, and transferred into pots under high Rc (90 umolm^{-2}s^{-1}).

Plasmid Construction and Plant Transformation

All plant transformation plasmids were constructed in the pBI and pGNT vectors with kanamycin-resistance and gentamicin-resistance markers, respectively (Clack et al., 2009). The N-termini of *PHYB*, *PHYB*^{c375s}, *PHYC*, *PHYD* and *PHYE* cDNA sequences were translationally directly fused to the myc$_6$-tagged BEM and his$_6$-tagged CDC regions, with the SV40 NLS at their C-termini. These chimeric transgenes, which are listed in APPENDIX A, were placed under the control of the constitutive *Cauliflower mosaic virus* 35S promoter.

Plant transformations were performed by the Agrobacterium tumefaciens-mediated floral dip method. The relevant transgenes were singly and doubly transformed into the host plant of No-0 *phyB-1* mutant. Transformed plants were selected on either GM medium (KanCarb or GentCarb) containing 25mg/ml kanamycin or 50mg/ml gentamicin or on both. After T2 segregation, multiple independent homozygous T3 lines expressing the *PHY* single and double transgenes were identified and used in experiments.

Proteasome and Protein Inhibitors

Carbobenzoxyl-leucinyl-leucinyl-leucinal (MG132), provided by A.G. Scientific, Inc , was dissolved in DMSO at a concentration of 25 mg ml^{-1} and stored for no more than 2 months at -80°C. For MG132 and DMSO treatments, seedlings were first grown on sterilized filter paper on GM plates with to desired stages, then they were collected

with filter paper soaked in liquid MS medium containing MG132 (50 mM, dissolved in DMSO) or 0.1% DMSO under R light conditions for 6h. After the incubation, the seedlings were thoroughly washed with liquid MS medium three times (5 min each) to remove residual DMSO or MG132 before proceeding with the experimental procedure. Protease inhibitor cocktails for plants (P9599, Sigma-Aldrich), was dissolved in DMSO and stored at -20°C. One ml is recommended for the inhibition of proteases extracted from 30 g of plant tissue in a total volume of 100ml.

Sequence (5'-3')	**Function**
AAGGAATTCAACCTACCAACTGTTCAAG (682)	Bem1 coding sequence PCR for yeast two-hybrid analysis
TAGGAATTCACAGCAACCTTTGCAACAG (684)	Bem2 coding sequence PCR for yeast two-hybrid analysis
TCTGAATTCCAATCAACTTCTGGATTGAAA (663)	Bem3 coding sequence PCR for yeast two-hybrid analysis
CAGGATCCTTCGTCTTCTAACACTAGATTC (683)	Bem1, Bem2 and Bem3 3' end PCR primers for yeast two-hybrid analysis
ATGGAATTCGAGCAGTTTAAGGCAAGAC (685)	Cdc1 coding sequence PCR for yeast two-hybrid analysis
TCTGAATTCTCTTCCATACTCTTCAGG (665)	Cdc2 coding sequence PCR for yeast two-hybrid analysis
ACGGATCCTCAATACAGACGAATGTTCAAG (686)	Cdc1 and Cdc2 3' end PCR primers for yeast two-hybrid analysis

Table 2.1 Oligonucleotide primers used in PCR for the yeast two-hybrid analysis.

Yeast Two-Hybrid Assay

Yeast two-hybrid assays were carried out with materials and protocols from the Matchmaker GAL4 System 3 (Clontech). Regions from the yeast genomic DNA sequences were amplified using forward primers containing EcoRI and reverse primers containing BamHI and cloned into the pGAD-T7 and pGBK-T7 vectors: Bem1 (N235-I551), Bem2 (D424-I551) and Bem3 (A470-I551), Cdc1 (E673-Y854) and Cdc2 (S760-Y854). The *NB-BEM3* and *NB-CDC2* fragments from the

pBI-35S:phyB-Bem3-myc6 and pGNT-35S:phyB-Cdc2-his6 plasmids were cloned into the pGAD-T7 and pGBK-T7 vectors using NdcI and StuI restriction sites. Primers used in PCR are listed in Table 2.1. Assays were performed under room light conditions.

Protein Extraction, SDS PAGE, and Western Blot

Fresh dark-, red or white light-grown seedlings were ground in an ice-cold mortar and pestle in Extraction buffer (50mM Tris pH 8.0, 150mM NaCl, 0.1% NP-40) with complete EDTA-free protease inhibitor mixture (Roche Diagnostics) at tissue weight buffer volume ratios of 1:1 for dark- and 1:2 for light-grown seedlings. Extracts were centrifuged for 5 min at 12,000g in a microcentrifuge at 4°C, and the supernatants were used for further experiments (immunoblot, immunoprecipitation and size-exclusion chromatography).

Proteins in gel were transferred to Hybond-ECL membranes (GE Healthcare), by using western blot apparatus (Bio-Rad, Laboratories, Hercules, CA). Membranes were then blocked of any nonspecific binding overnight at 4°C with blocking buffer (5% non fat dry milk, 0.2% tween 20 in TBS-T buffer pH7.6). Membranes were probed with blocking buffer containing primary antibody. The monoclonal antibodies (mAbs) were anti-phyA 073d (1:2000), anti-phyB B3B6 (1:1000), anti-phyC C11 (1:500), anti-phyD 2C1 (1:1000), and anti-phyE 7B3 (1:200) (Hirschfeld et al 1998), anti-myc 9E10 (1:1000; gift of Seth Pincus, Louisiana State University, Baton Rouge) and anti-his RGS (Qiagen). After 3 washes with the TBS-T buffer, chemiluminescent detection of primary antibodies was performed with horseradish peroxidase-conjugated secondary antibody and

Supersignal West Pico reagents (Thermo Fisher Scientific). Total protein was analyzed by the standard procedure of Bio-Rad Protein Assay (Bio-Rad, Hercules, CA).

Immunoprecipitation

One-milliliter aliquots of extracts were precleared by the addition of fifty microliters of tissue culture supernatant of the anti-myc monoclonal line 9E10 and incubation for 1h on ice. Fourty microliters of protein A-agarose beads (Santa Cruz Biotechnology) was added to the extract, the mixture was incubated shaking at 4°C for 1h, and the beads were pelleted by centrifugation at 1500 rpm for 20 sec at 4°C. The beads were washed four times in 500 ul of extraction buffer. Proteins bound to the beads were eluted by heating at 95°C for 5 min in 1×SDS sample buffer and pelleting the beads. The eluted proteins were analyzed by fractionation on 8% SDS PAGE, blotting to nitrocellulose and probing with mAbs. For each IP experiment, a set of gel lanes was loaded with the protein extract on the basis of protein concentration (Bio-Rad) and a set of gel lanes was loaded with IP samples as equivalent volumes from precipitations performed in parallel.

Size Exclusion Chromatography (SEC)

Protein extracts of dark-grown *phyB*(NB-Bem), *phyB*(NB-Cdc), *phyB*(NB-Bem/ NB-Cdc), *phyB*(NB-GAL[his6-NLS]), *phyB*(NB- GAL[myc6-NLS]) seedlings were prepared as above, and 1.0 ml samples containing about 1.0mg of total soluble protein were applied to a Superose 6 (GE healthcare) gel filtration column (25-ml bed volume). The column was eluted with the extraction buffer at 4°C at a rate of 0.5 ml/min, and 1.0

ml fractions were collected. Immunoblot analysis of column fractions were performed as described above. The column was calibrated with protein molecular weight standards (Pharmacia), and immunoblots were scanned and analyzed by using ImageJ software (National Institutes of Health).

CHAPTER 3

MODIFICATION OF THE ENDS OF PHYTOCHROME A INFLUENCES ITS ACTIVITY AND DEGRADATION PATTERN

Abstract

A five-membered phytochrome (phy) family in *Arabidopsis thaliana* is responsible for sensing Red (R)/Far-red (FR) light to modulate plant growth and development. Compared with the four light-stable family members, light labile photo-activated phyA is critical for mediating very low fluence (VLFR) and far-red high irradiance (FR-HIR) responses. A series of transgenic Arabidopsis plants was developed expressing epitope-tagged phyA fusion transgenes in a *phyA-201 null* phyA mutant or a wild-type Arabidopsis background. These phyA derivatives consist of the full-length phyA coding sequence attached to either a single myc epitope (myc_1) or six tandem myc epitopes (myc_6) on either end of phyA. The myc_1-tagged phyA fusion proteins are fully functional in VLFR and FR-HIR signaling, whereas the myc_6-tagged phyAs are impaired in FR-HIR signaling, confirming that both the N- and C-terminal ends of phyA are critical for FR-HIR. It is also demonstrated that the C-terminus is more sensitive in phyA-mediated FR-HIRs, but the N-terminus is more important in phyA-mediated VLFRs, raising the question of phyA differential interaction in its signaling. Further analysis shows that both the N- and C-terminal myc_6-tagged phyAs are degraded at a significantly slower rate than wild-type phyA and myc_1-tagged phyAs. This is consistent with a model in which FR-HIRs are more closely associated with phyA turnover than VLFR's. These results

suggest that phyA may fine-tune light signaling through differential interaction with its downstream factors.

Introduction

Plants have evolved various photoreceptor-mediated signal transduction pathways to better monitor and adapt to changes in their light environments. Red light (R)/far-red light (FR) sensing photoreceptor phytochrome (phy) isoforms are subject to photoconversion between a R-absorbing inactive Pr form and a FR-absorbing active Pfr form. In *Arabidopsis thaliana*, five phytochromes, phyA-phyE, are encoded by a small gene family. Unlike the light stable type II phyB-phyE, the type I phyA is predominant in dark-grown tissues, but its Pfr form is rapidly degraded with a half-life time of ~30 min upon transfer to light. This unique light-unstable property of phyA makes it suitable to the task of seed germination, and crosstalk with type II phys in the regulation of seedling de-etiolation and flowering. PhyA mediates two discrete phases of responses: the very low fluence responses (VLFRs) to a broad light spectrum within seconds and FR-dependent high irradiance responses (FR-HIRs) to prolonged or continuous FR irradiation (FRc) (Casal, Yanovsky, and Luppi, 2000).

Phytochrome consists of an N-terminal photosensory region and a C-terminal regulatory module, which are connected via a flexible hinge region. The phyA photosensory region is divided into a Per/Arnt/Sim (PAS)-like domain (PLD), a cGMP phosphodiesterase/adenyl cyclase/F*hl* domain (GAF), and a phytochrome domain (PHY). The C-terminal region of phyA, which is important for both signal transduction and

dimerization, contains two PAS-related domains and a histidine-kinase-related domain (HKRD). Structural studies show that phyA inter-domain crosstalk occurs during phyA Pr/Pfr conformational change (Park, Bhoo, and Song, 2000). Evidence suggests that phyA may be present in cells exists only as a homodimeric protein, compared with the mixed homo- and heterodimers of type II phys (Sharrock and Clack, 2002). Functionally key residues and sequence motifs in phyA have been identified. Deletion or missense mutations of phyA can both significantly influence its activity. For example, deletion of a small serine-rich region (Δ6-12) of the phyA N-terminal end reduces FR-HIRs and phyA stability, but does not affect VLFRs (Trupkin et al., 2007). A missense *eid4* mutation (E229K) of phyA enhances its light sensitivity by altering its degradation and subcellular partitioning (Dieterle et al., 2005). Missense mutations in the C-terminus of phyA have been identified as weak loss-of-function *phyA* alleles (Muller et al., 2009; Xu et al., 1995; Yanovsky et al., 2002). Although the C-terminus of phyB can be replaced by a heterologous dimerization domain and an NLS, the N-terminus of phyA in the nucleus, when dimerized, is still nonfunctional in the light (Wolf et al., 2011). A different phyA signal transduction pathway appears to act in the two distinct modes of phyA action (Shinomura, Uchida, and Furuya, 2000). The phyA-mediated VLFRs require Pfr as the active form which is generated in photoconversion from Pr to Pfr, whereas the phyA-mediated FR-HIRs depend on constant short-lived signals produced in the photocycling of phyA between Pr and Pfr. Therefore, phyA function tightly associates with its structural and photochemical properties.

Both photo-conversion of phyA Pr to Pfr and accumulation of Pfr in the nucleus are necessary for the initiation of phyA signaling. This is confirmed by the lack of activity of both a nuclear Pr phyA:NLS fusion protein and a cytosolic Pfr phyA-GFP-NES protein, both of which failed to initiate photomorphogenesis (Genoud et al., 2008; Toledo-Ortiz et al., 2010). Light-dependent translocation of phyA into the nucleus is the first critical signaling step for controlling phyA activity in an appropriate level to optimize light responsivity. Discovery of a specific nuclear translocation machinery for phyA resulted from the observation of movements of phyA-GFP fusion proteins in response to FRc. In darkness, phyA-GFP is present only in the cytosol as its inactive Pr form, whereas upon irradiation, the photo-activated phyA-GFP Pfr rapidly accumulates in the nucleus, where it aggregates and forms nuclear bodies (NBs) (Kircher et al., 2002; Kircher et al., 1999). Because of the lack of a nuclear localization signal (NLS), phyA requires two specific protein factors, FAR-RED ELONGATED HYPOCOTYL 1 (FHY1) and FHY1-LIKE (FHL). The *fhl/fhy1* double mutant shows a *phyA* mutant phenotype under both VLFR and FR-HIR conditions (Rosler, Klein, and Zeidler, 2007). These two phyA-specific proteins not only help phyA to translocate into the nucleus but also to avoid degradation (Genoud et al., 2008; Hiltbrunner et al., 2006; Hiltbrunner et al., 2005).

In Arabidopsis, rapid degradation of active phyA Pfr in the nucleus is also important for desensitizing phyA-mediated signaling. Upon exposure to Rc or continuous white light (Wc), nearly 99% of the phyA present in etiolated tissues is degraded before reaching a very low steady state equilibrium. In contrast, only a small portion of phyA

Pfr molecules are degraded under FRc resulting in a continuous low ratio of Pfr to P_{total} (Clough and Vierstra, 1997). The degradation of phyA depends on the ubiquitin/26S proteasome system. The CONSTITUTIVE PHOTOMORPHOGENIC 1 (COP1) E3 ligase protein specifically recognizes phyA by direct physical interaction (Seo et al., 2004) and targets it for ubiquitination and degradation. Large size NBs initiated by FRc or Rc, are proposed to be the sites for protein degradation, perhaps by facilitating COP1 to meet and recognize its preferred targets.

Post-translational modification of the phyA apoprotein also significantly affects phyA-mediated signal transduction by altering phyA inter-domain interaction, its binding affinity for downstream regulators and its stability. PhyA is proposed to contain endogenous Serine/thrine kinase activity, which can phosphorylate both itself and several potential signaling substrates such as PKS1, Aux/IAAs, and cryptochromes (Ahmad et al., 1998; Colon-Carmona et al., 2000; Fankhauser et al., 1999a; Yamaguchi et al., 1999). On the basis of the study of oat phyA, three phosphorylation sites were identified, including two autophosphorylated serine residues, Ser8 and Ser18 in the N-terminal extension region (NTE), and Ser599 in the hinge region (Han et al., 2010a; Lapko et al., 1999). PhyA phosphorylated at Ser599 shows low affinity for signaling transducers such as NDPK2 and PIF3 (Kim et al., 2004), and dephosphorylation of the Ser8 and Ser18 sites by phosphatase treatment or by site-directed mutations of these sites cause phyA hyperactivity and high phyA protein stability due to reduced recognition by the COP1/SPA complex (Han et al., 2010a; Ryu et al., 2005; Saijo et al., 2008b). Meanwhile, phyA can also be degraded in the cytoplasm but with a slower rate than that in the

nucleus (Debrieux and Fankhauser, 2010). However, Meng et al. (2010) suggested that phyA signaling requires phyA degradation, rather than just being desensitized by the proteolysis in cells based on the study of the *HMR* mutants.

This laboratory has been interested in using epitope-tagged Arabidopsis phytochromes as *in vivo* tools for investigating phy quaternary structure and interaction with downstream signaling proteins (Clack et al., 2009; Sharrock and Clack, 2004). Expression of transgenes encoding phytochrome apoprotein with modified ends, such as addition of florescent protein tags or epitope tags, or selective removal of amino acid sequences, is frequently used as an approach to investigating its *in vivo* properties and functions. Here, I describe the analysis of transgenic plants in either a *phyA-201*-null mutant or the wild-type background that express full-length phyA coding sequence from the *PHYA* promoter and with the relatively small modification of having one or six myc tags attached to its N or C terminus. We show that the myc_1-tagged fusion phyA proteins are able to fully complement the *phyA* mutant phenotype in de-etiolation and restore FR-HIR or nuclear VLFR types of signaling, whereas myc_6-tagged phyA fusion proteins have significantly reduced activities in those areas. I present evidence here that native phyA is homodimeric, and binds to myc-tagged phyA in a 1:1 ratio in cells and does not form detectable heterodimers with type II phytochromes. I also demonstrate that phyA degradation is correlated with reduced phyA activities in the transgenic lines, indicating that alteration of phyA architecture may impair the mechanism of protein-protein recognition so as to affect phyA destruction and downstream signaling.

Results

Myc_6 Epitopes Attenuate PhyA Biological Activity in FR-HIR Signaling

In order to investigate possible *in vivo* phyA heterodimerization with type II phy's and phyA interaction with downstream signaling proteins, lines with epitope-tagged ends were generated. As shown in Figure 3.1A, one set of two constructs, *PHYA*-m1, and *PHYA*-m6, were generated consisting of the full-length phyA coding sequence tagged with either a single myc epitope (myc_1) or six myc epitopes (myc_6) on its C-terminus. A second set of two transgenes, m1-*PHYA*, and m6-*PHYA*, were constructed encoding N-terminal (myc_1) or (myc_6)-tagged phyA fusion proteins. All of these epitope-tagged phyA derivatives were individually transformed into either a *phyA-201*-null *phyA* mutant or a L*er* wild-type Arabidopsis background under the control of the *PHYA* promoter. As a control, the unmodified full-length phyA coding sequence driven by the *PHYA* promoter was also expressed in the *phyA* mutant. Western blot analysis using antibodies specific to either the myc tag or the phyA protein shows that in the dark, the phyA levels in these transgenic lines are similar with that of endogenous phyA in the wild type (Figure 3.1B). A similar result for phyA transgene expression was also observed when seedlings of these lines were grown in pronged, very low FR light (0.37 $umolm^{-2}s^{-1}$), because of the low ratio of Pfr/P_{total} (Figure 3.2). It should be noted that m6-phyA expressed in the *phyA*(m6-*PHYA*) line, is easily degraded in cells to generate lower molecular weight unexpected bands in the phyA blot, which appear to be close in size to native, untagged phyA (Figure 3.1A).

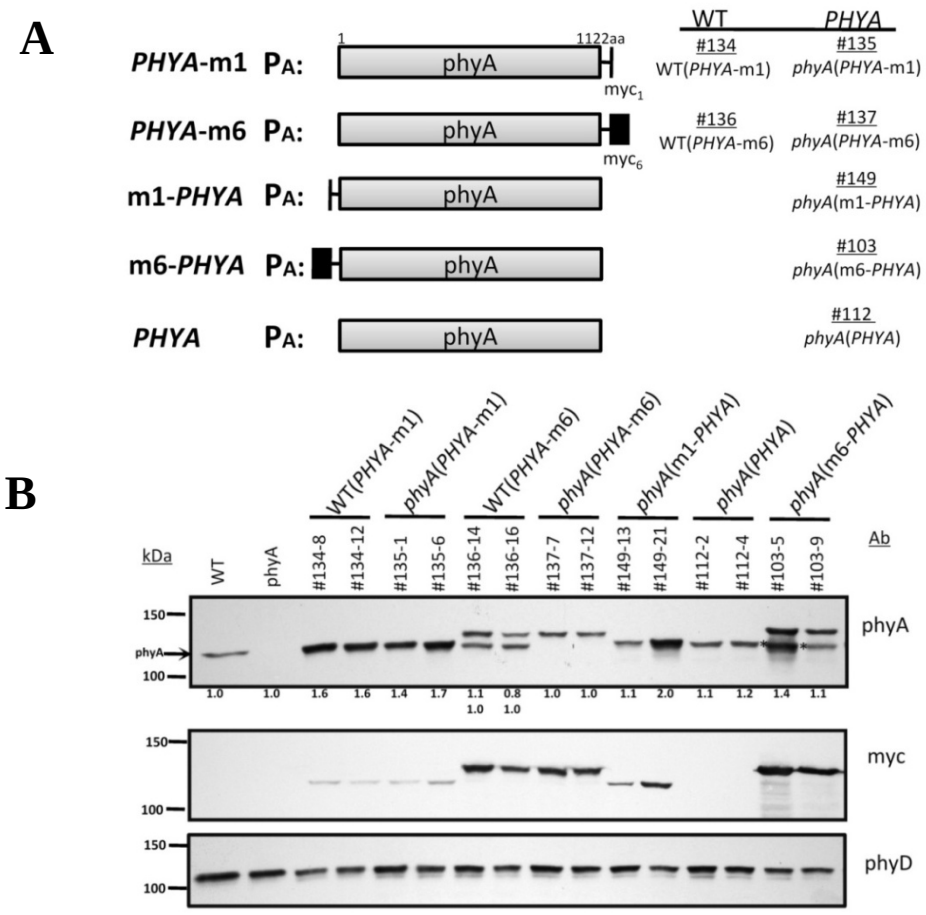


Figure 3.1. Generation of transgenic Arabidopsis lines expressing myc epitope-tagged phyA fusion transgenes. (A) Structures of the *PHYA*-m1, *PHYA*-m6, m1-*PHYA*, m6-*PHYA* and the full-length *PHYA*. myc_1 and myc_6 epitopes were translationally fused to the *PHYA* cDNA sequence on either its ends. All of these phyA derivatives were individually transformed into either a *phyA* mutant or a WT background under the control of the *PHYA* promoter (P_A). (B) Immunoblot detection of various phyA fusion proteins in 5-day-old dark-grown seedlings. The blots were probed with a monoclonal anti-phyA, anti-myc or anti-phyD antibody. The band marked with an asterisk on the anti-phyA blot of the #103 lines is a degradation product that is no longer detected by the anti-myc antibody.

FR-HIR response requires long irradiations at relatively high total fluence rates (higher than $6.1x10^4 umolm^{-2}$) (Mancinelli and Rabino, 1978). Therefore, FR-HIRs should be induced when seedlings are treated with 5 d prolonged, continuous FR equal to

or greater than 0.14 umolm^{-2}s^{-1}. Morphologies of 5-d-old seedlings of the myc-tagged phyA lines are shown in Figure 3.3A. Expression of m1-*PHYA* or *PHYA*-m1 fully complements the long hypocotyl phenotype of the *phyA* mutant under various moderate to high FRc fluences (0.37, 3.70 and 37.0 umolm^{-2}s^{-1}). Figure 3.3A and 3.3B demonstrate that all of the etiolated seedlings exhibited indistinguishable skotomorphogenesis and all of the FR-grown seedlings show a significant level of photomorphogenesis. However, the two myc$_6$ epitope-tagged phyAs, m6-phyA and phyA-m6, are notably attenuated for this FR-HIR signaling. At the two fluence levels below 0.1 umolm^{-2}s^{-1} in Figure 3.3B, the phenotypes of all the transgenic seedlings were identical in hypocotyl growth to that of the wild-type, with a small fluence-dependent component (Fig 3.3B). The biphasic response of WT under various continuous FR light shown in Figure 3.3B illustrates the two modes of action of phyA, VLFR below 0.1 umolm^{-2}s^{-1} and FR-HIR above 0.1 umolm^{-2}s^{-1}, and demonstrates that modification of either the N or C terminus with a large myc6 tag reduces signaling in FR-HIR but not VLFR.

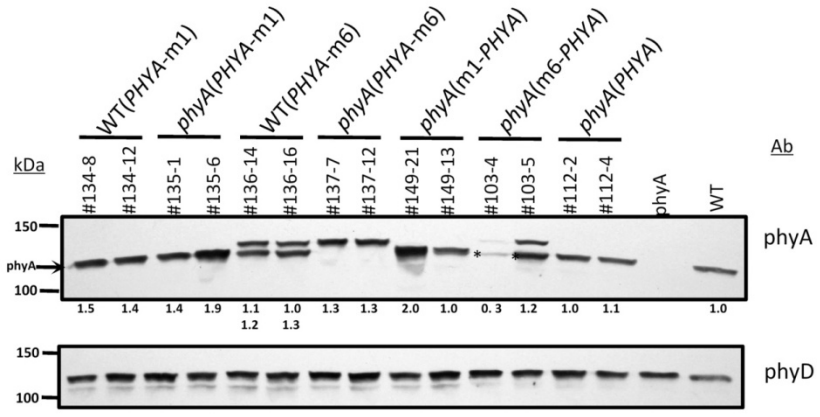


Figure 3.2. Expression levels of various phyA fusion proteins in 5-day-old FRc-grown seedlings (0.37 umolm^{-2}s^{-1}). The blots were probed with a monoclonal anti-phyA or anti-phyD antibody as in Figure 3.1 (above).

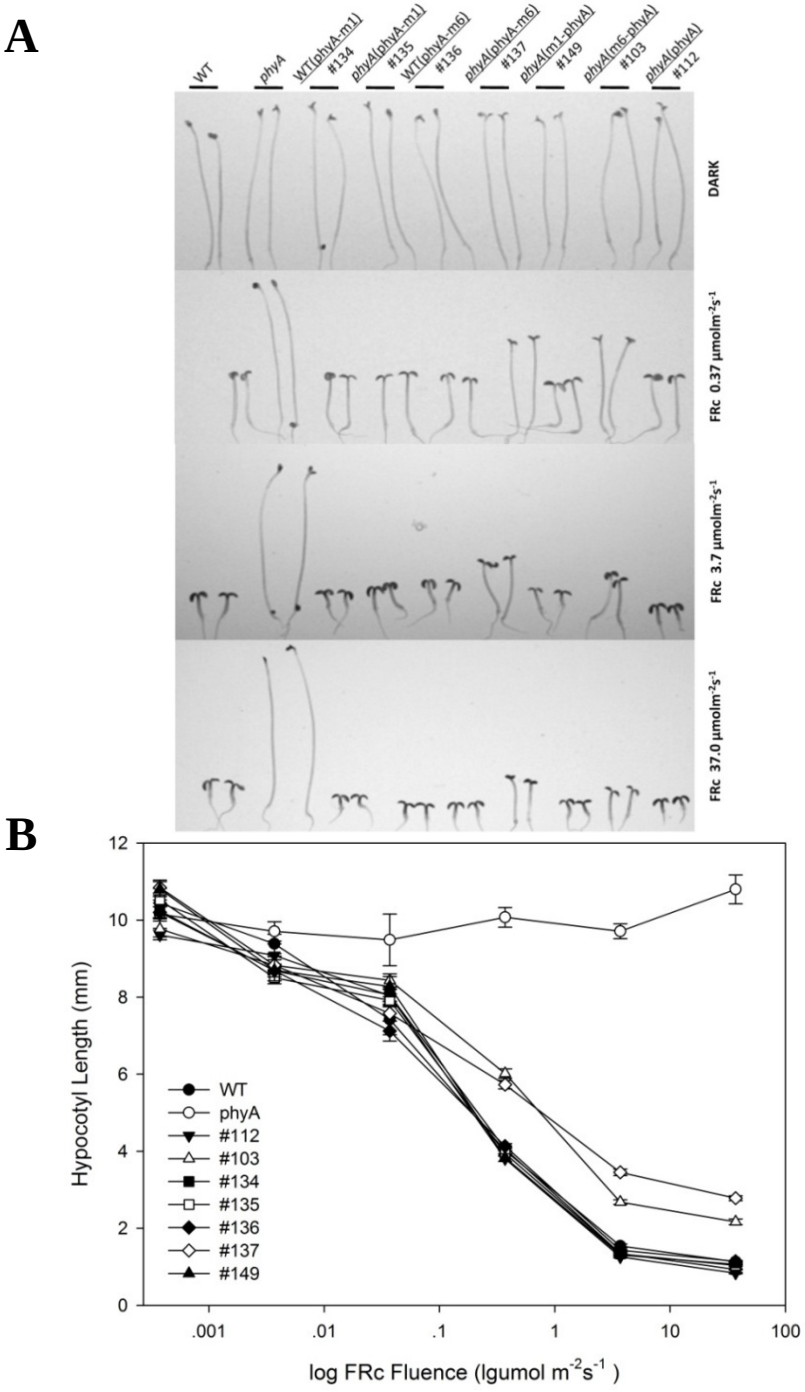


Figure 3.3. Myc_6 epitopes attenuate phyA-mediated FR-HIR signaling. (A) Morphology of the WT, *phyA* mutant and various transgenic phyA lines expressing myc1 or myc_6-tagged fusion phyA proteins. (B) Fluence response of hypocotyl length to dark and continuous FR. Seedlings of these corresponding lines were given 3h R to induce germination, incubated in darkness at 25°C for 24 h and then grown for 4 days in the dark or under a range of continuous FR (mean ± SE; n=40-60).

The PhyA N-terminus May be More Important for VLFR than its C-terminus

PhyA-mediated VLFRs can be detected by either a single pulse of FR or hourly pulses of FR. Seed germination and chlorophyll accumulation can be promoted when exposed to a brief pulse of FR light, whereas, following exposure to hourly pulses of FR, phyA-mediated VLFR in seedling de-etiolation is induced. This is represented by reduced hypocotyl elongation, increased cotyledon expansion, increased cotyledon angle separation, and increased anthocyanin accumulation (Botto et al., 1996; Lifschitz, Gepstein, and Horwitz, 1990; Shinomura et al., 1996b; Yanovsky, Casal, and Luppi, 1997). As shown in Figure 3.4, representative lines of *PHYA*-m1, *PHYA*-m6, m1-*PHYA*, and m6-*PHYA*, respond differently to hourly pulses of FR light (3min 200 $umolm^{-2}s^{-1}$ FR + 57min dark). Seedlings expressing *PHYA*-m1 or *PHYA*-m6 showed a short hypocotyl phenotype similar to that of the wild type after 5 d treatment of cyclic FR light pulses. However, both m1-phyA and m6-phyA result in a weaker photosensitivity to some extent than phyA-m1 and phyA-m6, respectively. Because the phyA fusion transgenes are expressed at similar levels (Figure 3.1B), these data suggest that the N-terminus of phyA may have an important role for signaling in the VLFR mode. In addition, the extra five myc epitopes attached to the ends of the N- or C- terminus of phyA in lines #137 and #103 also reduce phyA activities in the VLFRs in these lines.

Unmodified PhyA and Terminal-modified PhyA Function Similarly in Regulation of Flowering

The role of phyA in regulating flowering time has been extensively studied. Under extended short-day conditions (ESD), flowering in WT is significantly accelerated

relative to short-day conditions (SD), but the *phyA* mutant delays flowering under both conditions (Trupkin et al., 2007). Figure 3.5 shows the effects of the epitope-tagged phyA transgenes on flowering responses under an extended short-day treatment (Johnson et al., 1994b). Both the time of flowering and the number of rosette leaves at bolting were taken as a measure of flowering time. The *phyA* phenotype of prolonged vegetative growth and increased leaf number at the onset of flowering were fully complemented by expression of WT phyA and all of the four terminus-modified phyA transgenes, including m1-*PHYA*, m6-*PHYA*, *PHYA*-m1 and *PHYA*-m6. Although regulation of floral induction by phys is complicated, it appears that myc6 epitope tags do not significantly attenuate flowering when attached on either end of phyA.

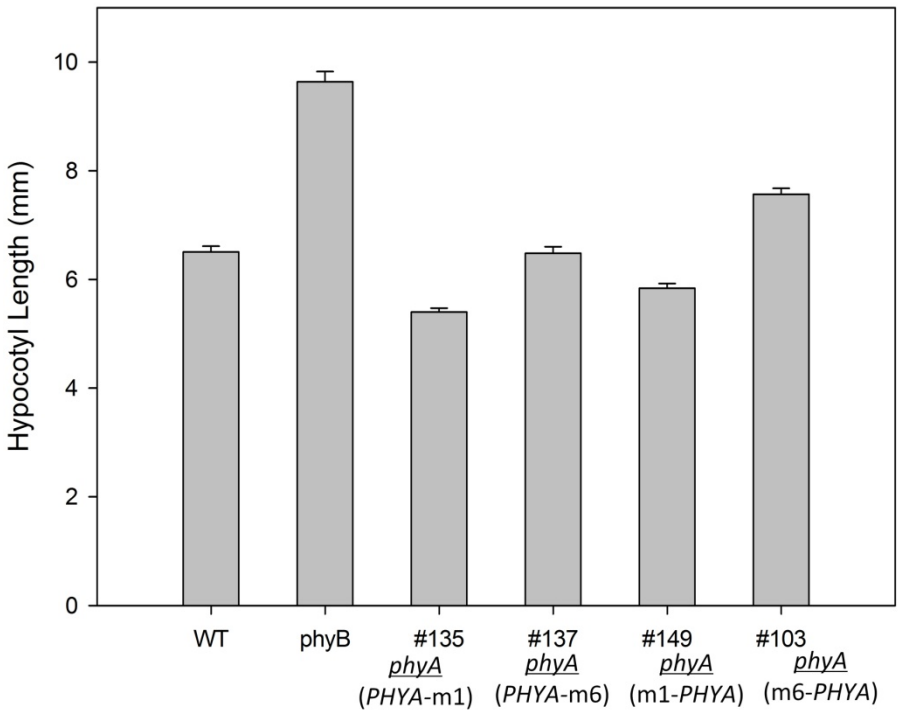


Figure 3.4. The N-terminus of phyA is critical for phyA-mediated VLFRs. Average hypocotyl length of 5-day-old seedlings grown under repeated FR pulses are shown. (mean ± SE; 2n=40-60).

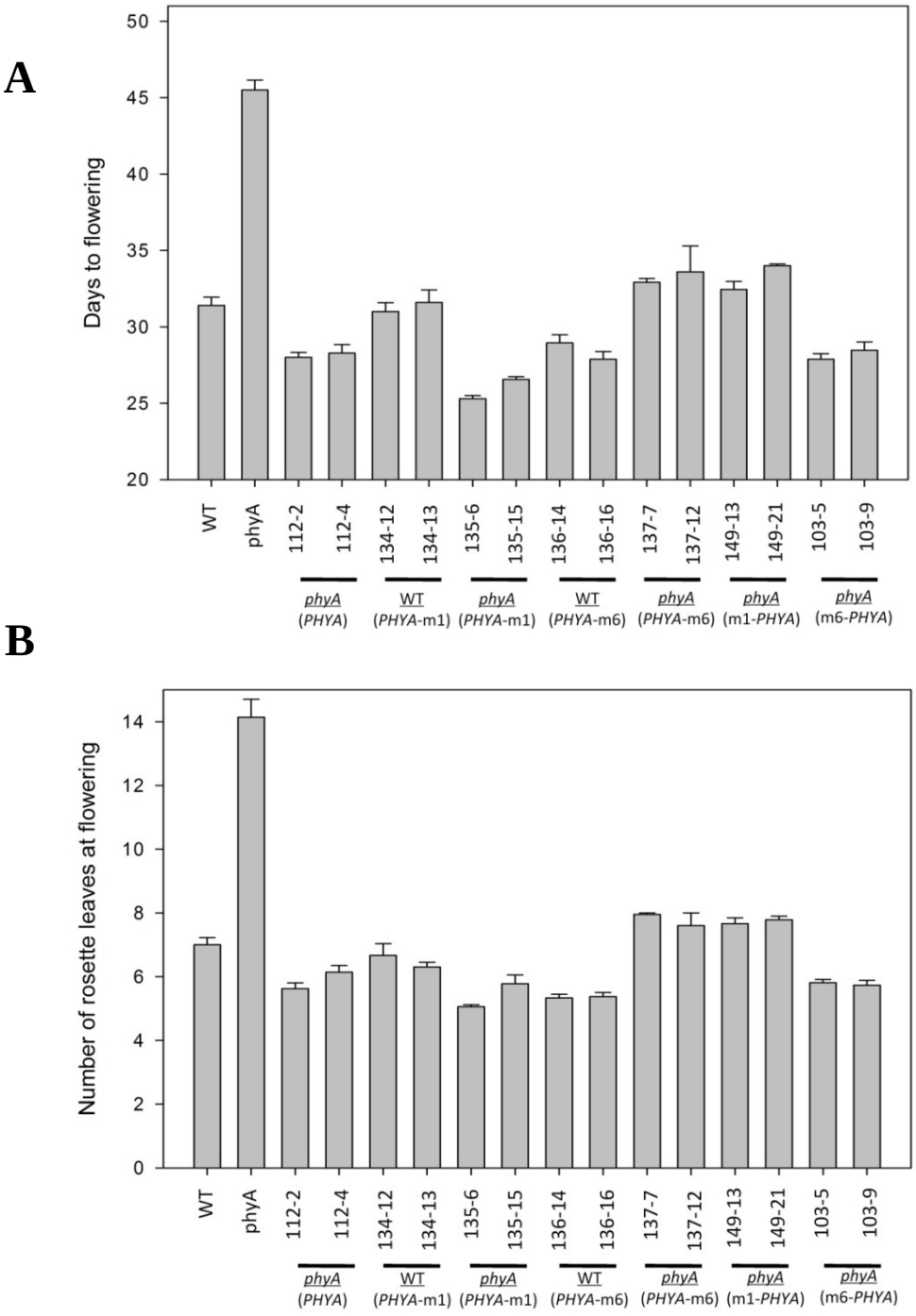


Figure 3.5. Epitope-tagged phyAs are biological active and complement the late flowering phyA mutant phenotype. Plants were grown under extended short day conditions (8 h cool-white fluorescent light/ 8h low-fluence incandescent light/ 8h darkness) at 21°C. At least two independent lines of each genotype plant were observed. (mean ± SE; 2n=10-14).

PhyA Forms Only Homodimers *in vivo*

We have previously shown that type II phys (phyB-E) form many different heterodimers *in vivo* (Clack et al., 2009). To investigate phyA dimerization specificity, individual myc-tagged phyA transgenes were pulled down with the anti-myc 9E10 mAb from extracts of FR-treated seedlings of the *phyA*(*PHYA*-m1), *phyA*(*PHYA*-m6) and WT(*PHYA*-m6) transgenic lines. As shown in Figure 3.6, endogenous phyA was coprecipitated from extracts of the WT(*PHYA*-m6) line, but endogenous phyB-phyE failed to be pulled down in this assay. Interestingly, the ratio of native phyA to phyA-m6 in the IP reaction is nearly 1:3 (0.3:0.8) in the WT(*PHYA*-m6) line #136-14, suggesting there is no differential interaction between native phyA and phyA-m6. These data confirm phyA homodimeric interactions *in vivo* and the independent structures of the type I phyA and the type II phyB-E phytochromes in plants.

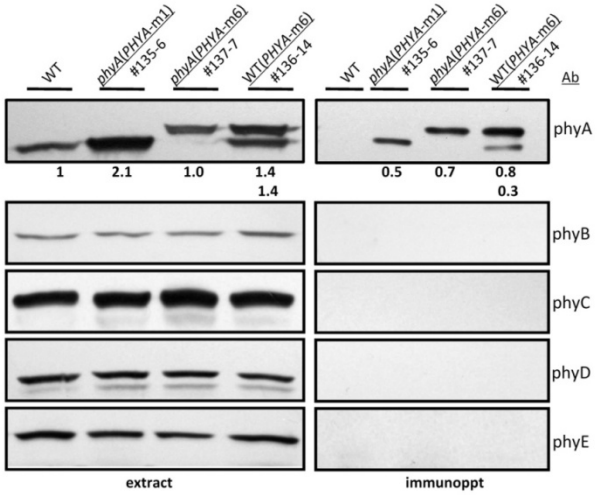


Figure 3.6. Assessment of coimmunoprecipitation of phyA-phyE with the phyA-m6 or phyA-m1 protein from seedling extracts. Samples of extracts of FR-grown seedlings of the WT, *phyA*(*PHYA*-m1), *phyA*(*PHYA*-m6), and WT(*PHYA*-m6) lines were immunoprecipitated with the anti-myc 9E10 mAb. Aliquots of the input extracted proteins and the immunoprecipitates were separated on 8% SDS gels, blotted, and probed with the indicated antibodies.

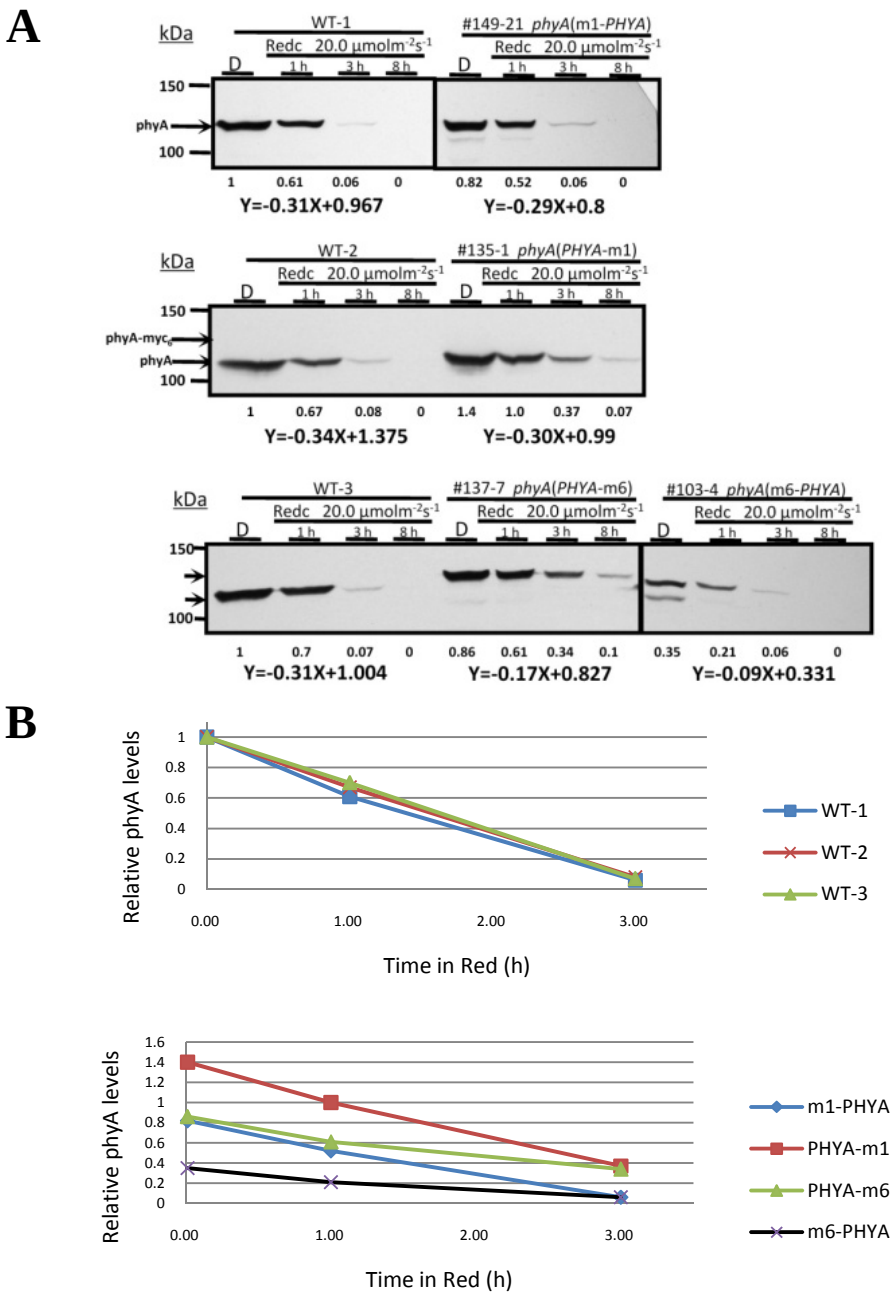


Figure 3.7. Kinetic analysis of phyA degradation following transfer to R. (A) The light-induced reduction of phyA levels is slower in phyA(PHYA-m6) and phyA(m6-PHYA) lines, but not in phyA(PHYA-m1) phyA(m1-PHYA) lines. Total protein extracts from 5-day-old etiolated seedlings of the WT and the phyA transgenic lines transferred for increasing amounts of time into R (20.0 umolm-2s-1) were separated, blotted and probed with anti phyA antibody. The first order equation of protein degradation was calculated based on the first 3h determined phyA degradation pattern. (B) Quantification of phyA levels in the WT (left) and myc-tagged phyA transgenic lines (right) under R.

Myc_6 Epitope tags Delay Degradation of PhyA in R Light

After absorbing R light, native phyA Pfr undergoes rapid proteolytic degradation in the nucleus with first order reaction kinetics (Franklin and Quail, 2010). To test whether the hyposensitive myc_6-tagged phyA derivatives in the HIRs and VLFRs show altered degradation kinetics or change the inherent degradation pattern of native phyA, the phyA protein levels were tested in five-day-old dark-grown seedlings and following transfer to R. As expected, the observation at 3 different time points (Dark, 1h and 3h) showed first order degradation of native phyA with a degradation rate slope around 0.3, and after 8h exposure, native phyA was undetectable on these blots (Figure 3.7A and B). Repeat experiment with WT phyA show a consistent degradation rate (Figure 3.7A). When treated with the same R fluence (20.0 $umolm^{-2}s^{-1}$), both m1-phyA in the #149-21 line and phyA-m1 in the #135-1 line are normally degraded with a degradation rate slope of around 0.3, similar to that of native phyA in WT. In contrast, phyA-m6 in the *phyA*(*PHYA*-m6) line #137-7 and m6-phyA in the *phyA*(m6-*PHYA*) line #103-4 showed a significantly slower degradation rate, 0.17 and 0.09, respectively (Figure 3.7). This indicates that the native phyA pool is degraded 2-3 times more rapidly than phyA-m6 and m6-phyA when exposed to Redc. It is worth noting that m6-phyA is much more stable in the red light than phyA-m6, indicating that the phyA N-terminus is sensitive for degradation.

Interaction Regulates the Degradation
Process of Native PhyA in the R Light

Under a lower Rc fluence condition (10.0 umolm^{-2}s^{-1}), native phyA still degraded rapidly with a slope around 0.27 (Figure 3.8), a little bit more slowly than under high Rc fluence (rate above 0.30). This suggests that high R fluence can accelerate phyA degradation. As expected, the slow degradation of phyA-m6 also occurred in several independent WT(*PHYA*-m6) #136 lines, whereas the degradation rate of native phyAs at the lower bands in the same #136 lines were degraded slowly with the same rate slope of phyA-m6 (rate=~0.11-0.19) (Figure 3.8). Associated with the evidences of phyA co-IPs, it is likely that phyA-m6 can successfully stabilize native phyA from proteolysis by direct dimeric interaction with each other.

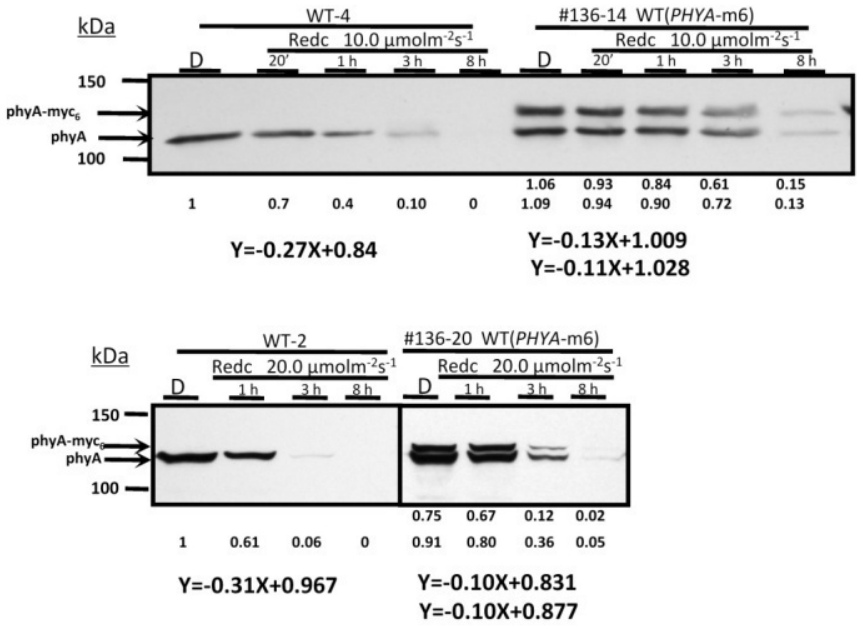


Figure 3.8. Interaction delays native phyA degradation in the WT(*PHYA*-m6) lines under R conditions. Total protein extracts from 5-day-old etiolated WT and WT(*PHYA*-m6) seedlings and seedlings exposed to R for the indicated periods were separated on 8% SDS-PAGE gels, blotted and detected with anti phyA antibodies. The phyA degradation equation was determined from the blot of each line above.

Discussion

How phyA regulates plant growth and development is one of the most extensively studied areas in plant photobiology. PhyA photo-conversion, nuclear translocation, phosphorylation and degradation have been shown by point mutation and deletion analysis to be emerging as key steps that control phyA signaling to diverse cellular processes in plants. However, a critical mutation of *PHYA* usually causes devastating effects on its structure and function. Due to its small size (N-EQKLISEEDL-C;1202 Da), a myc epitope tag, which is widely used to detect expression of target genes or for affinity chromatography, is unlikely to affect the protein's biochemical properties (Munro and Pelham, 1984). Therefore, to understand phyA signaling mechanisms of both VLFR and HIR in detail, a myc epitope tag or six myc tags were added to either end of phyA. The results presented here show that modification of the phyA ends can cause differential changes in photoreceptor function and sensitivity to light signals in different circumstances.

The transgenic plants that express myc6-tagged phyA fusion proteins under the control of the *PHYA* promoter show a significantly impaired hypocotyl elongation response under FRc (Figure 3.3). Previously, deletion or mutation in the N- or C-terminal domains of phyA have been reported to cause a hypoactive phyA (Dieterle et al., 2005; Trupkin et al., 2007; Yanovsky et al., 2002). Therefore, it seems clear that the phyA N- and C-termini are critical for phyA signaling and function in FR-HIR. However, the two myc_1-tagged phyA products produced in this study, phyA-m1 and m1-phyA, are equivalent to native phyA in their biological activities, suggesting that the size of the

epitope tag, rather than the mere presence of extra sequence on the ends of phyA, exerts direct and decisive influence on phyA attenuation. A limited alteration of the phyA quaternary structure by the relatively large-size myc_6 epitope tag, most likely influences the protein-protein interaction of phyA with other signaling factors. But, it is also possible that addition of the large myc_6 tag to either end changes the phyA Pr or Pfr absorption spectra, masks phosphorylation sites in the phyA NTE, or affects NB formation in the nucleus. It is notable that fusion of six tandem myc tags to phyD reduced its activity in hypocotyls previously (Sharrock and Clack, 2004).

Results of four replications of the VLFR experiment show that the *PHYA*-m6 gene can fully complement the *phyA* mutant hypocotyl elongation phenotype, but the m6-phyA activity is slightly reduced in the VLFR (Figure 3.4). These data suggest that the N-terminal domain of phyA may be more important in the VLFR mode than the C-terminus. Both the N- and C-termini of phyA are critical for FR-HIRs (Figure 3.3), Other researchers have observed that a PHYA-65-GFP-GUS-NLS product, consisting of the first 595 amino acids of oat phyA attached to GFP, followed by GUS and NLS, mediated VLFRs but not HIRs (Mateos et al., 2006). A PHY686-YFP-DD-NES (nuclear export signal) fusion protein was found to be functional only in cytoplasmic VLFR signaling (Wolf et al., 2011). Collectively, these observations indicate that there are two distinct phyA-mediated signal pathways between the VLFRs and HIRs and that various modifications of the phyA protein have differential effects on these responses.

It has been observed that biologically active m6-phyB, m6-phyD, m6-phyC or m6-phyE proteins fail to coprecipitate native phyA from extracts of dark-grown

Arabidopsis seedlings, suggesting that phyA is present in plants only in a homodimeric form (Clack et al., 2009; Sharrock and Clack, 2004). However, two possibilities that may result in the failure of phyA coprecipitation on blots need to be considered. First, as protein was extracted from dark-grown tissue, phyA rapid degradation may have occurred in the subsequent pull-down assays. Secondly, phyA possibly only binds to the type II phytochromes as its active Pfr form. As shown in Figure 3.6, FR-grown extracts containing at least small portion of active Pfr were tested for coprecipitation of native phyA-phyE with both the phyA-m6 and the phyA-m1 proteins, which are biological active. The conclusion that type I phyA does not heterodimerize with type II phyB-E was confirmed. Therefore, this experiment sufficiently illustrates that phyA only forms homodimers. Moreover, the Co-IP assay also showed phyA-m6 binds to itself and to native phyA with equivalent frequencies in the WT(*PHYA*-m6) plants (Figure 3.6), indicating that the myc_6 epitope tag likely does not affect phyA-phyA interaction to form a compact dimeric module. Further investigation showed that, upon transfer to R, co-expressed phyA-m6 and phyA have similar degradation rates (Figure 3.8), which is slower than that of native phyA dimers, but faster than that of phyA-m6 dimers. These observations indicate that phyA-m6 tends to retard the degradation of phyA by their physical interaction. Perhaps, intermittent interaction between single phyA molecules occurs in NBs as a common phenomenon. Certainly, proteolysis is a very complicated process, which may preferentially target and degrade the phyA/phyA-m6 molecules via the 26S proteasome in plant cells.

Rapid degradation of phyA Pfr appears to be closely related to phyA function. Two opposite interpretations have been proposed to explain phyA accumulation and degradation in the nucleus. Based on the fact that autophosphorylated phyA contains decreased activity and decreased protein stability, the degradation process has been considered as a mechanism to desensitize phyA signaling (Han et al., 2010b; Seo et al., 2004). However, the study of the *hmr* mutants shows that native phyA accumulates in R light in the mutant, while the phyA response is absent (Chen et al., 2010c), indicating that phyA degradation may in fact be required for phyA function. Our studies reveal that phyA activity in FR-HIRs and degradation show a close correlation. The end modifications on phyA-m6 and m6-phyA impair phyA activity and increase phyA stability. Meanwhile, phyA-m1 and m1-phyA, which do not impair phyA activity, maintain normal phyA degradation patterns. It is possible that downstream factors of phyA in its HIR signaling mechanism and the COP1-SPA E3 ligase complex, which ubiquitinates phyA Pfr (Saijo et al., 2008a), may recognize some of the same binding sites or regions of phyA. The COP1-SPA complex directly interacts with the PAS domain region (amino acids 591-850) in the phyA C-terminal half of the molecule (Seo et al., 2004). Because the PAS domain is nearly in the middle of the phyA protein sequence, it seems likely that both N- and C-terminal myc_6 tags are able to influence this spot and to hinder the subsequent interaction of the PAS domain with the COP-SPA complex.

The tight correlation of phyA activity with degradation may be true for phyA signaling only in the FR-HIR mode. The normal activity of phyA-m6 in mediating VLFR indicates that a wild-type rate of phyA degradation is not necessary in the VLFR (Figure

3.4). In addition, all of the myc-tagged phyA fusion proteins, which show various degradation patterns, successfully complement the late flowering phenotype of the *phyA*-deficient mutant under ESD (Figure 3.5). These findings suggest that, while end modifications of phyA influence its biochemical properties and its biological activities to a significant degree, some phyA responses are still really functional. VLFR depends on very small amounts of active Pfr in the nucleus, whereas FR-HIR depends on a repeated phyA photocycling which allows seedling de-etiolation. In Chapter 1, the hypothesis that there is a common signal transduction pathway and the same active phyA form (Pfr or phosphorylated Pfr) shared between VLFR and HIR was mentioned. However, data presented here indicate that activated phyA may interact with different downstream factors between VLFR and HIR signaling. A prolonged FR exposure might benefit the C-terminal Pfr binding with downstream factors such as PIFs in HIR. After this molecular recognition, co-degradation of the phyA-PIF complex will occur via the 26S proteasome. This constant interaction-degradation coupling process inactivates PIFs and finally results in seedling de-etiolation. In this way, rapid degradation may be required for phyA signaling in the FR-HIR mode. In addition, in FR-HIR active phyA Pfr might interact with some signaling factors that are induced after modification of the transcriptome in seedlings. In contrast, a short light pulse in VLFR possibly just activates one round of phyA-responsive early gene expression by interaction with basic downstream factors.

Materials and Methods

Plant Materials, Growth conditions, and Measurement

The *Arabidopsis thaliana* wild type and *phyA*-null allele *phyA-201* lines (Nagatani 1993; Reed 1994) and the established transgenic lines are in the *Landsberg erecta* background. Seeds were surface sterilized and planted on Murashige and Skoog medium containing 0.8% agar with or without 3% sucrose. The plates were incubated in the dark for 3 d at 4°C, exposed to continuous white light at room temperature for 3h to induce uniform germination, and then transferred to the respective light conditions described in the figure legends. R (670 nm) and FR (735 nm) light were supplied by LEDs in an E-30LED growth chamber (Percival).

For hypocotyl length measurements (HIRs and VLFRs), seedlings were grown on MS plates without 3% sucrose for 5 d at 21°C, then laid out on 0.8% agar plates, photographed, and measured (at least 20 per treatment) using ImageJ software (National Institutes of Health).

VLFR

Seeds were chilled and given a 3h R (25.0 $\mu molm^{-2}s^{-1}$), then incubated in darkness at 25°C for 24 h to allow germination and transferred to hourly pulses of far-red light (3min/h at 200$\mu molm^{-2}s^{-1}$) for 4 days.

Flowering Time

For extended SD (ESD) flowering-time experiments, seedlings were germinated and grown for 7 d under SD on MS plates with 3% sucrose before being transferred into

pots. These pots were placed under ESD condition of 8h cool-white fluorescent light (200 $\mu molm^{-2}s^{-1}$) followed by 8 h of low-fluence rate incandescent light ($2\mu molm^{-2}s^{-1}$) and 8 h of darkness (Johnson et al., 1994b). Flowering time was measured as the day on which the first floral bud became visible at the center of the rosette.

CHAPTER 4

COMPLEMENTATION OF EARLY FLOWERING PHENOTYPE IN ARABIDOPSIS BY EXPRESSION OF PHYTOCHROME E

Introduction

Identification of null mutations in the members of the phytochrome gene family in Arabidopsis is a critical step in determination of their functions. The *phyA* null mutant has a severe deficiency in the high-irradiance responses under far-red light and the very low fluence responses after a brief light of exposure, whereas the lack of phyB results in reduced sensitivity of many red light-induced responses, including the inhibition of hypocotyl suppression and cotyledon expansion in seedlings, elongation of petioles and stems in the vegetative phase, and early flowering (Halliday, Koornneef, and Whitelam, 1994; Parks and Quail, 1993). The function of phyC, phyD and phyE in Arabidopsis are more subtle, and depend upon heterdimerization with phyB (Clack et al., 2009).

Phytochrome-mediated signaling pathways mediate the timing of Arabidopsis floral transition via control of a threshold level of the transcriptional regulator CONSTANS (CO). CO promotes flowering by up-regulating the expression of the floral integrator FLOWERING TIME (FT) and TWIN SISTER OF FT (TSF). FT moves from the leaves to the meristem through the phloem, where it induces the program that leads to floral development. Studies of flowering time have shown interactions between phytochrome pathways in the control of flowering. Under long day conditions (16h light/8 h dark), *phyA* mutants show delayed flowering, with more rosette leaves produced

before reproduction than the wild type. In contrast, *phyB* mutants show accelerated flowering. The *phyAphyB* double mutant was intermediate between the single mutants, demonstrating the activities of phyA and phyB are antagonistic (Neff and Chory, 1998a). Type II phytochromes phyB-E function redundantly in the suppression of flowering in high R:FR conditions. phyE has been shown to mediate floral repression in the *phyB* mutation background under EOD-FR light and short day conditions (Devlin, Patel, and Whitelam, 1998b). However, the *PHYE* gene, driven by its own promoter expressed in the transgenic *phyB* mutant did not complement the *phyB* early-flowering phenotype in the long day conditions (Sharrock, Clack, and Goosey, 2003). phyE also plays a dominant role in temperature-mediated flowering. The *phyAphyBphyD* triple mutant began to flower at the same time as wild type when grown in short photoperiods at 16°C. In contrast, the *phyAphyBphyDphyE* mutant showed early flowering response in the same conditions (Halliday et al., 2003).

To better understand phyE activity in regulating the time of flowering, we measured the flowering responses in wild-type, the *phyE* and *phyBphyE* double mutant lines, and in their corresponding transgenic lines in which the *PHYE-m6* transgene was expressed. The results showed that, phyE delays flowering in Arabidopsis under short day conditions. In this paper, we also deduced that phyD/phyE heterodimers may be more active than phyB/phyE heterodimers based on the average data we obtained.

Results

To determine the phyE activity *in vivo*, a P*PHYE*:phyE-myc$_6$ transgene (*PHYE*-m6) was expressed in L*er* wild-type, *phyE*, and *phyBphyE* (abbreviated *phyBE*) host plants. Figure 4.1 shows that deficiency of phyE protein in the monogenic *phyE* mutant results in flowering a few days earlier than the wild type under short days, but the *phyE* mutation causes a stronger early flowering response in the *phyB* background. The number of rosette leaves present when flowering occurred also showed the same result (4.1B). Subsequently, the levels of phyE-myc6 proteins in the transgenic lines were assayed on immunoblots of tissue extracts probed with anti-phyE antibody (7B3), showing the *PHYE-m6* transgene is expressed at a similar level to the wild type (Clack et al., 2009). The early flowering phenotypes of the *phyE* and *phyBphyE* mutants were complemented by the *PHYE-m6* transgene with respect to both days to flowering and the number of rosette leaves at flowering. The transgenic WT(*PHYE*-m6) lines, which overexpressed the *PHYE-m6* transgene in the wild type plants, also greatly delayed the time of flowering (Figure 4.1). All these observations demonstrate that the phyE-myc6 protein is biologically active. As shown in Figure 4.2, phyE can significantly affect the rosette leaf morphoglogy and greening between the *phyBE* mutant and the transgenic *phyBE*(*PHYE*-m6) #119 line.

Discussion

Phytochrome E has been considered to have the overlapping functions with the closely related phytochromes, phyB and phyD (Franklin and Quail, 2010). In our present study, phyE is shown to act as an active factor reversing early flowering in Arabidopsis. The effects of phyE deficiency in the *phyBE* and *phyE* mutants were strongly complemented by expression of the epitope-tagged phyE transgene in these mutant lines. Through yeast two-hybrid and immunoprecipitation experiments, three forms of phyE have been identified in Arabidopsis, the majority of phyB/phyE and phyD/phyE heterodimers and maybe a small portion of phyE monomers in the *phyBE* mutant (Clack et al., 2009).

A synergistic relationship between phyB and phyD was demonstrated in seedling de-etiolation when a greater hypocotyl elongation occurred in the double *phyBphyD* mutant, compared to the combined increases in both monogenic mutants (Aukerman et al., 1997). As shown in Figure 4.3, a synergistic effect was also observed in the *phyBphyE* mutant, showing that the *phyB*, *phyE* or *phyB/phyE* mutants cause 11.7 days, 7.1 days or 22.8 days earlier flowering on everage than WT, respectively. Thus, compared to the phyE mutant, additional phyB/phyE and phyD/phyE dimers in WT delayed flowering 7.1 days. However, phyD/phyE alone caused 11.1 days later flowering in the *phyB* mutant than the the *phyBE* mutant. This indicates that phyD/phyE dimers may play a larger role than phyB/phyE dimers in the flowering reponse.

Compared to the *phyBE* mutant, expression of phyE protein in the *phyBE*(*PHYE*-m6) line postponed flowering for 11.5 days. But, expression of phyE

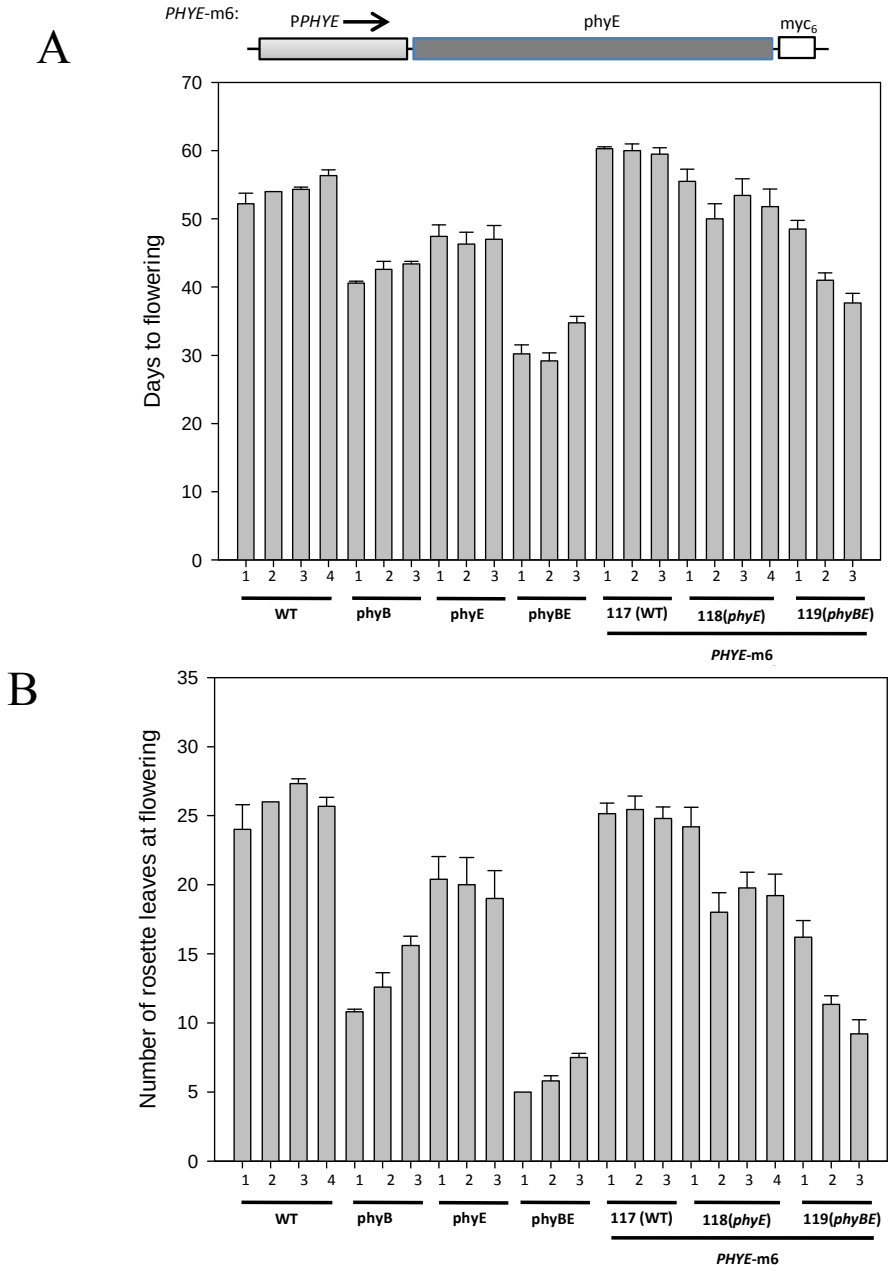


Figure 4.1. Biological activity of epitope-tagged phyE delays flowering. Structure of the *PHYE-m6* transgene and complementation of the *phyE* mutant early flowering response. The *PHYE-m6* coding sequence was fused to a 1.8-kb PHYE promoter region and transformed into the Ler wild-type, *phyE*, and *phyBE* genetic backgrounds. Plants were grown under short days (8 h light/16 h dark) at 21°C. At least three independent lines of each genotype plant were observed.

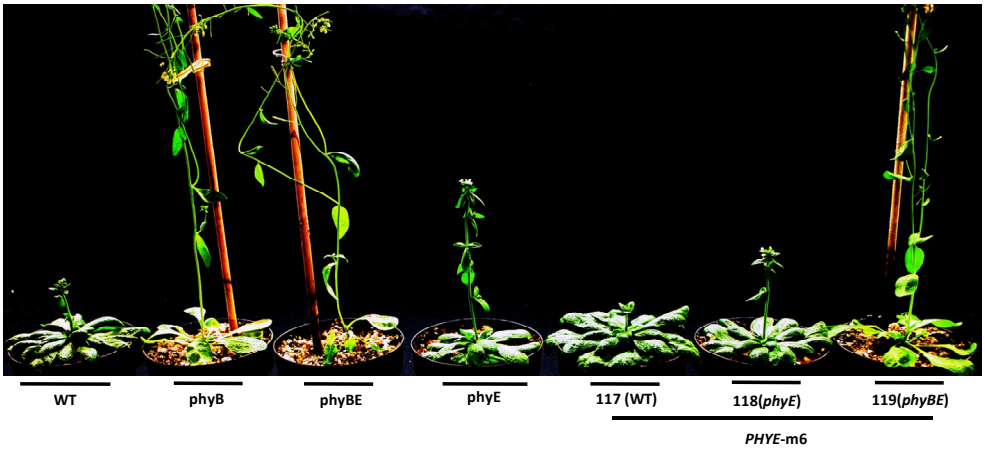
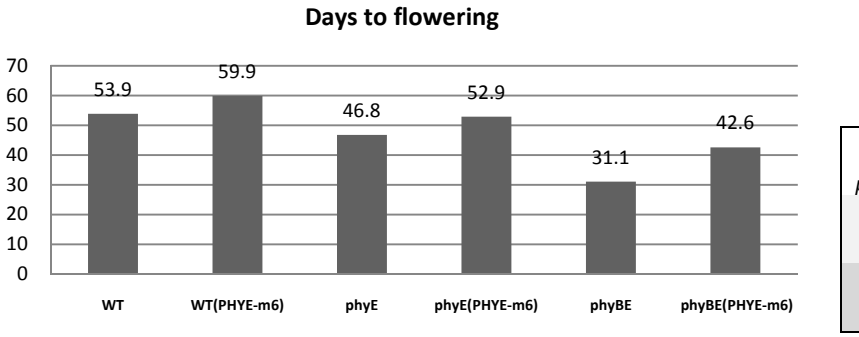
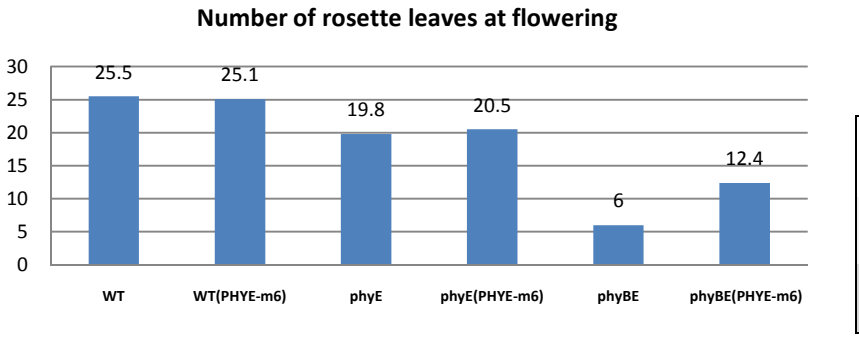


Figure 4.2. Post-flowering phenotypes of representatives of Wild-Type, *phyB*, *phyBE*, *phyE*, WT(*PHYE*-m6), *phyE*(*PHYE*-m6) and *phyBE*(*PHYE*-m6). Plants were grown as in Figure 1.



Lines	Days
phyBE	0
phyBE(*PHYE*-m6)	11.5
phyE	0
phyE(*PHYE*-m6)	6.1
WT	0
WT(*PHYE*-m6)	6



Lines	Leaves
phyBE	0
phyBE(*PHYE*-m6)	6.4
phyE	0
phyE(*PHYE*-m6)	0.7
WT	0
WT(*PHYE*-m6)	-0.4

Figure 4.3. The phyD/phyE heterodimers and the phyB/phyE heterodimers play major roles in controlling flowering time. The average of times and leaf numbers of the mutant and transgenic lines were caculated from the data from Figure 4.1A. Different days and leaf numbers at the right tables existed between the couple lines, the mutants and their relative phyE-m6-containing transgenic lines.

protein in the *phyE*(*PHYE*-m6) and WT(*PHYE*-m6) lines only resulted in earlier flowering of 6.1 and 6.0 days compared to their corresponding control lines, respectively (Figure 4.3). Because phyE only interacts with phyD in the *phyBE* mutant, it is clear that phyD/phyE dimers greatly enhance the complementation of the *phyBE* early flower phenotype. Moreover, a similar conclusion can also be drawn based on the calculation of the number of rosette leaves at flowering (Figure 4.3).

Compared to the *phyBE* mutant, expression of phyE protein in the *phyBE*(*PHYE*-m6) line postponed flowering for 11.5 days. But, expression of phyE protein in the *phyE*(*PHYE*-m6) and WT(*PHYE*-m6) lines only resulted in earlier flowering of 6.1 and 6.0 days compared to their corresponding control lines, respectively (Figure 4.3). Because phyE only interacts with phyD in the *phyBE* mutant, it is clear that phyD/phyE dimers greatly enhance the complementation of the *phyBE* early flower phenotype. Moreover, a similar conclusion can also be drawn based on the calculation of the number of rosette leaves at flowering (Figure 4.3).

Materials and Methods

Plant Materials, Growth Conditions, and Measurement

The *Arabidopsis thaliana phyB-1, phyE-1* and *phyBphyE* double mutant lines and the corresponding transgenic lines generated from these are in the Landsberg *erecta* (L*er*) genetic background. Seeds were surface-sterilized, plated on GM agar medium (3% sucrose), and cold-treated for 4 d in the dark. Seedlings were grown for 7 d and transferred into pots at 21°C in a Conviron PGR15 growth chamber. Flowering time was

measured under a short day (8h light/16h dark) as the date of the first appearance of a floral bud, and as the number of rosette leaves at flowering.

REFERENCES CITED

Abdurakhmonov, I. Y., Buriev, Z. T., Logan-Young, C. J., Abdukarimov, A., and Pepper, A. E. (2010). Duplication, divergence and persistence in the Phytochrome photoreceptor gene family of cottons (Gossypium spp.). *BMC Plant Biology* **10,** Article No.: 119.

Abe, H., Yamamoto, K. T., Nagatani, A., and Furuya, M. (1985). Characterization of Green Tissue-Specific Phytochrome Isolated Immunochemically from Pea Pisum-Sativum Seedlings. *Plant and Cell Physiology* **26**(7)**,** 1387-1400.

Ahmad, M., Jarillo, J. A., Smirnova, O., and Cashmore, A. R. (1998). The CRY1 blue light photoreceptor of Arabidopsis interacts with phytochrome A in vitro. *Molecular Cell* **1**(7)**,** 939-948.

Aida, M., Ishida, T., and Tasaka, M. (1999). Shoot apical meristem and cotyledon formation during Arabidopsis embryogenesis: Interaction among the CUP-SHAPED COTYLEDON and SHOOT MERISTEMLESS genes. *Development (Cambridge)* **126**(8)**,** 1563-1570.

Al-Sady, B., Ni, W., Kircher, S., Schafer, E., and Quail, P. H. (2006). Photoactivated phytochrome induces rapid PIF3 phosphorylation prior to proteasome-mediated degradation. *Mol Cell* **23**(3)**,** 439-46.

Alabadi, D., Gallego-Bartolome, J., Orlando, L., Garcia-Carcel, L., Rubio, V., Martinez, C., Frigerio, M., Iglesias-Pedraz, J. M., Espinosa, A., Deng, X. W., and Blazquez, M. A. (2008). Gibberellins modulate light signaling pathways to prevent Arabidopsis seedling de-etiolation in darkness. *Plant J* **53**(2)**,** 324-35.

Aukerman, M. J., Hirschfeld, M., Wester, L., Weaver, M., Clack, T., Amasino, R. M., and Sharrock, R. A. (1997). A deletion in the PHYD gene of the Arabidopsis Wassilewskija ecotype defines a role for phytochrome D in red/far-red light sensing. *Plant Cell* **9**(8)**,** 1317-26.

Bae, G., and Choi, G. (2008). Decoding of light signals by plant phytochromes and their interacting proteins. *Annu Rev Plant Biol* **59,** 281-311.

Bagnall, D. J., King, R. W., Whitelam, G. C., Boylan, M. T., Wagner, D., and Quail, P. H. (1995). Flowering responses to altered expression of phytochrome in mutants and transgenic lines of Arabidopsis thaliana (L.) Heynh. *Plant Physiol* **108**(4)**,** 1495-503.

Ballare, C. L. (2003). Stress under the sun: spotlight on ultraviolet-B responses. *Plant Physiol* **132**(4)**,** 1725-7.

Basu, D., Dehesh, K., Schneider-Poetsch, H. J., Harrington, S. E., McCouch, S. R., and Quail, P. H. (2000). Rice PHYC gene: structure, expression, map position and evolution. *Plant Mol Biol* **44**(1)**,** 27-42.

Bauer, D., Viczian, A., Kircher, S., Nobis, T., Nitschke, R., Kunkel, T., Panigrahi, K. C., Adam, E., Fejes, E., Schafer, E., and Nagy, F. (2004). Constitutive photomorphogenesis 1 and multiple photoreceptors control degradation of phytochrome interacting factor 3, a transcription factor required for light signaling in Arabidopsis. *Plant Cell* **16**(6)**,** 1433-45.

Beggs, C. J., Holmes, M. G., Jabben, M., and Schaefer, E. (1980). Action Spectra for the Inhibition of Hypocotyl Growth by Continuous Irradiation in Light and Dark Grown Sinapis-Alba Seedlings. *Plant Physiology (Rockville)* **66**(4)**,** 615-618.

Belles-Boix, E., Hamant, O., Witiak, S. M., Morin, H., Traas, J., and Pautot, V. (2006). KNAT6: an Arabidopsis homeobox gene involved in meristem activity and organ separation. *Plant Cell* **18**(8)**,** 1900-1907.

Bhattacharyya, R. P., Remenyi, A., Yeh, B. J., and Lim, W. A. (2006). Domains, motifs, and scaffolds: the role of modular interactions in the evolution and wiring of cell signaling circuits. *Annu Rev Biochem* **75,** 655-80.

Borthwick, H. A., Hendricks, S. B., Parker, M. W., Toole, E. H., and Toole, V. K. (1952). A Reversible Photoreaction Controlling Seed Germination. *Proc Natl Acad Sci U S A* **38**(8)**,** 662-6.

Botto, J. F., Sanchez, R. A., Whitelam, G. C., and Casal, J. J. (1996). Phytochrome A mediates the promotion of seed germination by very low fluences of light and canopy shade light in arabidopsis. *Plant Physiology (Rockville)* **110**(2)**,** 439-444.

Bowman, J. L., Floyd, S. K., and Sakakibara, K. (2007). Green genes-comparative genomics of the green branch of life. *Cell* **129**(2)**,** 229-34.

Briggs, W. R., and Christie, J. M. (2002). Phototropins 1 and 2: versatile plant blue-light receptors. *Trends Plant Sci* **7**(5)**,** 204-10.

Briggs, W. R., and Huala, E. (1999). Blue-light photoreceptors in higher plants. *Annu Rev Cell Dev Biol* **15,** 33-62.

Brockmann, J., Rieble, S., Kazarinova-Fukshansky, N., Seyfried, M., and Schaefer, E. (1987). Phytochrome Behaves as a Dimer in-Vivo. *Plant Cell and Environment* **10**(2)**,** 105-112.

Butler, W. L., Norris, K. H., Siegelman, H. W., and Hendricks, S. B. (1959). Detection, Assay, and Preliminary Purification of the Pigment Controlling Photoresponsive Development of Plants. *Proc Natl Acad Sci U S A* **45**(12)**,** 1703-8.

Carey, M., Kakidani, H., Leatherwood, J., Mostashari, F., and Ptashne, M. (1989). An amino-terminal fragment of GAL4 binds DNA as a dimer. *J Mol Biol* **209**(3)**,** 423-32.

Casal, J. J., Yanovsky, M. J., and Luppi, J. P. (2000). Two photobiological pathways of phytochrome A activity, only one of which shows dominant negative suppression by phytochrome B. *Photochem Photobiol* **71**(4)**,** 481-6.

Castle, L. A., and Meinke, D. W. (1994). A FUSCA gene of Arabidopsis encodes a novel protein essential for plant development. *Plant Cell* **6**(1)**,** 25-41.

Chandler, J. W., Cole, M., and Werr, W. (2008). The role of DORNROESCHEN (DRN) and DRN-LIKE (DRNL) in Arabidopsis embryonic patterning. *Plant Signal Behav* **3**(1)**,** 49-51.

Chattopadhyay, S., Ang, L.-H., Puente, P., Deng, X.-W., and Wei, N. (1998). Arabidopsis bZIP protein HY5 directly interacts with light-responsive promoters in mediating light control of gene expression. *Plant Cell* **10**(5)**,** 673-683.

Chen, H., Huang, X., Gusmaroli, G., Terzaghi, W., Lau, O. S., Yanagawa, Y., Zhang, Y., Li, J., Lee, J. H., Zhu, D., and Deng, X. W. (2010a). Arabidopsis CULLIN4-damaged

DNA binding protein 1 interacts with CONSTITUTIVELY PHOTOMORPHOGENIC1-SUPPRESSOR OF PHYA complexes to regulate photomorphogenesis and flowering time. *Plant Cell* **22**(1)**,** 108-23.

Chen, M., Galvao, R. M., Li, M., Burger, B., Bugea, J., Bolado, J., and Chory, J. (2010b). Arabidopsis HEMERA/pTAC12 initiates photomorphogenesis by phytochromes. *Cell* **141**(7)**,** 1230-40.

Chen, M., Galvao, R. M., Li, M., Burger, B., Bugea, J., Bolado, J., and Chory, J. (2010c). Arabidopsis HEMERA/pTAC12 Initiates Photomorphogenesis by Phytochromes. *Cell* **141**(7)**,** 1230.

Chen, M., Schwab, R., and Chory, J. (2003). Characterization of the requirements for localization of phytochrome B to nuclear bodies. *Proc Natl Acad Sci U S A* **100**(24)**,** 14493-8.

Chen, M., Tao, Y., Lim, J., Shaw, A., and Chory, J. (2005). Regulation of phytochrome B nuclear localization through light-dependent unmasking of nuclear-localization signals. *Curr Biol* **15**(7)**,** 637-42.

Cherry, J. R., Hondred, D., Walker, J. M., and Vierstra, R. D. (1992). Phytochrome requires the 6-kDa N-terminal domain for full biological activity. *Proc Natl Acad Sci U S A* **89**(11)**,** 5039-43.

Chory, J., Peto, C., Feinbaum, R., Pratt, L., and Ausubel, F. (1989). Arabidopsis thaliana mutant that develops as a light-grown plant in the absence of light. *Cell* **58**(5)**,** 991-9.

Clack, T., Mathews, S., and Sharrock, R. A. (1994). The phytochrome apoprotein family in Arabidopsis is encoded by five genes: the sequences and expression of PHYD and PHYE. *Plant Mol Biol* **25**(3)**,** 413-27.

Clack, T., Shokry, A., Moffet, M., Liu, P., Faul, M., and Sharrock, R. A. (2009). Obligate Heterodimerization of Arabidopsis Phytochromes C and E and Interaction with the PIF3 Basic Helix-Loop-Helix Transcription Factor. *Plant Cell* **21**(3)**,** 786-99.

Clough, R. C., and Vierstra, R. D. (1997). Phytochrome degradation. *Plant Cell and Environment* **20**(6)**,** 713-721.

Colbert, J. T., Hershey, H. P., and Quail, P. H. (1983). Autoregulatory control of translatable phytochrome mRNA levels. *Proc Natl Acad Sci U S A* **80**(8)**,** 2248-52.

Colon-Carmona, A., Chen, D. L., Yeh, K. C., and Abel, S. (2000). Aux/IAA proteins are phosphorylated by phytochrome in vitro. *Plant Physiol* **124**(4)**,** 1728-38.

Cordonnier, M. M., and Pratt, L. H. (1982). Immunopurification and initial characterization of dicotyledonous phytochrome. *Plant Physiol* **69**(2)**,** 360-5.

Cornilescu, G., Ulijasz, A. T., Cornilescu, C. C., Markley, J. L., and Vierstra, R. D. (2008). Solution structure of a cyanobacterial phytochrome GAF domain in the red-light-absorbing ground state. *J Mol Biol* **383**(2)**,** 403-13.

Correll, M. J., and Kiss, J. Z. (2005). The roles of phytochromes in elongation and gravitropism of roots. *Plant and Cell Physiology* **46**(2)**,** 317-323.

Davis, S. J., Vener, A. V., and Vierstra, R. D. (1999). Bacteriophytochromes: phytochrome-like photoreceptors from nonphotosynthetic eubacteria. *Science* **286**(5449)**,** 2517-20.

de Lucas, M., Daviere, J. M., Rodriguez-Falcon, M., Pontin, M., Iglesias-Pedraz, J. M., Lorrain, S., Fankhauser, C., Blazquez, M. A., Titarenko, E., and Prat, S. (2008). A molecular framework for light and gibberellin control of cell elongation. *Nature* **451**(7177)**,** 480-4.

Debrieux, D., and Fankhauser, C. (2010). Light-induced degradation of phyA is promoted by transfer of the photoreceptor into the nucleus. *Plant Molecular Biology* **73**(6)**,** 687-695.

Deng, X. W., Caspar, T., and Quail, P. H. (1991). cop1: a regulatory locus involved in light-controlled development and gene expression in Arabidopsis. *Genes Dev* **5**(7)**,** 1172-82.

Devlin, P. F., and Kay, S. A. (2000). Cryptochromes are required for phytochrome signaling to the circadian clock but not for rhythmicity. *Plant Cell* **12**(12)**,** 2499-2510.

Devlin, P. F., Patel, S. R., and Whitelam, G. C. (1998a). Phytochrome E influences internode elongation and flowering time in Arabidopsis. *Plant Cell* **10**(9)**,** 1479-1487.

Devlin, P. F., Patel, S. R., and Whitelam, G. C. (1998b). Phytochrome E influences internode elongation and flowering time in Arabidopsis. *Plant Cell* **10**(9)**,** 1479-87.

Devlin, P. F., Robson, P. R., Patel, S. R., Goosey, L., Sharrock, R. A., and Whitelam, G. C. (1999). Phytochrome D acts in the shade-avoidance syndrome in Arabidopsis by controlling elongation growth and flowering time. *Plant Physiol* **119**(3)**,** 909-15.

Devlin, P. F., Yanovsky, M. J., and Kay, S. A. (2003). A genomic analysis of the shade avoidance response in Arabidopsis. *Plant Physiol* **133**(4)**,** 1617-29.

Dieterle, M., Bauer, D., Bueche, C., Krenz, M., Schaefer, E., and Kretsch, T. (2005). A new type of mutation in phytochrome A causes enhanced light sensitivity and alters the degradation and subcellular partitioning of the photoreceptor. *Plant Journal* **41**(1)**,** 146-161.

Elich, T. D., and Chory, J. (1997). Biochemical characterization of Arabidopsis wild-type and mutant phytochrome B holoproteins. *Plant Cell* **9**(12)**,** 2271-80.

Emery, J. F., Floyd, S. K., Alvarez, J., Eshed, Y., Hawker, N. P., Izhaki, A., Baum, S. F., and Bowman, J. L. (2003). Radial patterning of Arabidopsis shoots by class III HD-ZIP and KANADI genes. *Curr Biol* **13**(20)**,** 1768-74.

Eshed, Y., Baum, S. F., Perea, J. V., and Bowman, J. L. (2001). Establishment of polarity in lateral organs of plants. *Curr Biol* **11**(16)**,** 1251-60.

Essen, L. O., Mailliet, J., and Hughes, J. (2008). The structure of a complete phytochrome sensory module in the Pr ground state. *Proc Natl Acad Sci U S A* **105**(38)**,** 14709-14.

Esteban, B., Carrascal, M., Abian, J., and Lamparter, T. (2005). Light-induced conformational changes of cyanobacterial phytochrome Cph1 probed by limited proteolysis and autophosphorylation. *Biochemistry* **44**(2)**,** 450-61.

Fankhauser, C., Yeh, K.-C., Lagarias, J. C., Zhang, H., Elich, T. D., and Chory, J. (1999a). PKS1, a substrate phosphorylated by phytochrome that modulates light signaling in Arabidopsis. *Science (Washington D C)* **284**(5419)**,** 1539.

Fankhauser, C., Yeh, K. C., Lagarias, J. C., Zhang, H., Elich, T. D., and Chory, J. (1999b). PKS1, a substrate phosphorylated by phytochrome that modulates light signaling in Arabidopsis. *Science* **284**(5419)**,** 1539-41.

Feng, S., Martinez, C., Gusmaroli, G., Wang, Y., Zhou, J., Wang, F., Chen, L., Yu, L., Iglesias-Pedraz, J. M., Kircher, S., Schaefer, E., Fu, X., Fan, L.-M., and Deng, X. W. (2008). Coordinated regulation of Arabidopsis thaliana development by light and gibberellins. *Nature (London)* **451**(7177)**,** 475.

Finkelstein, R. R., and Lynch, T. J. (2000). The Arabidopsis abscisic acid response gene ABI5 encodes a basic leucine zipper transcription factor. *Plant Cell* **12**(4)**,** 599-609.

Fornara, F., de Montaigu, A., and Coupland, G. (2010). SnapShot: Control of flowering in Arabidopsis. *Cell* **141**(3)**,** 550, 550 e1-2.

Franklin, K. A., Allen, T., and Whitelam, G. C. (2007). Phytochrome A is an irradiance-dependent red light sensor. *Plant J* **50**(1)**,** 108-17.

Franklin, K. A., Davis, S. J., Stoddart, W. M., Vierstra, R. D., and Whitelam, G. C. (2003a). Mutant analyses define multiple roles for phytochrome C in Arabidopsis photomorphogenesis. *Plant Cell* **15**(9)**,** 1981-1989.

Franklin, K. A., Praekelt, U., Stoddart, W. M., Billingham, O. E., Halliday, K. J., and Whitelam, G. C. (2003b). Phytochromes B, D, and E act redundantly to control multiple physiological responses in Arabidopsis. *Plant Physiology (Rockville)* **131**(3)**,** 1340-1346.

Franklin, K. A., and Quail, P. H. (2010). Phytochrome functions in Arabidopsis development. *J Exp Bot* **61**(1)**,** 11-24.

Froehlich, A. C., Noh, B., Vierstra, R. D., Loros, J., and Dunlap, J. C. (2005). Genetic and molecular analysis of phytochromes from the filamentous fungus Neurospora crassa. *Eukaryot Cell* **4**(12)**,** 2140-52.

Furuya, M. (1989). Molecular properties and biogenesis of phytochrome I and II. *Adv Biophys* **25,** 133-67.

Geddie, M. L., and Matsumura, I. (2007). Antibody-induced oligomerization and activation of an engineered reporter enzyme. *J Mol Biol* **369**(4)**,** 1052-9.

Gendreau, E., Traas, J., Desnos, T., Grandjean, O., Caboche, M., and Hofte, H. (1997). Cellular basis of hypocotyl growth in Arabidopsis thaliana. *Plant Physiol* **114**(1)**,** 295-305.

Genoud, T., Millar, A. J., Nishizawa, N., Kay, S. A., Schafer, E., Nagatani, A., and Chua, N. H. (1998). An Arabidopsis mutant hypersensitive to red and far-red light signals. *Plant Cell* **10**(6)**,** 889-904.

Genoud, T., Schweizer, F., Tscheuschler, A., Debrieux, D., Casal, J. J., Schafer, E., Hiltbrunner, A., and Fankhauser, C. (2008). FHY1 mediates nuclear import of the light-activated phytochrome A photoreceptor. *PLoS Genet* **4**(8)**,** e1000143.

Gil, P., Kircher, S., Adam, E., Bury, E., Kozma-Bognar, L., Schafer, E., and Nagy, F. (2000). Photocontrol of subcellular partitioning of phytochrome-B:GFP fusion protein in tobacco seedlings. *Plant J* **22**(2)**,** 135-45.

Goosey, L., Palecanda, L., and Sharrock, R. A. (1997). Differential patterns of expression of the Arabidopsis PHYB, PHYD, and PHYE phytochrome genes. *Plant Physiol* **115**(3)**,** 959-69.

Goto, N., Kumagai, T., and Koornneef, M. (1991). Flowering Responses to Light-Breaks in Photomorphogenic Mutants of Arabidopsis-Thaliana, a Long-Day Plant. *Physiologia Plantarum* **83**(2)**,** 209-215.

Goto, N., Kumagai, T., and Korrnneef, M. (1991). Flowering Responses to Light-Breaks in Photomorphogenic Mutants of Arabidopsis-Thaliana a Long-Day Plant. *Physiologia Plantarum* **83**(2)**,** 209-215.

Grimm, R. E., C. Lottspeich, F. Zenger, C. Ru¨diger,W. (1988). Sequence analysis of proteolytic fragments of 124-kilodalton phytochrome from etiolatedAvena sativa L.: Conclusions on the conformation of the native protein *planta* **174**(3)**,** 396-401.

Halliday, K. J., Koornneef, M., and Whitelam, G. C. (1994). Phytochrome B and at Least One Other Phytochrome Mediate the Accelerated Flowering Response of Arabidopsis thaliana L. to Low Red/Far-Red Ratio. *Plant Physiol* **104**(4)**,** 1311-1315.

Halliday, K. J., Salter, M. G., Thingnaes, E., and Whitelam, G. C. (2003). Phytochrome control of flowering is temperature sensitive and correlates with expression of the floral integrator FT. *Plant J* **33**(5)**,** 875-85.

Hamazato, F., Shinomura, T., Hanzawa, H., Chory, J., and Furuya, M. (1997). Fluence and wavelength requirements for Arabidopsis CAB gene induction by different phytochromes. *Plant Physiol* **115**(4)**,** 1533-40.

Han, Y.-J., Kim, H.-S., Kim, Y.-M., Shin, A.-Y., Lee, S.-S., Bhoo, S. H., Song, P.-S., and Kim, J.-I. (2010a). Functional Characterization of Phytochrome Autophosphorylation in Plant Light Signaling. *Plant and Cell Physiology* **51**(4)**,** 596-609.

Han, Y. J., Kim, H. S., Kim, Y. M., Shin, A. Y., Lee, S. S., Bhoo, S. H., Song, P. S., and Kim, J. I. (2010b). Functional characterization of phytochrome autophosphorylation in plant light signaling. *Plant Cell Physiol* **51**(4)**,** 596-609.

Han, Y. J., Kim, H. S., Song, P. S., and Kim, J. I. (2010c). Autophosphorylation desensitizes phytochrome signal transduction. *Plant Signal Behav* **5**(7)**,** 868-71.

Hardtke, C. S., Gohda, K., Osterlund, M. T., Oyama, T., Okada, K., and Deng, X. W. (2000). HY5 stability and activity in arabidopsis is regulated by phosphorylation in its COP1 binding domain. *EMBO J* **19**(18)**,** 4997-5006.

Haynes, K. A., and Silver, P. A. (2009). Eukaryotic systems broaden the scope of synthetic biology. *Journal of Cell Biology* **187**(5)**,** 589-596.

Hennig, L., Stoddart, W. M., Dieterle, M., Whitelam, G. C., and Schaefer, E. (2002). Phytochrome E controls light-induced germination of Arabidopsis. *Plant Physiology (Rockville)* **128**(1)**,** 194-200.

Hershey, H. P., Barker, R. F., Idler, K. B., Lissemore, J. L., and Quail, P. H. (1985). Analysis of cloned cDNA and genomic sequences for phytochrome: complete amino acid sequences for two gene products expressed in etiolated Avena. *Nucleic Acids Res* **13**(23)**,** 8543-59.

Hershey, H. P., Barker, R. F., Idler, K. B., Murray, M. G., and Quail, P. H. (1987). Nucleotide sequence and characterization of a gene encoding the phytochrome polypeptide from Avena. *Gene* **61**(3)**,** 339-48.

Hershey, H. P., Colbert, J. T., Lissemore, J. L., Barker, R. F., and Quail, P. H. (1984). Molecular cloning of cDNA for Avena phytochrome. *Proc Natl Acad Sci U S A* **81**(8)**,** 2332-6.

Hiltbrunner, A., Tscheuschler, A., Viczian, A., Kunkel, T., Kircher, S., and Schafer, E. (2006). FHY1 and FHL act together to mediate nuclear accumulation of the phytochrome A photoreceptor. *Plant Cell Physiol* **47**(8)**,** 1023-34.

Hiltbrunner, A., Viczian, A., Bury, E., Tscheuschler, A., Kircher, S., Toth, R., Honsberger, A., Nagy, F., Fankhauser, C., and Schafer, E. (2005). Nuclear accumulation of the phytochrome A photoreceptor requires FHY1. *Curr Biol* **15**(23)**,** 2125-30.

Hirose, Y., Shimada, T., Narikawa, R., Katayama, M., and Ikeuchi, M. (2008). Cyanobacteriochrome CcaS is the green light receptor that induces the expression of phycobilisome linker protein. *Proceedings of the National Academy of Sciences of the United States of America* **105**(28)**,** 9528-9533.

Hoecker, U. (2005). Regulated proteolysis in light signaling. *Curr Opin Plant Biol* **8**(5)**,** 469-76.

Hughes, J. (2010). Phytochrome three-dimensional structures and functions. *Biochem Soc Trans* **38**(2)**,** 710-6.

Huq, E., Al-Sady, B., Hudson, M., Kim, C., Apel, K., and Quail, P. H. (2004). Phytochrome-interacting factor 1 is a critical bHLH regulator of chlorophyll biosynthesis. *Science* **305**(5692)**,** 1937-41.

Inomata, K., Khawn, H., Chen, L. Y., Kinoshita, H., Zienicke, B., Molina, I., and Lamparter, T. (2009). Assembly of Agrobacterium phytochromes Agp1 and Agp2 with doubly locked bilin chromophores. *Biochemistry* **48**(12)**,** 2817-27.

Ito, T., Matsui, Y., Ago, T., Ota, K., and Sumimoto, H. (2001). Novel modular domain PB1 recognizes PC motif to mediate functional protein-protein interactions. *EMBO J* **20**(15)**,** 3938-46.

Jang, I. C., Henriques, R., Seo, H. S., Nagatani, A., and Chua, N. H. (2010). Arabidopsis PHYTOCHROME INTERACTING FACTOR proteins promote phytochrome B polyubiquitination by COP1 E3 ligase in the nucleus. *Plant Cell* **22**(7)**,** 2370-83.

Jiao, Y., Lau, O. S., and Deng, X. W. (2007). Light-regulated transcriptional networks in higher plants. *Nat Rev Genet* **8**(3)**,** 217-30.

Johnson, E., Bradley, M., Harberd, N. P., and Whitelam, G. C. (1994a). Photoresponses of Light-Grown phyA Mutants of Arabidopsis (Phytochrome A Is Required for the Perception of Daylength Extensions). *Plant Physiol* **105**(1)**,** 141-149.

Johnson, E., Bradley, M., Harberd, N. P., and Whitelam, G. C. (1994b). Photoresponses of light-grown phyA mutants of Arabidopsis: Phytochrome A is required for the perception of daylength extensions. *Plant Physiology (Rockville)* **105**(1)**,** 141-149.

Jones, A. M., Allen, C. D., Gardner, G., and Quail, P. H. (1986). Synthesis of phytochrome apoprotein and chromophore are not coupled obligatorily. *Plant Physiol* **81**(4)**,** 1014-6.

Jones, A. M., and Erickson, H. P. (1989). Domain structure of phytochrome from Avena sativa visualized by electron microscopy. *Photochem Photobiol* **49**(4)**,** 479-83.

Jones, A. M., and Quail, P. H. (1986). Quaternary Structure of 124-Kilodalton Phytochrome from Avena-Sativa. *Biochemistry* **25**(10)**,** 2987-2995.

Karniol, B., Wagner, J. R., Walker, J. M., and Vierstra, R. D. (2005). Phylogenetic analysis of the phytochrome superfamily reveals distinct microbial subfamilies of photoreceptors. *Biochem J* **392**(Pt 1)**,** 103-16.

Kay, S. A., Keith, B., Shinozaki, K., and Chua, N. H. (1989). The sequence of the rice phytochrome gene. *Nucleic Acids Res* **17**(7)**,** 2865-6.

Kelly, J. M., and Lagarias, J. C. (1985). Photochemistry of 124-Kilodalton Avena Phytochrome under Constant Illumination in-Vitro. *Biochemistry* **24**(21)**,** 6003-6010.

Kevei, E., Schafer, E., and Nagy, F. (2007). Light-regulated nucleo-cytoplasmic partitioning of phytochromes. *J Exp Bot* **58**(12)**,** 3113-24.

Khanna, R., Huq, E., Kikis, E. A., Al-Sady, B., Lanzatella, C., and Quail, P. H. (2004). A novel molecular recognition motif necessary for targeting photoactivated phytochrome signaling to specific basic helix-loop-helix transcription factors. *Plant Cell* **16**(11)**,** 3033-44.

Khanna, R., Shen, Y., Marion, C. M., Tsuchisaka, A., Theologis, A., Schafer, E., and Quail, P. H. (2007). The basic helix-loop-helix transcription factor PIF5 acts on ethylene biosynthesis and phytochrome signaling by distinct mechanisms. *Plant Cell* **19**(12)**,** 3915-29.

Kidokoro, S., Maruyama, K., Nakashima, K., Imura, Y., Narusaka, Y., Shinwari, Z. K., Osakabe, Y., Fujita, Y., Mizoi, J., Shinozaki, K., and Yamaguchi-Shinozaki, K. (2009). The phytochrome-interacting factor PIF7 negatively regulates DREB1 expression under circadian control in Arabidopsis. *Plant Physiol* **151**(4)**,** 2046-57.

Kiel, C., Yus, E., and Serrano, L. (2010). Engineering signal transduction pathways. *Cell* **140**(1)**,** 33-47.

Kim, D. H., Kang, J. G., Yang, S. S., Chung, K. S., Song, P. S., and Park, C. M. (2002). A phytochrome-associated protein phosphatase 2A modulates light signals in flowering time control in Arabidopsis. *Plant Cell* **14**(12)**,** 3043-56.

Kim, J. I., Shen, Y., Han, Y. J., Park, J. E., Kirchenbauer, D., Soh, M. S., Nagy, F., Schafer, E., and Song, P. S. (2004). Phytochrome phosphorylation modulates light signaling by influencing the protein-protein interaction. *Plant Cell* **16**(10)**,** 2629-40.

Kircher, S., Gil, P., Kozma-Bognar, L., Fejes, E., Speth, V., Husselstein-Muller, T., Bauer, D., Adam, E., Schafer, E., and Nagy, F. (2002). Nucleocytoplasmic partitioning of the plant photoreceptors phytochrome A, B, C, D, and E is regulated differentially by light and exhibits a diurnal rhythm. *Plant Cell* **14**(7)**,** 1541-55.

Kircher, S., Kozma-Bognar, L., Kim, L., Adam, E., Harter, K., Schafer, E., and Nagy, F. (1999). Light quality-dependent nuclear import of the plant photoreceptors phytochrome A and B. *Plant Cell* **11**(8)**,** 1445-56.

Koini, M. A., Alvey, L., Allen, T., Tilley, C. A., Harberd, N. P., Whitelam, G. C., and Franklin, K. A. (2009). High temperature-mediated adaptations in plant architecture require the bHLH transcription factor PIF4. *Curr Biol* **19**(5)**,** 408-13.

Koornneef, M. (1991). Isolation of higher plant developmental mutants. *Symp Soc Exp Biol* **45,** 1-19.

Koyama, T., Furutani, M., Tasaka, M., and Ohme-Takagi, M. (2007). TCP transcription factors control the morphology of shoot lateral organs via negative regulation of the expression of boundary-specific genes in Arabidopsis. *Plant Cell* **19**(2)**,** 473-84.

Krall, L., and Reed, J. W. (2000a). The histidine kinase-related domain participates in phytochrome B function but is dispensable. *Proceedings of the National Academy of Sciences of the United States of America* **97**(14)**,** 8169-8174.

Krall, L., and Reed, J. W. (2000b). The histidine kinase-related domain participates in phytochrome B function but is dispensable. *Proc Natl Acad Sci U S A* **97**(14)**,** 8169-74.

Lagarias, J. C., Kelly, J. M., Cyr, K. L., and Smith, W. O. J. (1987). Comparative Photochemical Analysis of Highly Purified 124-Kilodalton Oat and Rye Phytochromes in-Vitro. *Photochemistry and Photobiology* **46**(1)**,** 5-14.

Lagarias, J. C., and Mercurio, F. M. (1985). Structure function studies on phytochrome. Identification of light-induced conformational changes in 124-kDa Avena phytochrome in vitro. *J Biol Chem* **260**(4)**,** 2415-23.

Lamparter, T., Michael, N., Mittmann, F., and Esteban, B. (2002). Phytochrome from Agrobacterium tumefaciens has unusual spectral properties and reveals an N-terminal chromophore attachment site. *Proceedings of the National Academy of Sciences of the United States of America* **99**(18)**,** 11628-11633.

Lapko, V. N., Jiang, X. Y., Smith, D. L., and Song, P. S. (1999). Mass spectrometric characterization of oat phytochrome A: isoforms and posttranslational modifications. *Protein Sci* **8**(5)**,** 1032-44.

Lau, O. S., and Deng, X. W. (2010). Plant hormone signaling lightens up: integrators of light and hormones. *Curr Opin Plant Biol* **13**(5)**,** 571-7.

Laubinger, S., Fittinghoff, K., and Hoecker, U. (2004). The SPA quartet: a family of WD-repeat proteins with a central role in suppression of photomorphogenesis in arabidopsis. *Plant Cell* **16**(9)**,** 2293-306.

Laufs, P., Peaucelle, A., Morin, H., and Traas, J. (2004). MicroRNA regulation of the CUC genes is required for boundary size control in Arabidopsis meristems. *Development* **131**(17)**,** 4311-22.

Lee, J., He, K., Stolc, V., Lee, H., Figueroa, P., Gao, Y., Tongprasit, W., Zhao, H., Lee, I., and Deng, X. W. (2007). Analysis of transcription factor HY5 genomic binding sites revealed its hierarchical role in light regulation of development. *Plant Cell* **19**(3)**,** 731-49.

Leivar, P., Monte, E., Al-Sady, B., Carle, C., Storer, A., Alonso, J. M., Ecker, J. R., and Quail, P. H. (2008a). The Arabidopsis phytochrome-interacting factor PIF7, together with PIF3 and PIF4, regulates responses to prolonged red light by modulating phyB levels. *Plant Cell* **20**(2)**,** 337-352.

Leivar, P., Monte, E., Oka, Y., Liu, T., Carle, C., Castillon, A., Huq, E., and Quail, P. H. (2008b). Multiple phytochrome-interacting bHLH transcription factors repress premature seedling photomorphogenesis in darkness. *Curr Biol* **18**(23)**,** 1815-23.

Leivar, P., and Quail, P. H. (2010). PIFs: pivotal components in a cellular signaling hub. *Trends Plant Sci*.

Leivar, P., and Quail, P. H. (2011). PIFs: pivotal components in a cellular signaling hub. *Trends Plant Sci* **16**(1)**,** 19-28.

Leivar, P., Tepperman, J. M., Monte, E., Calderon, R. H., Liu, T. L., and Quail, P. H. (2009). Definition of early transcriptional circuitry involved in light-induced reversal

of PIF-imposed repression of photomorphogenesis in young Arabidopsis seedlings. *Plant Cell* **21**(11)**,** 3535-53.

Levskaya, A., Chevalier, A. A., Tabor, J. J., Simpson, Z. B., Lavery, L. A., Levy, M., Davidson, E. A., Scouras, A., Ellington, A. D., Marcotte, E. M., and Voigt, C. A. (2005). Synthetic biology: engineering Escherichia coli to see light. *Nature* **438**(7067)**,** 441-2.

Levskaya, A., Weiner, O. D., Lim, W. A., and Voigt, C. A. (2009). Spatiotemporal control of cell signalling using a light-switchable protein interaction. *Nature* **461**(7266)**,** 997-1001.

Li, H., Zhang, J., and Vierstra, R. D. (2010). Quaternary organization of a phytochrome dimer as revealed by cryoelectron microscopy. *Proc Natl Acad Sci U S A* **107**(24)**,** 10872-7.

Lifschitz, S., Gepstein, S., and Horwitz, B. A. (1990). Phytochrome Regulation of Greening in Wild Type and Long-Hypocotyl Mutants of Arabidopsis-Thaliana. *Planta (Heidelberg)* **181**(2)**,** 234-238.

Lim, W. A. (2010). Designing customized cell signalling circuits. *Nat Rev Mol Cell Biol* **11**(6)**,** 393-403.

Lorrain, S., Trevisan, M., Pradervand, S., and Fankhauser, C. (2009). Phytochrome interacting factors 4 and 5 redundantly limit seedling de-etiolation in continuous far-red light. *Plant Journal* **60**(3)**,** 449-461.

Mackenzie, J. M., Jr., Coleman, R. A., Briggs, W. R., and Pratt, L. H. (1975). Reversible redistribution of phytochrome within the cell upon conversion to its physiologically active form. *Proc Natl Acad Sci U S A* **72**(3)**,** 799-803.

Mancinelli, A. L., and Rabino, I. (1978). High Irradiance Responses of Plant Photomorphogenesis. *Botanical Review* **44**(2)**,** 129-180.

Marina, A., Waldburger, C. D., and Hendrickson, W. A. (2005). Structure of the entire cytoplasmic portion of a sensor histidine-kinase protein. *EMBO J* **24**(24)**,** 4247-59.

Marmorstein, R., Carey, M., Ptashne, M., and Harrison, S. C. (1992). DNA recognition by GAL4: structure of a protein-DNA complex. *Nature* **356**(6368)**,** 408-14.

Mateos, J. L., Luppi, J. P., Ogorodnikova, O. B., Sineshchekov, V. A., Yanovsky, M. J., Braslavsky, S. E., Gartner, W., and Casal, J. J. (2006). Functional and biochemical analysis of the N-terminal domain of phytochrome A. *J Biol Chem* **281**(45)**,** 34421-9.

Mathews, R. A. S. a. S. (2006a). phytochrome genes in higher plants:structure, expression, and evolution. *In* "photomorphogenesis in plants and bacteria 3rd Edition" (e. s. a. f. nagy, Ed.), pp. 99-129.

Mathews, S. (2006b). Phytochrome-mediated development in land plants: red light sensing evolves to meet the challenges of changing light environments. *Mol Ecol* **15**(12)**,** 3483-503.

Mathews, S. (2010). Evolutionary studies illuminate the structural-functional model of plant phytochromes. *Plant Cell* **22**(1)**,** 4-16.

Mathews, S., Clements, M. D., and Beilstein, M. A. (2010). A duplicate gene rooting of seed plants and the phylogenetic position of flowering plants. *Philos Trans R Soc Lond B Biol Sci* **365**(1539)**,** 383-95.

Mathews, S., and Sharrock, R. A. (1997). Photochrome gene diversity. *Plant Cell and Environment* **20**(6)**,** 666-671.

Matsushita, T., Mochizuki, N., and Nagatani, A. (2003). Dimers of the N-terminal domain of phytochrome B are functional in the nucleus. *Nature* **424**(6948)**,** 571-4.

Monte, E., Al-Sady, B., Leivar, P., and Quail, P. H. (2007). Out of the dark: how the PIFs are unmasking a dual temporal mechanism of phytochrome signalling. *J Exp Bot* **58**(12)**,** 3125-33.

Monte, E., Alonso, J. M., Ecker, J. R., Zhang, Y., Li, X., Young, J., Austin-Phillips, S., and Quail, P. H. (2003a). Isolation and characterization of phyC mutants in Arabidopsis reveals complex crosstalk between phytochrome signaling pathways. *Plant Cell* **15**(9)**,** 1962-80.

Monte, E., Alonso, J. M., Ecker, J. R., Zhang, Y., Li, X., Young, J., Austin-Phillips, S., and Quail, P. H. (2003b). Isolation and characterization of phyC mutants in Arabidopsis reveals complex crosstalk between phytochrome signaling pathways. *Plant Cell* **15**(9)**,** 1962-1980.

Muller, R., Fernandez, A. P., Hiltbrunner, A., Schafer, E., and Kretsch, T. (2009). The histidine kinase-related domain of Arabidopsis phytochrome a controls the spectral sensitivity and the subcellular distribution of the photoreceptor. *Plant Physiol* **150**(3)**,** 1297-309.

Munro, S., and Pelham, H. R. (1984). Use of peptide tagging to detect proteins expressed from cloned genes: deletion mapping functional domains of Drosophila hsp 70. *EMBO J* **3**(13)**,** 3087-93.

Nagatani, A., Reed, J. W., and Chory, J. (1993). Isolation and Initial Characterization of Arabidopsis Mutants That Are Deficient in Phytochrome A. *Plant Physiol* **102**(1)**,** 269-277.

Nagy, E. S. a. F. (2006). Historical Overview. 3 ed. *In* " photomorphogenesis in plants and bacteria", Vol. 1, pp. 1-24. 5 vols.

Neff, M. M., and Chory, J. (1998a). Genetic interactions between phytochrome A, phytochrome B, and cryptochrome 1 during Arabidopsis development. *Plant Physiology (Rockville)* **118**(1)**,** 27-36.

Neff, M. M., and Chory, J. (1998b). Genetic interactions between phytochrome A, phytochrome B, and cryptochrome 1 during Arabidopsis development. *Plant Physiology* **118**(1)**,** 27-36.

Nemhauser, J. L. (2008). Dawning of a new era: photomorphogenesis as an integrated molecular network. *Curr Opin Plant Biol* **11**(1)**,** 4-8.

Osterlund, M. T., and Deng, X. W. (1998). Multiple photoreceptors mediate the light-induced reduction of GUS-COP1 from Arabidopsis hypocotyl nuclei. *Plant J* **16**(2)**,** 201-8.

Osterlund, M. T., Hardtke, C. S., Wei, N., and Deng, X. W. (2000). Targeted destabilization of HY5 during light-regulated development of Arabidopsis. *Nature* **405**(6785)**,** 462-6.

Osterlund, M. T., Wei, N., and Deng, X. W. (2000). The roles of photoreceptor systems and the COP1-targeted destabilization of HY5 in light control of Arabidopsis seedling development. *Plant Physiol* **124**(4)**,** 1520-4.

Oyama, T., Shimura, Y., and Okada, K. (1997). The Arabidopsis HY5 gene encodes a bZIP protein that regulates stimulus-induced development of root and hypocotyl. *Genes Dev* **11**(22)**,** 2983-95.

Palagyi, A., Terecskei, K., Adam, E., Kevei, E., Kircher, S., Merai, Z., Schafer, E., Nagy, F., and Kozma-Bognar, L. (2010). Functional analysis of amino-terminal domains of the photoreceptor phytochrome B. *Plant Physiol* **153**(4)**,** 1834-45.

Park, C. M., Bhoo, S. H., and Song, P. S. (2000). Inter-domain crosstalk in the phytochrome molecules. *Semin Cell Dev Biol* **11**(6)**,** 449-56.

Parks, B. M., and Quail, P. H. (1993). hy8, a new class of arabidopsis long hypocotyl mutants deficient in functional phytochrome A. *Plant Cell* **5**(1)**,** 39-48.

Phee, B. K., Kim, J. I., Shin, D. H., Yoo, J., Park, K. J., Han, Y. J., Kwon, Y. K., Cho, M. H., Jeon, J. S., Bhoo, S. H., and Hahn, T. R. (2008). A novel protein phosphatase indirectly regulates phytochrome-interacting factor 3 via phytochrome. *Biochem J* **415**(2)**,** 247-55.

Poppe, C., Hangarter, R. P., Sharrock, R. A., Nagy, F., and Schaefer, E. (1996). The light-induced reduction of the gravitropic growth-orientation of seedlings of Arabidopsis thaliana (L.) Heynh. is a photomorphogenic response mediated synergistically by the far-red-absorbing forms of phytochromes A and B. *Planta (Heidelberg)* **199**(4)**,** 511-514.

Pratt, L. H., Kidd, G. H., and Coleman, R. A. (1974). An immunochemical characterization of the phytochrome destruction reaction. *Biochim Biophys Acta* **365**(1)**,** 93-107.

Quail, P. H. (1994). Photosensory perception and signal transduction in plants. *Curr Opin Genet Dev* **4**(5)**,** 652-61.

Quail, P. H. (2002). Phytochrome photosensory signalling networks. *Nat Rev Mol Cell Biol* **3**(2)**,** 85-93.

Quail, P. H., Boylan, M. T., Parks, B. M., Short, T. W., Xu, Y., and Wagner, D. (1995). Phytochromes: photosensory perception and signal transduction. *Science* **268**(5211)**,** 675-80.

Reed, J. W., Nagatani, A., Elich, T. D., Fagan, M., and Chory, J. (1994). Phytochrome A and Phytochrome B Have Overlapping but Distinct Functions in Arabidopsis Development. *Plant Physiol* **104**(4)**,** 1139-1149.

Reed, J. W., Nagpal, P., Poole, D. S., Furuya, M., and Chory, J. (1993a). Mutations in the gene for the red/far-red light receptor phytochrome B alter cell elongation and physiological responses throughout arabidopsis development. *Plant Cell* **5**(2)**,** 147-157.

Reed, J. W., Nagpal, P., Poole, D. S., Furuya, M., and Chory, J. (1993b). Mutations in the gene for the red/far-red light receptor phytochrome B alter cell elongation and physiological responses throughout Arabidopsis development. *Plant Cell* **5**(2)**,** 147-57.

Rizzini, L., Favory, J. J., Cloix, C., Faggionato, D., O'Hara, A., Kaiserli, E., Baumeister, R., Schafer, E., Nagy, F., Jenkins, G. I., and Ulm, R. (2011). Perception of UV-B by the Arabidopsis UVR8 protein. *Science* **332**(6025)**,** 103-6.

Robson, P. R. H., and Smith, H. (1996). Genetic and transgenic evidence that phytochromes A and B act to modulate the gravitropic orientation of Arabidopsis thaliana hypocotyls. *Plant Physiology (Rockville)* **110**(1)**,** 211-216.

Rockwell, N. C., and Lagarias, J. C. (2006). The structure of phytochrome: a picture is worth a thousand spectra. *Plant Cell* **18**(1)**,** 4-14.

Rockwell, N. C., Shang, L., Martin, S. S., and Lagarias, J. C. (2009). Distinct classes of red/far-red photochemistry within the phytochrome superfamily. *Proceedings of the National Academy of Sciences of the United States of America* **106**(15)**,** 6123-6127.

Rockwell, N. C., Su, Y. S., and Lagarias, J. C. (2006). Phytochrome structure and signaling mechanisms. *Annu Rev Plant Biol* **57,** 837-58.

Romanowski, M., and Song, P. S. (1992). Structural domains of phytochrome deduced from homologies in amino acid sequences. *J Protein Chem* **11**(2)**,** 139-55.

Rosler, J., Klein, I., and Zeidler, M. (2007). Arabidopsis fhl/fhy1 double mutant reveals a distinct cytoplasmic action of phytochrome A. *Proc Natl Acad Sci U S A* **104**(25)**,** 10737-42.

Ryu, J. S., Kim, J. I., Kunkel, T., Kim, B. C., Cho, D. S., Hong, S. H., Kim, S. H., Fernandez, A. P., Kim, Y., Alonso, J. M., Ecker, J. R., Nagy, F., Lim, P. O., Song, P. S., Schafer, E., and Nam, H. G. (2005). Phytochrome-specific type 5 phosphatase controls light signal flux by enhancing phytochrome stability and affinity for a signal transducer. *Cell* **120**(3)**,** 395-406.

Sage, L. C. (1992). "Pigment of the Imagination: A History of Phytochrome Research." Academic Press, San Diego.

Saijo, Y., Sullivan, J. A., Wang, H., Yang, J., Shen, Y., Rubio, V., Ma, L., Hoecker, U., and Deng, X. W. (2003). The COP1-SPA1 interaction defines a critical step in phytochrome A-mediated regulation of HY5 activity. *Genes Dev* **17**(21)**,** 2642-7.

Saijo, Y., Zhu, D., Li, J., Rubio, V., Zhou, Z., Shen, Y., Hoecker, U., Wang, H., and Deng, X. W. (2008a). Arabidopsis COP1/SPA1 complex and FHY1/FHY3 associate with distinct phosphorylated forms of phytochrome A in balancing light signaling. *Mol Cell* **31**(4)**,** 607-13.

Saijo, Y., Zhu, D., Li, J., Rubio, V., Zhou, Z., Shen, Y., Hoecker, U., Wang, H., and Deng, X. W. (2008b). Arabidopsis COP1/SPA1 complex and FHY1/FHY3 associate with distinct phosphorylated forms of phytochrome a in balancing light signaling. *Molecular Cell* **31**(4)**,** 607-613.

Sakamoto, K., and Nagatani, A. (1996). Nuclear localization activity of phytochrome B. *Plant J* **10**(5)**,** 859-68.

Salter, M. G., Franklin, K. A., and Whitelam, G. C. (2003). Gating of the rapid shade-avoidance response by the circadian clock in plants. *Nature* **426**(6967)**,** 680-3.

Sato, N. (1988). Nucleotide sequence and expression of the phytochrome gene in *Pisum sativum*: Differential regulation by light of multiple transcripts. *Plant Mol Biol* **11,** 697-710.

Schafer, E., Lassig, T. U., and Schopfer, P. (1975). Photocontrol of phytochrome destruction in grass seedlings. The influence of wavelength and irradiance. *Photochem Photobiol* **22**(5)**,** 193-202.

Schfer, E., Schmidt, W., and Mohr, H. (1973). COMPARATIVE MEASUREMENTS OF PHYTOCHROME IN COTYLEDONS AND HYPOCOTYL HOOK OF MUSTARD (SINAPIS ALBA L.). *phtochemistry and photobiology* **18**(4)**,** 331-334.

Seibeck, S., Borucki, B., Otto, H., Inomata, K., Khawn, H., Kinoshita, H., Michael, N., Lamparter, T., and Heyn, M. P. (2007). Locked 5Zs-biliverdin blocks the Meta-RA to Meta-RC transition in the functional cycle of bacteriophytochrome Agp1. *FEBS Lett* **581**(28)**,** 5425-9.

Seo, H. S., Watanabe, E., Tokutomi, S., Nagatani, A., and Chua, N. H. (2004). Photoreceptor ubiquitination by COP1 E3 ligase desensitizes phytochrome A signaling. *Genes Dev* **18**(6)**,** 617-22.

Seo, H. S., Yang, J. Y., Ishikawa, M., Bolle, C., Ballesteros, M. L., and Chua, N. H. (2003). LAF1 ubiquitination by COP1 controls photomorphogenesis and is stimulated by SPA1. *Nature* **423**(6943)**,** 995-9.

Sharrock, R. A. (2008). The phytochrome red/far-red photoreceptor superfamily. *Genome Biol* **9**(8)**,** 230.

Sharrock, R. A., and Clack, T. (2002). Patterns of expression and normalized levels of the five Arabidopsis phytochromes. *Plant Physiol* **130**(1)**,** 442-56.

Sharrock, R. A., and Clack, T. (2004). Heterodimerization of type II phytochromes in Arabidopsis. *Proc Natl Acad Sci U S A* **101**(31)**,** 11500-5.

Sharrock, R. A., Clack, T., and Goosey, L. (2003). Differential activities of the Arabidopsis phyB/D/E phytochromes in complementing phyB mutant phenotypes. *Plant Mol Biol* **52**(1)**,** 135-42.

Sharrock, R. A., Lissemore, J. L., and Quail, P. H. (1986). Nucleotide and amino acid sequence of a Cucurbita phytochrome cDNA clone: identification of conserved features by comparison with Avena phytochrome. *Gene* **47**(2-3)**,** 287-95.

Sharrock, R. A., and Quail, P. H. (1989). Novel phytochrome sequences in Arabidopsis thaliana: structure, evolution, and differential expression of a plant regulatory photoreceptor family. *Genes Dev* **3**(11)**,** 1745-57.

Shimizu-Sato, S., Huq, E., Tepperman, J. M., and Quail, P. H. (2002). A light-switchable gene promoter system. *Nat Biotechnol* **20**(10)**,** 1041-4.

Shin, J., Park, E., and Choi, G. (2007). PIF3 regulates anthocyanin biosynthesis in an HY5-dependent manner with both factors directly binding anthocyanin biosynthetic gene promoters in Arabidopsis. *Plant J* **49**(6)**,** 981-94.

Shinomura, T., Nagatani, A., Hanzawa, H., Kubota, M., Watanabe, M., and Furuya, M. (1996a). Action spectra for phytochrome A- and B-specific photoinduction of seed germination in Arabidopsis thaliana. *Proc Natl Acad Sci U S A* **93**(15)**,** 8129-33.

Shinomura, T., Nagatani, A., Hanzawa, H., Kubota, M., Watanabe, M., and Furuya, M. (1996b). Action spectra for phytochrome A- and B-specific photoinduction of seed germination in Arabidopsis thaliana. *Proceedings of the National Academy of Sciences of the United States of America* **93**(15)**,** 8129-8133.

Shinomura, T., Uchida, K., and Furuya, M. (2000). Elementary processes of photoperception by phytochrome A for high-irradiance response of hypocotyl elongation in Arabidopsis. *Plant Physiol* **122**(1)**,** 147-56.

Smith, H. (1983). The natural radiation environment: limitations on the biology of photoreceptors. Phytochrome as a case study. *Symp Soc Exp Biol* **36,** 1-18.

Smith, H., and Whitelam, G. C. (1990). Phytochrome a Family of Photoreceptors with Multiple Physiological Roles. *Plant Cell and Environment* **13**(7)**,** 695-708.

Somers, D. E., Devlin, P. F., and Kay, S. A. (1998). Phytochromes and cryptochromes in the entrainment of the Arabidopsis circadian clock. *Science* **282**(5393)**,** 1488-90.

Stephenson, P. G., Fankhauser, C., and Terry, M. J. (2009). PIF3 is a repressor of chloroplast development. *Proceedings of the National Academy of Sciences of the United States of America* **106**(18)**,** 7654-7659.

Stockhaus, J., Nagatani, A., Halfter, U., Kay, S., Furuya, M., and Chua, N. H. (1992). Serine-to-alanine substitutions at the amino-terminal region of phytochrome A result in an increase in biological activity. *Genes Dev* **6**(12A)**,** 2364-72.

Strauss, H. M., Hughes, J., and Schmieder, P. (2005). Heteronuclear solution-state NMR studies of the chromophore in cyanobacterial phytochrome Cph1. *Biochemistry* **44**(23)**,** 8244-50.

Strauss, H. M., Schmieder, P., and Hughes, J. (2005). Light-dependent dimerisation in the N-terminal sensory module of cyanobacterial phytochrome 1. *FEBS Lett* **579**(18)**,** 3970-4.

Su, Y. S., and Lagarias, J. C. (2007). Light-independent phytochrome signaling mediated by dominant GAF domain tyrosine mutants of Arabidopsis phytochromes in transgenic plants. *Plant Cell* **19**(7)**,** 2124-39.

Sullivan, J. A., Shirasu, K., and Deng, X. W. (2003). The diverse roles of ubiquitin and the 26S proteasome in the life of plants. *Nat Rev Genet* **4**(12)**,** 948-58.

Sullivan, T. D., Christensen, A. H., and Quail, P. H. (1989). Isolation and Characterization of a Maize Chlorophyll a-B Binding Protein Gene That Produces High Levels of Messenger Rna in the Dark. *Molecular and General Genetics* **215**(3)**,** 431-440.

Takano, M., Inagaki, N., Xie, X., Yuzurihara, N., Hihara, F., Ishizuka, T., Yano, M., Nishimura, M., Miyao, A., Hirochika, H., and Shinomura, T. (2005). Distinct and cooperative functions of phytochromes A, B, and C in the control of deetiolation and flowering in rice. *Plant Cell* **17**(12)**,** 3311-25.

Tanaka, R., and Tanaka, A. (2007). Tetrapyrrole biosynthesis in higher plants. *Annu Rev Plant Biol* **58,** 321-46.

Tepperman, J. M., Hudson, M. E., Khanna, R., Zhu, T., Chang, S. H., Wang, X., and Quail, P. H. (2004). Expression profiling of phyB mutant demonstrates substantial

contribution of other phytochromes to red-light-regulated gene expression during seedling de-etiolation. *Plant J* **38**(5)**,** 725-39.

Toledo-Ortiz, G., Kiryu, Y., Kobayashi, J., Oka, Y., Kim, Y., Nam, H. G., Mochizuki, N., and Nagatani, A. (2010). Subcellular Sites of the Signal Transduction and Degradation of Phytochrome A. *Plant and Cell Physiology* **51**(10)**,** 1648-1660.

Trupkin, S. A., Debrieux, D., Hiltbrunner, A., Fankhauser, C., and Casal, J. J. (2007). The serine-rich N-terminal region of Arabidopsis phytochrome A is required for protein stability. *Plant Mol Biol* **63**(5)**,** 669-78.

Tsukaya, H., Tsuge, T., and Uchimiya, H. (1994). The cotyledon: A superior system for studies of leaf development. *Planta (Heidelberg)* **195**(2)**,** 309-312.

Ulijasz, A. T., Cornilescu, G., Cornilescu, C. C., Zhang, J., Rivera, M., Markley, J. L., and Vierstra, R. D. (2010). Structural basis for the photoconversion of a phytochrome to the activated Pfr form. *Nature* **463**(7278)**,** 250-4.

van Thor, J. J., Mackeen, M., Kuprov, I., Dwek, R. A., and Wormald, M. R. (2006). Chromophore structure in the photocycle of the cyanobacterial phytochrome Cph1. *Biophys J* **91**(5)**,** 1811-22.

Vandenbussche, F., Habricot, Y., Condiff, A. S., Maldiney, R., Van der Straeten, D., and Ahmad, M. (2007). HY5 is a point of convergence between cryptochrome and cytokinin signalling pathways in Arabidopsis thaliana. *Plant Journal* **49**(3)**,** 428-441.

Vierstra, R. D. (1996). Proteolysis in plants: mechanisms and functions. *Plant Mol Biol* **32**(1-2)**,** 275-302.

Vierstra, R. D., and Quail, P. H. (1982). Native phytochrome: Inhibition of proteolysis yields a homogeneous monomer of 124 kilodaltons from Avena. *Proc Natl Acad Sci U S A* **79**(17)**,** 5272-6.

Wagner, D., Hoecker, U., and Quail, P. H. (1997). RED1 is necessary for phytochrome B-mediated red light-specific signal transduction in arabidopsis. *Plant Cell* **9**(5)**,** 731-743.

Wagner, J. R., Brunzelle, J. S., Forest, K. T., and Vierstra, R. D. (2005). A light-sensing knot revealed by the structure of the chromophore-binding domain of phytochrome. *Nature* **438**(7066)**,** 325-31.

Wagner, J. R., Zhang, J., Brunzelle, J. S., Vierstra, R. D., and Forest, K. T. (2007). High resolution structure of Deinococcus bacteriophytochrome yields new insights into phytochrome architecture and evolution. *J Biol Chem* **282**(16)**,** 12298-309.

Wall, J. K., and Johnson, C. B. (1983). An Analysis of Phytochrome Action in the High Irradiance Response. *Planta (Heidelberg)* **159**(5)**,** 387-397.

Wang, H., Ma, L. G., Li, J. M., Zhao, H. Y., and Deng, X. W. (2001). Direct interaction of Arabidopsis cryptochromes with COP1 in light control development. *Science* **294**(5540)**,** 154-8.

Ward, W. W., and Cormier, M. J. (1979). An energy transfer protein in coelenterate bioluminescence. Characterization of the Renilla green-fluorescent protein. *J Biol Chem* **254**(3)**,** 781-8.

Wei, N., Kwok, S. F., von Arnim, A. G., Lee, A., McNellis, T. W., Piekos, B., and Deng, X. W. (1994). Arabidopsis COP8, COP10, and COP11 genes are involved in repression of photomorphogenic development in darkness. *Plant Cell* **6**(5)**,** 629-43.

Weller, J. L., Hecht, V., Vander Schoor, J. K., Davidson, S. E., and Ross, J. J. (2009). Light regulation of gibberellin biosynthesis in pea is mediated through the COP1/HY5 pathway. *Plant Cell* **21**(3)**,** 800-13.

Whitelam, G. C., and Smith, H. (1991). Retention of Phytochrome-Mediated Shade Avoidance Responses in Phytochrome-Deficient Mutants of Arabidopsis Cucumber and Tomato. *Journal of Plant Physiology* **139**(1)**,** 119-125.

Wolf, I., Kircher, S., Fejes, E., Kozma-Bognar, L., Schafer, E., Nagy, F., and Adam, E. (2011). Light-regulated nuclear import and degradation of Arabidopsis phytochrome-A N-terminal fragments. *Plant Cell Physiol* **52**(2)**,** 361-72.

Woodward, A. W., and Bartel, B. (2005). Auxin: regulation, action, and interaction. *Ann Bot* **95**(5)**,** 707-35.

Wu, G., and Spalding, E. P. (2007). Separate functions for nuclear and cytoplasmic cryptochrome 1 during photomorphogenesis of Arabidopsis seedlings. *Proc Natl Acad Sci U S A* **104**(47)**,** 18813-8.

Xu, Y., Parks, B. M., Short, T. W., and Quail, P. H. (1995). Missense mutations define a restricted segment in the C-terminal domain of phytochrome A critical to its regulatory activity. *Plant Cell* **7**(9)**,** 1433-43.

Yamaguchi, R., Nakamura, M., Mochizuki, N., Kay, S. A., and Nagatani, A. (1999). Light-dependent translocation of a phytochrome B-GFP fusion protein to the nucleus in transgenic Arabidopsis. *J Cell Biol* **145**(3)**,** 437-45.

Yamashino, T., Matsushika, A., Fujimori, T., Sato, S., Kato, T., Tabata, S., and Mizuno, T. (2003). A Link between circadian-controlled bHLH factors and the APRR1/TOC1 quintet in Arabidopsis thaliana. *Plant Cell Physiol* **44**(6)**,** 619-29.

Yang, H. Q., Tang, R. H., and Cashmore, A. R. (2001). The signaling mechanism of Arabidopsis CRY1 involves direct interaction with COP1. *Plant Cell* **13**(12)**,** 2573-87.

Yang, S. W., Jang, I. C., Henriques, R., and Chua, N. H. (2009). FAR-RED ELONGATED HYPOCOTYL1 and FHY1-LIKE associate with the Arabidopsis transcription factors LAF1 and HFR1 to transmit phytochrome A signals for inhibition of hypocotyl elongation. *Plant Cell* **21**(5)**,** 1341-59.

Yang, X., Kuk, J., and Moffat, K. (2008). Crystal structure of Pseudomonas aeruginosa bacteriophytochrome: photoconversion and signal transduction. *Proc Natl Acad Sci U S A* **105**(38)**,** 14715-20.

Yang, X., Kuk, J., and Moffat, K. (2009). Conformational differences between the Pfr and Pr states in Pseudomonas aeruginosa bacteriophytochrome. *Proc Natl Acad Sci U S A* **106**(37)**,** 15639-44.

Yang, X., Stojkovic, E. A., Kuk, J., and Moffat, K. (2007). Crystal structure of the chromophore binding domain of an unusual bacteriophytochrome, RpBphP3, reveals residues that modulate photoconversion. *Proc Natl Acad Sci U S A* **104**(30)**,** 12571-6.

Yanovsky, M. J., Casal, J. J., and Luppi, J. P. (1997). The VLF loci, polymorphic between ecotypes Landsberg erecta and Columbia, dissect two branches of phytochrome A signal transduction that correspond to very-low-fluence and high-irradiance responses. *Plant Journal* **12**(3)**,** 659-667.

Yanovsky, M. J., Luppi, J. P., Kirchbauer, D., Ogorodnikova, O. B., Sineshchekov, V. A., Adam, E., Kircher, S., Staneloni, R. J., Schafer, E., Nagy, F., and Casal, J. J. (2002). Missense mutation in the PAS2 domain of phytochrome A impairs subnuclear localization and a subset of responses. *Plant Cell* **14**(7)**,** 1591-603.

Yeh, K. C., and Lagarias, J. C. (1998). Eukaryotic phytochromes: light-regulated serine/threonine protein kinases with histidine kinase ancestry. *Proc Natl Acad Sci U S A* **95**(23)**,** 13976-81.

Yeh, K. C., Wu, S. H., Murphy, J. T., and Lagarias, J. C. (1997). A cyanobacterial phytochrome two-component light sensory system. *Science* **277**(5331)**,** 1505-8.

Zhang, H., He, H., Wang, X., Yang, X., Li, L., and Deng, X. W. (2011). Genome-wide mapping of the HY5-mediated genenetworks in Arabidopsis that involve both transcriptional and post-transcriptional regulation. *Plant J* **65**(3)**,** 346-58.

APPENDIX A

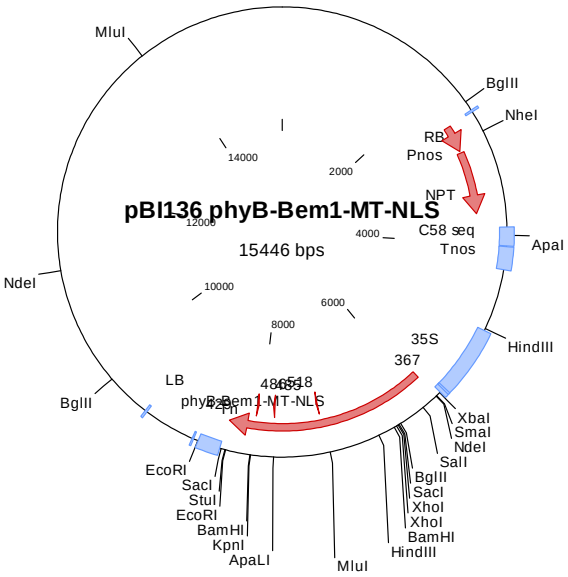
SEQENCES OF OBLIGATE DIMERS OF THE N-TERMINAL PHY PSRS

1: NB-Bem-myc6-NLS

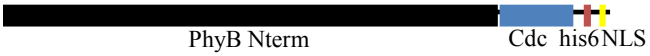



```
   1  mvsgvggsgg grgggrggee epssshtpnn rrggeqaqss gtkslrprsn
  51  tesmskaiqq ytvdarlhav feqsgesgks fdysqslktt tygssvpeqq
 101  itaylsriqr ggyiqpfgcm iavdessfri igysenarem lgimpqsvpt
 151  lekpeilamg tdvrslftss ssillerafv areitllnpv wihskntgkp
 201  fyailhridv gvvidlepar tedpalsiag avqsqklavr aisqlqalpg
 251  gdikllcdtv vesvrdltgy drvmvykfhe dehgevvaes krddlepyig
 301  lhypatdipq asrflfkqnr vrmivdcnat pvlvvqddrl tqsmclvgst
 351  lraphgchsq ymanmgsias lamaviingn eddgsnvasg rssmrlwglv
 401  vchhtssrci pfplryacef lmqafglqln melqlalqms ekrvlrtqtl
 451  lcdmllrdsp agivtqspsi mdlvkcdgaa flyhgkyypl gvapsevqik
 501  dvvewllanh adstglstds lgdagypgaa algdavcgma vayitkrdfl
 551  fwfrshtake ikwggakhhp edkddgqrmh prssfqafle vvksrsqpwe
 601  taemdaihsl qlilrdsfke seaamnskvv dgvvqpcrdm ageqgidelg
 651  ahqstsglkt tkikfyykdd ifalmlkgdt tykelrskia pridtdnfkl
 701  qtklfdgsge eiktdsqvsn iiqaklkisv hdicgtgshr fkameqklis
 751  eedlnemeqk liseedlnem eqkliseedl nemeqklise edlnemeqkl
 801  iseedlneme slgdltmeqk liseedlnsr pldpkkkrkv gg
```

NB = aa 1-651
Bem = aa 652-733
Myc6 = aa 744-828
SV40 NLS = aa 835-839

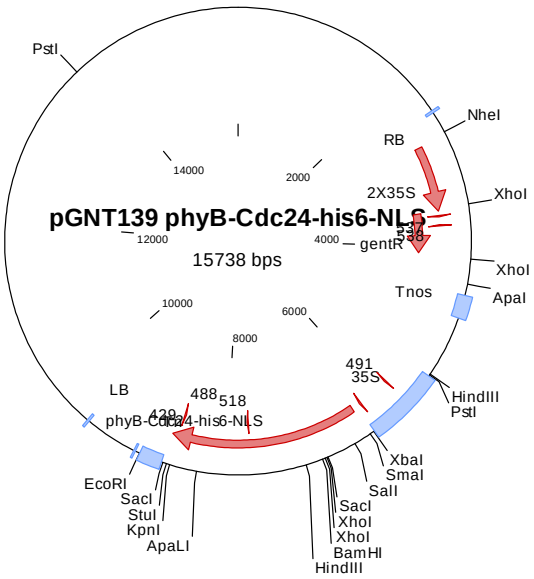


2: NB-Cdc-his6-NLS

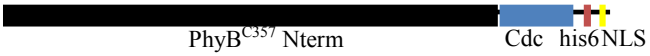



```
   1  MVSGVGGSGG GRGGGRGGEE EPSSSHTPNN RRGGEQAQSS GTKSLRPRSN
  51  TESMSKAIQQ YTVDARLHAV FEQSGESGKS FDYSQSLKTT TYGSSVPEQQ
 101  ITAYLSRIQR GGYIQPFGCM IAVDESSFRI IGYSENAREM LGIMPQSVPT
 151  LEKPEILAMG TDVRSLFTSS SSILLERAFV AREITLLNPV WIHSKNTGKP
 201  FYAILHRIDV GVVIDLEPAR TEDPALSIAG AVQSQKLAVR AISQLQALPG
 251  GDIKLLCDTV VESVRDLTGY DRVMVYKFHE DEHGEVVAES KRDDLEPYIG
 301  LHYPATDIPQ ASRFLFKQNR VRMIVDCNAT PVLVVQDDRL TQSMCLVGST
 351  LRAPHGCHSQ YMANMGSIAS LAMAVIINGN EDDGSNVASG RSSMRLWGLV
 401  VCHHTSSRCI PFPLRYACEF LMQAFGLQLN MELQLALQMS EKRVLRTQTL
 451  LCDMLLRDSP AGIVTQSPSI MDLVKCDGAA FLYHGKYYPL GVAPSEVQIK
 501  DVVEWLLANH ADSTGLSTDS LGDAGYPGAA ALGDAVCGMA VAYITKRDFL
 551  FWFRSHTAKE IKWGGAKHHP EDKDDGQRMH PRSSFQAFLE VVKSRSQPWE
 601  TAEMDAIHSL QLILRDSFKE SEAAMNSKVV DGVVQPCRDM AGEQGIDELG
 651  AQSSILFRIS YNNNSNNTSS SEIFTLLVEK VWNFDDLIMA INSKISNTHN
 701  NNISPITKIK YQDEDGDFVV LGSDEDWNVA KEMLAENNEK FLNIRLYCGT
 751  MRGSHHHHHH RPLDPKKKRK VGG
```

NB = aa 1-651
Cdc = aa 652-747
his6 = aa 754-760
SV40 NLS = aa 766-770

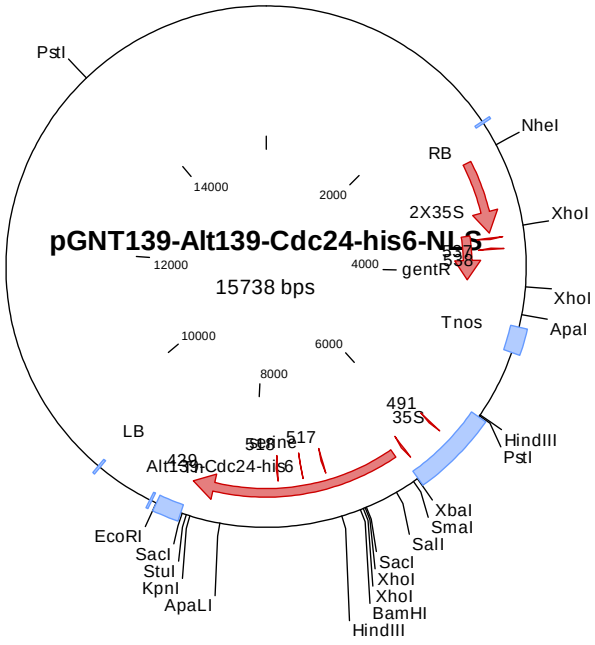


3: NB^{C357S}-Cdc-his6-NLS

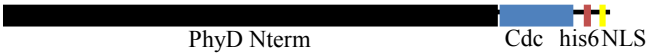



```
   1  MVSGVGGSGG GRGGGRGGEE EPSSSHTPNN RRGGEQAQSS GTKSLRPRSN
  51  TESMSKAIQQ YTVDARLHAV FEQSGESGKS FDYSQSLKTT TYGSSVPEQQ
 101  ITAYLSRIQR GGYIQPFGCM IAVDESSFRI IGYSENAREM LGIMPQSVPT
 151  LEKPEILAMG TDVRSLFTSS SSILLERAFV AREITLLNPV WIHSKNTGKP
 201  FYAILHRIDV GVVIDLEPAR TEDPALSIAG AVQSQKLAVR AISQLQALPG
 251  GDIKLLCDTV VESVRDLTGY DRVMVYKFHE DEHGEVVAES KRDDLEPYIG
 301  LHYPATDIPQ ASRFLFKQNR VRMIVDCNAT PVLVVQDDRL TQSMCLVGST
 351  LRAPHGSHSQ YMANMGSIAS LAMAVIINGN EDDGSNVASG RSSMRLWGLV
 401  VCHHTSSRCI PFPLRYACEF LMQAFGLQLN MELQLALQMS EKRVLRTQTL
 451  LCDMLLRDSP AGIVTQSPSI MDLVKCDGAA FLYHGKYYPL GVAPSEVQIK
 501  DVVEWLLANH ADSTGLSTDS LGDAGYPGAA ALGDAVCGMA VAYITKRDFL
 551  FWFRSHTAKE IKWGGAKHHP EDKDDGQRMH PRSSFQAFLE VVKSRSQPWE
 601  TAEMDAIHSL QLILRDSFKE SEAAMNSKVV DGVVQPCRDM AGEQGIDELG
 651  AQSSILFRIS YNNNSNNTSS SEIFTLLVEK VWNFDDLIMA INSKISNTHN
 701  NNISPITKIK YQDEDGDFVV LGSDEDWNVA KEMLAENNEK FLNIRLYCGT
 751  MRGSHHHHHH RPLDPKKKRK VGG
```

NB^{C357S} = aa 1-651
Cdc = aa 652-747
his6 = aa 754-760
SV40 NLS = aa 766-770

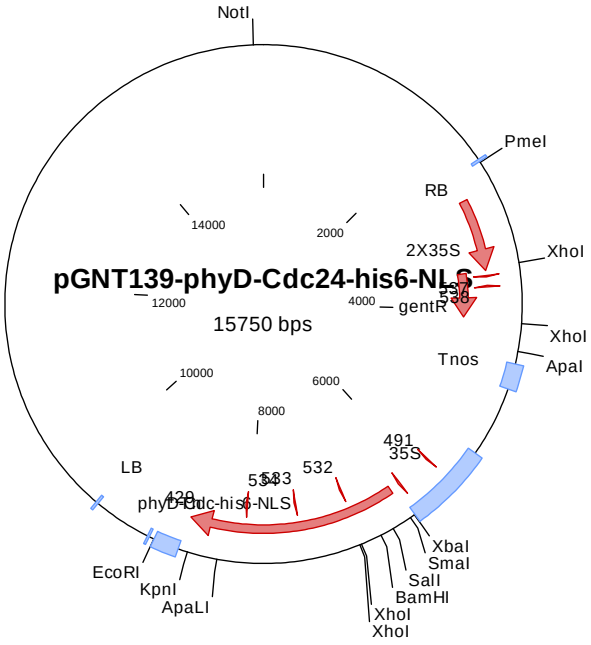


4: ND-Cdc-his6-NLS

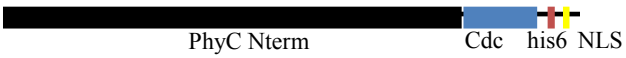



```
  1  MVSGGGSKTS GGEAASSGHR RSRHTSAAEQ AQSSANKALR SQNQQPQNHG
 51  GGTESTNKAI QQYTVDARLH AVFEQSGESG KSFDYSQSLK TAPYDSSVPE
101  QQITAYLSRI QRGGYTQPFG CLIAVEESTF TIIGYSENAR EMLGLMSQSV
151  PSIEDKSEVL TIGTDLRSLF KSSSYLLLER AFVAREITLL NPIWIHSNNT
201  GKPFYAILHR VDVGILIDLE PARTEDPALS IAGAVQSQKL AVRAISHLQS
251  LPSGDIKLLC DTVVESVRDL TGYDRVMVYK FHEDEHGEVV AESKRNDLEP
301  YIGLHYPATD IPQASRFLFK QNRVRMIVDC YASPVRVVQD DRLTQFICLV
351  GSTLRAPHGC HAQYMTNMGS IASLAMAVII NGNEEDGNGV NTGGRNSMRL
401  WGLVVCHHTS ARCIPFPLRY ACEFLMQAFG LQLNMELQLA LQVSEKRVLR
451  MQTLLCDMLL RDSPAGIVTQ RPSIMDLVKC NGAAFLYQGK YYPLGVTPTD
501  SQINDIVEWL VANHSDSTGL STDSLGDAGY PRAAALGDAV CGMAVACITK
551  RDFLFWFRSH TEKEIKWGGA KHHPEDKDDG QRMNPRSSFQ TFLEVVKSRC
601  QPWETAEMDA IHSLQLILRD SFKESEAMDS KAAAAGAVQP HGDDMVQQGM
651  QEIGAQSSIL FRISYNNNSN NTSSSEIFTL LVEKVWNFDD LIMAINSKIS
701  NTHNNNISPI TKIKYQDEDG DFVVLGSDED WNVAKEMLAE NNEKFLNIRL
751  YCGTMRGSHH HHHHRPLDPK KKRKVGG
```

ND = aa 1-655
Cdc = aa 656-751
his6 = aa 758-764
SV40 NLS = aa 769-774

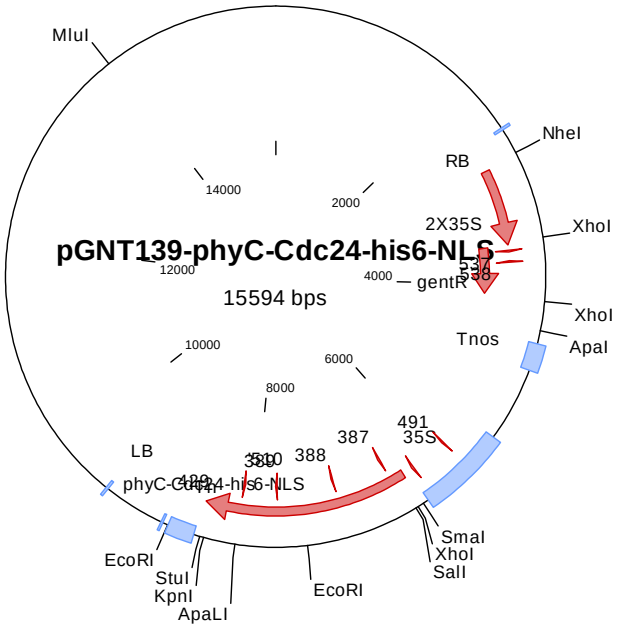


5: NC-Cdc-his6-NLS

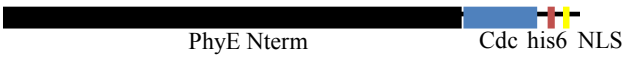



```
  1  MSSNTSRSCS TRSRQNSRVS SQVLVDAKLH GNFEESERLF DYSASINLNM
 51  PSSSCEIPSS AVSTYLQKIQ RGMLIQPFGC LIVVDEKNLK VIAFSENTQE
101  MLGLIPHTVP SMEQREALTI GTDVKSLFLS PGCSALEKAV DFGEISILNP
151  ITLHCRSSSK PFYAILHRIE EGLVIDLEPV SPDEVPVTAA GALRSYKLAA
201  KSISRLQALP SGNMLLLCDA LVKEVSELTG YDRVMVYKFH EDGHGEVIAE
251  CCREDMEPYL GLHYSATDIP QASRFLFMRN KVRMICDCSA VPVKVVQDKS
301  LSQPISLSGS TLRAPHGCHA QYMSNMGSVA SLVMSVTING SDSDEMNRDL
351  QTGRHLWGLV VCHHASPRFV PFPLRYACEF LTQVFGVQIN KEAESAVLLK
401  EKRILQTQSV LCDMLFRNAP IGIVTQSPNI MDLVKCDGAA LYYRDNLWSL
451  GVTPTETQIR DLIDWVLKSH GGNTGFTTES LMESGYPDAS VLGESICGMA
501  AVYISEKDFL FWFRSSTAKQ IKWGGARHDP NDRDGKRMHP RSSFKAFMEI
551  VRWKSVPWDD MEMDAINSLQ LIIKGSLQEE HSKTVVDVPL VDNRVQKVDE
601  LCAQSSILFR ISYNNNSNNT SSSEIFTLLV EKVWNFDDLI MAINSKISNT
651  HNNNISPITK IKYQDEDGDF VVLGSDEDWN VAKEMLAENN EKFLNIRLYC
701  GTMRGSHHHH HHRPLDPKKK RKVGG
```

NC = aa 1-603
Cdc = aa 604-700
his6 = aa 705-712
SV40 NLS = aa 718-722

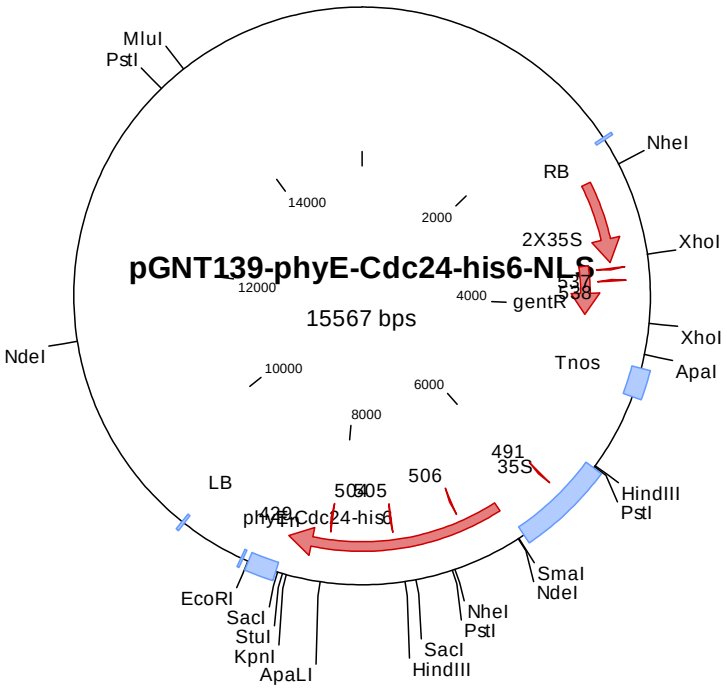


6: NE-Cdc-his6-NLS

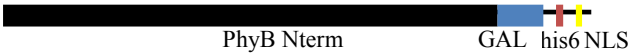



```
   1  MGFESSSSAA SNMKPQPQKS NTAQYSVDAA LFADFAQSIY TGKSFNYSKS
  51  VISPPNHVPD EHITAYLSNI QRGGLVQPFG CLIAVEEPSF RILGLSDNSS
 101  DFLGLLSLPS TSHSGEFDKV KGLIGIDART LFTPSSGASL SKAASFTEIS
 151  LLNPVLVHSR TTQKPFYAIL HRIDAGIVMD LEPAKSGDPA LTLAGAVQSQ
 201  KLAVRAISRL QSLPGGDIGA LCDTVVEDVQ RLTGYDRVMV YQFHEDDHGE
 251  VVSEIRRSDL EPYLGLHYPA TDIPQAARFL FKQNRVRMIC DCNATPVKVV
 301  QSEELKRPLC LVNSTLRAPH GCHTQYMANM GSVASLALAI VVKGKDSSKL
 351  WGLVVGHHCS PRYVPFPLRY ACEFLMQAFG LQLQMELQLA SQLAEKKAMR
 401  TQTLLCDMLL RDTVSAIVTQ SPGIMDLVKC DGAALYYKGK CWLVGVTPNE
 451  SQVKDLVNWL VENHGDDSTG LTTDSLVDAG YPGAISLGDA VCGVAAAGIS
 501  SKDYLLWFRS NTASAIKWGG AKHHPKDKDD AGRMHPRSSF TAFLEVAKSR
 551  SLPWEISEID AIHSLRLIMR ESFTSSRPVL SGNGVARDAN ELSAQSSILF
 601  RISYNNNSNN TSSSEIFTLL VEKVWNFDDL IMAINSKISN THNNNISPIT
 651  KIKYQDEDGD FVVLGSDEDW NVAKEMLAEN NEKFLNIRLY CGTMRGSHHH
 701  HHHRPLDPKK KRKVGG
```

NE = aa 1-592
Cdc = aa 595-691
his6 = aa 698-703
SV40 NLS = aa 709-713

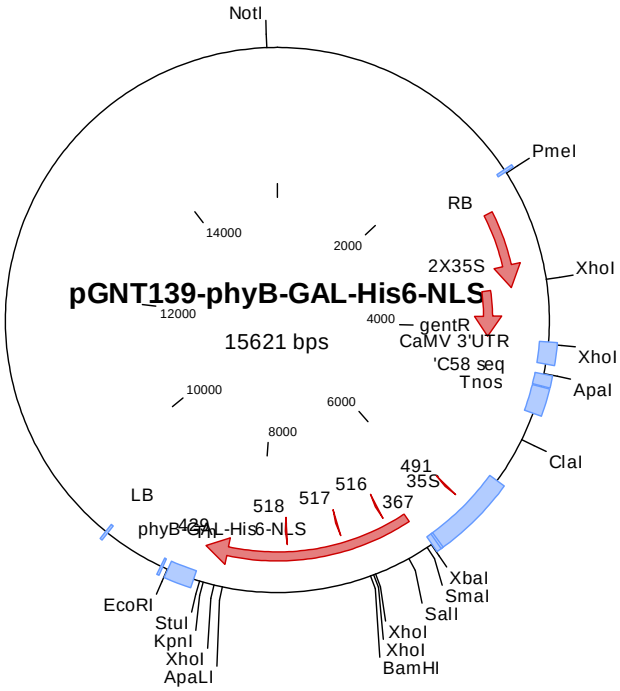


7: NB-GAL-his6-NLS

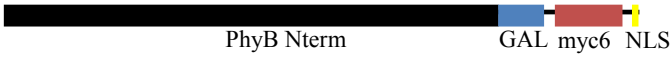



```
   1  MVSGVGGSGG GRGGGRGGEE EPSSSHTPNN RRGGEQAQSS GTKSLRPRSN
  51  TESMSKAIQQ YTVDARLHAV FEQSGESGKS FDYSQSLKTT TYGSSVPEQQ
 101  ITAYLSRIQR GGYIQPFGCM IAVDESSFRI IGYSENAREM LGIMPQSVPT
 151  LEKPEILAMG TDVRSLFTSS SSILLERAFV AREITLLNPV WIHSKNTGKP
 201  FYAILHRIDV GVVIDLEPAR TEDPALSIAG AVQSQKLAVR AISQLQALPG
 251  GDIKLLCDTV VESVRDLTGY DRVMVYKFHE DEHGEVVAES KRDDLEPYIG
 301  LHYPATDIPQ ASRFLFKQNR VRMIVDCNAT PVLVVQDDRL TQSMCLVGST
 351  LRAPHGCHSQ YMANMGSIAS LAMAVIINGN EDDGSNVASG RSSMRLWGLV
 401  VCHHTSSRCI PFPLRYACEF LMQAFGLQLN MELQLALQMS EKRVLRTQTL
 451  LCDMLLRDSP AGIVTQSPSI MDLVKCDGAA FLYHGKYYPL GVAPSEVQIK
 501  DVVEWLLANH ADSTGLSTDS LGDAGYPGAA ALGDAVCGMA VAYITKRDFL
 551  FWFRSHTAKE IKWGGAKHHP EDKDDGQRMH PRSSFQAFLE VVKSRSQPWE
 601  TAEMDAIHSL QLILRDSFKE SEAAMNSKVV DGVVQPCRDM AGEQGIDELG
 651  ALTRAHLTEV ESRLERLEQL FLLIFPREDL DMILKMDSLQ DIKALLTGLF
 701  VQDNVNKDAG TMRGSHHHHH HRPLDPKKKR KVGG
```

NB = aa 1-651
GAL = aa 652-709
his6 = aa 716-721
SV40 NLS = aa 727-731

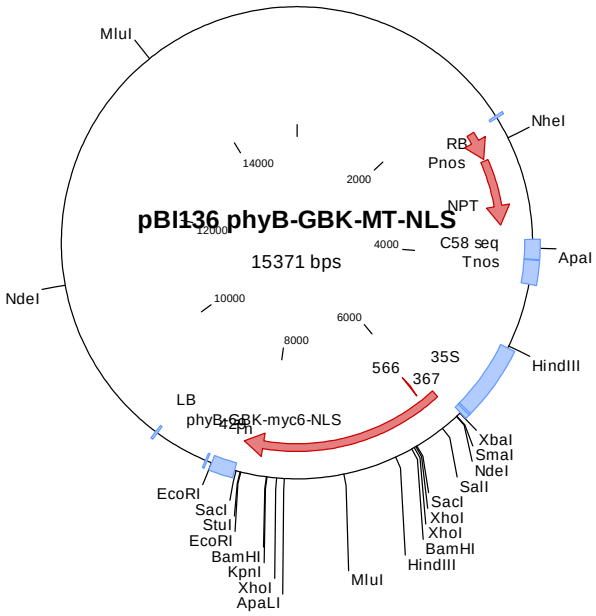


8: NB-GAL-mcy6-NLS

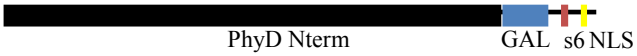



```
  1  MVSGVGGSGG GRGGGRGGEE EPSSSHTPNN RRGGEQAQSS GTKSLRPRSN
 51  TESMSKAIQQ YTVDARLHAV FEQSGESGKS FDYSQSLKTT TYGSSVPEQQ
101  ITAYLSRIQR GGYIQPFGCM IAVDESSFRI IGYSENAREM LGIMPQSVPT
151  LEKPEILAMG TDVRSLFTSS SSILLERAFV AREITLLNPV WIHSKNTGKP
201  FYAILHRIDV GVVIDLEPAR TEDPALSIAG AVQSQKLAVR AISQLQALPG
251  GDIKLLCDTV VESVRDLTGY DRVMVYKFHE DEHGEVVAES KRDDLEPYIG
301  LHYPATDIPQ ASRFLFKQNR VRMIVDCNAT PVLVVQDDRL TQSMCLVGST
351  LRAPHGCHSQ YMANMGSIAS LAMAVIINGN EDDGSNVASG RSSMRLWGLV
401  VCHHTSSRCI PFPLRYACEF LMQAFGLQLN MELQLALQMS EKRVLRTQTL
451  LCDMLLRDSP AGIVTQSPSI MDLVKCDGAA FLYHGKYYPL GVAPSEVQIK
501  DVVEWLLANH ADSTGLSTDS LGDAGYPGAA ALGDAVCGMA VAYITKRDFL
551  FWFRSHTAKE IKWGGAKHHP EDKDDGQRMH PRSSFQAFLE VVKSRSQPWE
601  TAEMDAIHSL QLILRDSFKE SEAAMNSKVV DGVVQPCRDM AGEQGIDELG
651  ALTRAHLTEV ESRLERLEQL FLLIFPREDL DMILKMDSLQ DIKALLTGLF
701  VQDNVNKDAG TGSHRFKAME QKLISEEDLN EMEQKLISEE DLNEMEQKLI
751  SEEDLNEMEQ KLISEEDLNE MEQKLISEED LNEMESLGDL TMEQKLISEE
801  DLNSRPLDPK KKRKVGG
```

NB = aa 1-651
GAL = aa 652-709
myc6 = aa 719-803
NLS = aa 810-814

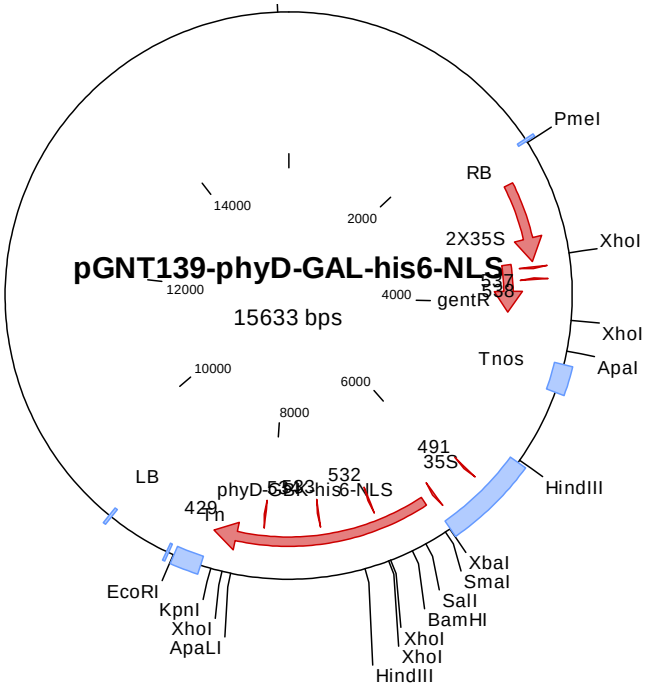


9: ND-GAL-his6-NLS

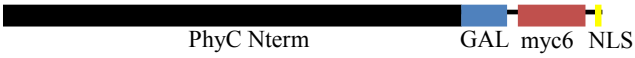



```
  1  MVSGGGSKTS GGEAASSGHR RSRHTSAAEQ AQSSANKALR SQNQQPQNHG
 51  GGTESTNKAI QQYTVDARLH AVFEQSGESG KSFDYSQSLK TAPYDSSVPE
101  QQITAYLSRI QRGGYTQPFG CLIAVEESTF TIIGYSENAR EMLGLMSQSV
151  PSIEDKSEVL TIGTDLRSLF KSSSYLLLER AFVAREITLL NPIWIHSNNT
201  GKPFYAILHR VDVGILIDLE PARTEDPALS IAGAVQSQKL AVRAISHLQS
251  LPSGDIKLLC DTVVESVRDL TGYDRVMVYK FHEDEHGEVV AESKRNDLEP
301  YIGLHYPATD IPQASRFLFK QNRVRMIVDC YASPVRVVQD DRLTQFICLV
351  GSTLRAPHGC HAQYMTNMGS IASLAMAVII NGNEEDGNGV NTGGRNSMRL
401  WGLVVCHHTS ARCIPFPLRY ACEFLMQAFG LQLNMELQLA LQVSEKRVLR
451  MQTLLCDMLL RDSPAGIVTQ RPSIMDLVKC NGAAFLYQGK YYPLGVTPTD
501  SQINDIVEWL VANHSDSTGL STDSLGDAGY PRAAALGDAV CGMAVACITK
551  RDFLFWFRSH TEKEIKWGGA KHHPEDKDDG QRMNPRSSFQ TFLEVVKSRC
601  QPWETAEMDA IHSLQLILRD SFKESEAMDS KAAAAGAVQP HGDDMVQQGM
651  QEIGALTRAH LTEVESRLER LEQLFLLIFP REDLDMILKM DSLQDIKALL
701  TGLFVQDNVN KDAGTMRGSH HHHHHRPLDP KKKRKVGG
```

ND = aa 1-655
GAL = aa 656-713
his6 = aa 720-725
SV40 NLS = aa 731-735



10: NC-GAL-mcy6-NLS



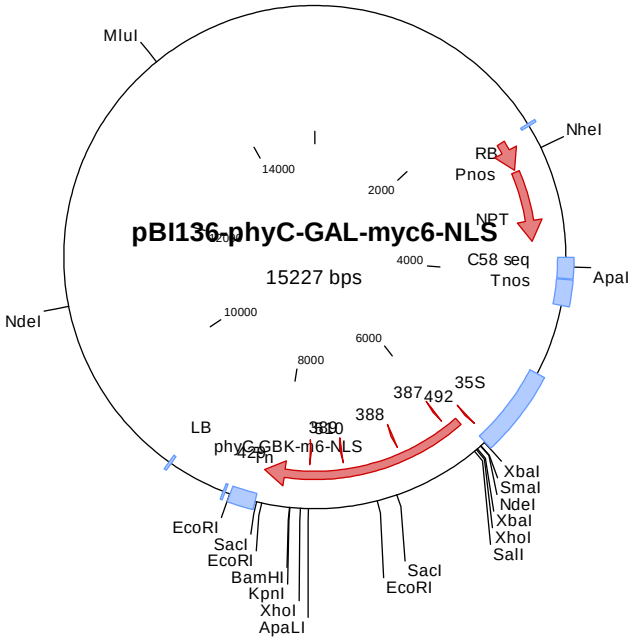

```
   1  MSSNTSRSCS TRSRQNSRVS SQVLVDAKLH GNFEESERLF DYSASINLNM
  51  PSSSCEIPSS AVSTYLQKIQ RGMLIQPFGC LIVVDEKNLK VIAFSENTQE
 101  MLGLIPHTVP SMEQREALTI GTDVKSLFLS PGCSALEKAV DFGEISILNP
 151  ITLHCRSSSK PFYAILHRIE EGLVIDLEPV SPDEVPVTAA GALRSYKLAA
 201  KSISRLQALP SGNMLLLCDA LVKEVSELTG YDRVMVYKFH EDGHGEVIAE
 251  CCREDMEPYL GLHYSATDIP QASRFLFMRN KVRMICDCSA VPVKVVQDKS
 301  LSQPISLSGS TLRAPHGCHA QYMSNMGSVA SLVMSVTING SDSDEMNRDL
 351  QTGRHLWGLV VCHHASPRFV PFPLRYACEF LTQVFGVQIN KEAESAVLLK
 401  EKRILQTQSV LCDMLFRNAP IGIVTQSPNI MDLVKCDGAA LYYRDNLWSL
 451  GVTPTETQIR DLIDWVLKSH GGNTGFTTES LMESGYPDAS VLGESICGMA
 501  AVYISEKDFL FWFRSSTAKQ IKWGGARHDP NDRDGKRMHP RSSFKAFMEI
 551  VRWKSVPWDD MEMDAINSLQ LIIKGSLQEE HSKTVVDVPL VDNRVQKVDE
 601  LCALTRAHLT EVESRLERLE QLFLLIFPRE DLDMILKMDS LQDIKALLTG
 651  LFVQDNVNKD AGTGSHRFKA MEQKLISEED LNEMEQKLIS EEDLNEMEQK
 701  LISEEDLNEM EQKLISEEDL NEMEQKLISE EDLNEMESLG DLTMEQKLIS
 751  EEDLNSRPLD PKKKRKVGG
```

NC = aa 1-602

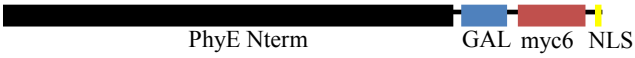
GAL = aa 604-661

Myc6 = aa 671-755

NLS = aa 762-766



11: NE-GAL-mcy6-NLS




```
  1  MGFESSSSAA SNMKPQPQKS NTAQYSVDAA LFADFAQSIY TGKSFNYSKS
 51  VISPPNHVPD EHITAYLSNI QRGGLVQPFG CLIAVEEPSF RILGLSDNSS
101  DFLGLLSLPS TSHSGEFDKV KGLIGIDART LFTPSSGASL SKAASFTEIS
151  LLNPVLVHSR TTQKPFYAIL HRIDAGIVMD LEPAKSGDPA LTLAGAVQSQ
201  KLAVRAISRL QSLPGGDIGA LCDTVVEDVQ RLTGYDRVMV YQFHEDDHGE
251  VVSEIRRSDL EPYLGLHYPA TDIPQAARFL FKQNRVRMIC DCNATPVKVV
301  QSEELKRPLC LVNSTLRAPH GCHTQYMANM GSVASLALAI VVKGKDSSKL
351  WGLVVGHHCS PRYVPFPLRY ACEFLMQAFG LQLQMELQLA SQLAEKKAMR
401  TQTLLCDMLL RDTVSAIVTQ SPGIMDLVKC DGAALYYKGK CWLVGVTPNE
451  SQVKDLVNWL VENHGDDSTG LTTDSLVDAG YPGAISLGDA VCGVAAAEFS
501  SKDYLLWFRS NTASAIKWGG AKHHPKDKDD AGRMHPRSSF TAFLEVAKSR
551  SLPWEISEID AIHSLRLIMR ESFTSSRPVL SGNGVARDAN ELSALTRAHL
601  TEVESRLERL EQLFLLIFPR EDLDMILKMD SLQDIKALLT GLFVQDNVNK
651  DAGTGSHRFK AMEQKLISEE DLNEMEQKLI SEEDLNEMEQ KLISEEDLNE
701  MEQKLISEED LNEMEQKLIS EEDLNEMESL GDLTMEQKLI SEEDLNSRPL
751  DPKKKRKVGG
```

NC = aa 1-592
GAL = aa 595-652
his6 = aa 662-746
NLS = aa 753-757

